BIFURCATIONS IN MAPS WITH MEMORY AND PREDATOR PREY MODELS WITH MODULATED CONTROL

THESIS SUBMITTED FOR THE DEGREE OF

DOCTOR OF PHILOSOPHY (SCIENCE)

OF

WEST BENGAL UNIVERSITY OF TECHNOLOGY

DEBABRATA DUTTA

DEPARTMENT OF THEORETICAL SCIENCES

S. N. BOSE NATIONAL CENTRE FOR BASIC SCIENCES

BLOCK-JD, SECTOR-III

SALTLAKE , KOLKATA–700098 , INDIA

AUGUST 2008

THESIS CERTIFICATE

This is to certify that the thesis titled **Bifurcations in maps with memory and predator prey models with modulated control**, submitted by **Debabrata Dutta** to the West Bengal University of Technology for the award of the degree of **Doctor of Philosophy**, is a bona fide record of the research work done by him under my supervision. The contents of this thesis, in full or in part, have not been submitted to any other Institute or University for the award of any degree or diploma.

Jayanta Bhattacharjee
Research Guide

Professor
Department of Theoretical Sciences
S. N. Bose National Centre for Basic Sciences
Block-JD, Sector-III, Salt Lake
Kolkata 700098, India.

To Alaka and Sumana

Acknowledgements

My warmest thanks go to my supervisor, Prof. J. K. Bhattacharjee, for motivation, inspiration, guidance and for the many helpful discussions which were invaluable lessons in how to conduct research. I also had the opportunity to attend his classes that had given enough motivation to take Physics as a career. Without him writing this thesis would have been quite difficult.

Additional thanks are due to all those people-both from within and outside the institute here-who gave me the opportunity to discuss my work with them and respond with helpful suggestions. I thank prof. R. Ramaswamy of J.N.U., New Delhi and his student Amitabha for their collaboration with us. I also thank Prof. R. E. Amritkar for his support and motivation to conduct research. My special thanks to Prof. Marc Timme and Prof. Theo Geisel for their academic and financial support to carry out research in MPIDS, Göttingen.

Its my pleasure to be also a part of the research group at the department of theoretical physics of the Indian Association for the Cultivation of Science, I gratefully recall the help and pleasant company of my friends and colleagues Ankur, Debaprasad, Debottam, Dipanjan, Shyamal, Sudipto, Soumya Prasad, Soumya, Nabakumar, Pradipta, Dwipesh, Jaydeep, my seniors Himadrida, Arnabda, Devashishda, Palashda, Sougatada and Arijitda. At the same department I also recall the cooperation extended to me in administrative matters by Bhudebda, Sureshda, Tapanda and Subrata who never let me feel external. I also pay my gratitude to Dr. Koushik Ray, Dr. Utpal Chattopadhaya for their help in computation.

In my Institute, S. N. Bose National Centre for Basic Sciences, I enjoyed the warm affection of my seniors Abhisekda, Mukulbhai, Anujda and Manida. Stay in SNBNCBS has been a pleasure

with my batch mates Abhishek, Mrinal, Navin, Manas, Venkat, Shashank, Sunandan and Swati and juniors Sagar, Arnab and Ashis . Its my pleasure to thank Mrinal, Venkat and Abhishek who helped changing my attitude towards experiments and to Swati for her support in research. Working with fun loving Sagar is also a pleasure.

Thanks to those people in Jadavpur University who have helped to make my graduate studies a pleasure, including Abhishek, Amaresh, Arindam, saptarshi, Soumyadeep and Stego.

Finally, I am especially grateful my aunt Alaka Mondal and Maternal Grand Parents for their active contribution and involvement in my life, for their motivation, inspiration, support and for introducing me to Physics.

Synopsis

We have done a systematic study of dynamical behaviours of nonlinear chaotic systems under memory modulation. Control and enhancement of chaos have their applications in real systems. For last two decades it has been a field of active research. However memory modulation has recently been recognised as an effective method of chaos control and our work indicates the richness of this method. Dynamics of chaotic systems are usually governed by system parameters. We propose to control the system parameter(s) according to the past and present states of the system. We have shown systems are able to show much richer dynamics under memory modulated control. We started with memory modulated parameter control in one dimensional maps and moved to higher dimensional discrete maps. We have made slight modification of our prescription to apply this method to more realistic continuous dynamical systems.

Our choice of delayed feedback modulation makes the dynamics of one dimensional (logistic) maps non–Abelian, and since the choice of (noninvertible) map depends on the history, the system is deterministic and also non-Markovian. These new features give rise to novel dynamical features. The zones of dynamical stability have a complicated and hierarchically organized structure.Our main method for understanding the organization of periodic orbits in such driven systems is through a generalization of the results of MSS for the organization of periodic orbits in unimodal maps, and we show how this scheme helps in rationalizing the different periodic orbits that can arise in the driven system. In addition, we find that there are non–MSS periodic orbits, namely the stabilization of “forbidden” itineraries for periodic orbits which results from the choice of delayed feedback forcing.There also appear to be regions in parameter space where there are no periodic windows and our preliminary studies of the dynamics here have revealed a peculiar characteristic of the attendant tangent bifurcations. Although they are still of Type-I, owing to the interplay of two different

mappings in determining the dynamics, the actual mechanics of the re-injection process leads to the scaling exponents being quite different from $\frac{1}{2}$. When applied with little modification memory dependent control enriches dynamics of one dimensional maps to greater extent. We introduce a single step memory dependence in the fully chaotic logistic map. However, we show that by using composite functions to define two one dimensional maps, it is possible to obtain some analytic results for the bifurcation structure. Numerical results support the calculated bifurcation scheme and in addition yields a further insight which allows the calculation of convergence ratio for a new period adding scenario. It can be shown that the convergence ratio can be calculated in the similar way for any quadratic modulated maps. It is also shown that the mechanism of period adding bifurcation is quite different from the dynamics of piecewise continuous maps where period adding phenomenon is quite common.

The mechanism of period adding bifurcation is explained more with the analysis of two dimensional discrete Lotka-Volterra system. We have shown that the period adding bifurcation is an outcome of interplay of chaotic dynamics with ordered (periodic) dynamics. We have shown when the dynamics with of positive and negative Lyapunov exponents get coupled, period adding occurs. Neimark-Sacker Bifurcation is observed in this two dimensional discrete system. As the system parameter changes the system moves from invariant curves to chaotic bands. Center manifold theory is used to explain this scenario. Invariant curves are coupled with chaotic bands to ensure period adding bifurcation does not occur with weakly stable attractors. Attractors with sufficiently large negative Lyapunov exponents cause period adding bifurcation as it couple with chaotic ones.

Single-step memory dependent parameter modulation was modified to fit into dynamics of continuous systems. Memory dependent delay feedback was used in stead of single-step one. This modulation is shown to have great effect on continuous dynamical systems in controlling their Lyapunov exponents. Limit cycles are shown as a outcome of quantization of delay time. We hope our work contributes to the ongoing research of control of chaos and consider memory modulated parameter control as a standard method of controlling chaos.

List of Publications

This thesis has been based on the following papers.

- **The phase-modulated logistic map**

  Amitabha Nandi, Debabrata Dutta, Jayanta K. Bhattacharjee and *Ramakrishna Ramaswamy*

  Published in *Chaos* **15** 023107 (2005)

- **Period adding bifurcation in a logistic map with memory**

  Debabrata Dutta, J. K. Bhattacharjee

  Published in *Physica D in press* **doi:10.1016/j.physd.2008.05.014**

- **Discrete Lotka Volterra under memory modulation**

  Debabrata Dutta , J. K. Bhattacharjee (To be communicated).

- **A study on bifurcation diagrams in relation to synchronisation in chaotic systems**

  Debabrata Dutta, J. K. Bhattacharjee

  Communicated, ***nlin:0612020***.

- **Controlling dynamical systems by memory dependent switching: a variation on the Pyragas scheme**

  Debabrata Dutta, J. K. Bhattacharjee (Communicated).

Table of Contents

Chapter 1

Control of chaos in dynamical systems

1.1 Introduction

The concept of chaos has been introduced into science quite recently, in the seventies. Chaotic systems provided researchers with a new tool for modelling the uncertainty which differs from the classical probabilistic concepts. Chaotic motions are modelled as the solutions of deterministic non-linear differential or difference equation with floating frequency and amplitude.

The attention of many physicists, mathematicians and engineers was drawn to the study of chaotic systems by the paper by D. Ruelle and F Takens (1971) who coined the term ‘strange attractor’ for chaotic attractors (1), and by the paper of T. Li and J. Yorke (1975) who introduced the term ‘chaos’ (2). Serious investigations of a similar complex dynamics were performed in the former soviet union by A. Kolmogorov, Y. Sinai, V. Arnold, V. Melnikov, Yu. Neimark, L. Shinikov and A. Sharkovsky in the 60s-70s. Later chaotic phenomena was discovered in enormous number of systems in mechanics, physics, chemistry, biology etc. Chaotic models were reported to be useful for financial time series prediction and for training. Moreover such models were also found useful in the study of neural networks and genetic algorithms.

From the point of view of control, chaotic systems are a particular class of nonlinear dynamical systems having irregular oscillating solutions. Control of chaos can be considered as a subarea of

controlling the nonlinear oscillatory systems. However problems of the control of chaos have certain distinctive features. The most important of them was pointed out by E. Ott, C. Grebogi and J. Yorke (3). They showed that the trajectory of chaotic motion can be turned into periodic one by means of arbitrarily small control that stabilizes the inherent periodic orbits. That concept opened new perspectives both in natural sciences and in technology and also initiated an avalanche of research in this area.

One of the reasons for interest in the control of chaos is the wide range of its potential applications covering the entire area of science and technology. We will illustrate here some of these.

1.1.1 Mechanics and mechanical engineering

A variety of oscillatory as well as synchronization problems for mechanical systems arises when one intends to design a vibration equipment. The control of a ship becomes important when it rolls and the rolling is affected by lateral ocean waves. The motion of the ship can exhibit chaos even for waves purely periodic in time due to the nonlinear dynamics of the ship. Thus the problem is to decrease the amplitude of chaotic oscillations under disturbances. Again only a low level of control is admissible. The problem of suppressing vibrations, which can be interpreted as damping the system to bring it down to a desired energy level, is of a similar nature.

Techniques of creating or suppressing chaos can be applied in washing machines. It is known that washing may be accelerated when the angular velocity of the rotor is oscillating. Moreover the desirable kind of oscillations is chaotic due to the fact that the chaotic changes in the rotor speed provide a better mixing and a better dissolving of the detergent.

1.1.2 Electrical engineering and telecommunications

Till recent years, investigations were mainly concerned with periodic oscillations (4). For many years the chaotic modes were either overlooked or considered to be undesirable. Van der Pol and Van der Mark (5) made the brief remark “Often an irregular noise is heard in the telephone re-

ceiver before the frequency jumps" and never discusses the issue further. However during last three decades, the interest in chaotic oscillations within the theory of circuits rose tremendously.The most popular applications of chaos lie in the field of telecommunications.

A few ways of using chaos for signal storage of transmission were reported in (6; 7; 8; 9; 10). Chaotic signal are used as the carrier instead of periodic one. To realize this electrical circuits of transmitter as well as receiver need to be synchronized. Many technique of controlling periodic signal fails in synchronizing chaotic one; hence new ways of controlling chaos synchronization were developed. Synchronization of chaotic system has its application in the field of cryptography (11).

One of the first experiments on controlling chaotic oscillations was devoted to control of lasers, where the system consisting of neodymium-yttrium-aluminium-garnate laser and a frequency doubling crystal was considered (12). At the high levels of input power the intensity of the laser output power fluctuates chaotically. With the feedback algorithm proposed by Hunt, the laser can be driven into periodic mode. Later many successful experiments on chaos control have been performed by different kinds of laser source (13; 14; 15; 16).

Another important field of application of chaos control is power systems. These systems under certain natural stress fall into 'crisis' which can be controlled using chaos control methods (17). Electrical generators in power systems can be controlled by broadening the attraction region of the normal operation mode. Control of irregular oscillations of the output is achieved through the method of transient stabilization.

1.1.3 Chemistry and chemical engineering

Studies of chaotic dynamics in chemistry has started with Belusov-Zhabotinsky reaction.Once the existence of periodic and chaotic oscillatory modes was recognized, the idea of controlling it in chemical reaction became quite natural. The control goal can be formulated as achieving the steady state mode of the reaction. In other cases it can be necessary to create chaotic oscillations. In combustion applications chaos is desirable as it enhances the mixing of fuel with air. In chemical reaction there are fewer parameters to control than in electronic circuits. So problem of small or

restricted control is truly practical. Adaptive control method is very effective in controlling chemical reactions for producing chaotic as well as oscillatory reactions.

Chaotic phenomena are already used in chemical technology. Chaotic mixing is much faster and more efficient than diffusion. A better mixing yields a more uniform reaction and therefore less impurity is present in the product. This process makes the reactions more cost effective and is heavily used in chemical industry.

1.1.4 Biology biochemistry and medicine.

Unlike chemistry and telecommunication chaotic oscillations have been known to biologists for long. The famous logistic map, whose role in chaos is that of the Hydrogen atom in quantum mechanics, has its origin in population dynamics (18). Rhythmic behaviour is a basic property in living organisms and it facilitates the survival and evolution of them. Chaotic rhythms are also quite common in biological systems. These systems are pierced by positive and negative feedbacks which make them suitable for control purposes.

During the last two decades research in biochemistry and molecular biology has gained much attention. Models of molecular dynamics are based on Hamiltonian formulation and control methods for the Hamiltonian systems are of much importance. These methods are applied to create oscillations in bio-molecular structures and also to synchronize oscillations in different parts of the structures.

The potential applications in medicine include treatment of cardiac arrhythmia and pathological brain activities. These motions are primarily chaotic and treatments are performed by enhancing chaos. Both theoretical and experimental results on controlling cardiac rhythms (19; 20; 21) and brain rhythms (22; 23) were reported in the literature.

1.1.5 Economics and finance

The existence and importance of oscillations in economic activities have been widely recognized since 19^{th} century. Quite recently an interest in models of nonlinear dynamics and chaos arose in financial studies. Though far less attention was paid to the prediction and control of those economic

activities. Recent studies showed that the dynamics of many financial time series is better described by chaotic models than by conventional ones based the Brownian motion (24; 25). Chaos theory and neural networks has become very important in studying modern financial theory. We can forecast an increasing significance of economics and finance as a new market for the control of oscillations and chaos.

1.2 Methods of chaos control

The presence of chaos in physical systems has been extensively demonstrated and is very common. In practice, however, it is often desired that chaos be avoided. In most cases we expect the systems to show nice periodic behaviour. For last two decades there has been extensive research on controlling chaos and numerous research papers were published. The idea of controlling chaos started with the seminal paper of Ott, Grebogi and Yorke (3).

The processes of controlling chaos in dynamical systems can be divided into following three main categories.

1.2.1 Stabilizing unstable periodic orbits

This method was suggested by Ott, Grebogi and Yorke and addressed the following question:“Given a chaotic attractor, how can one obtain improved performance and a desired attracting time-periodic motion by making only *small* time-dependent perturbations in an *accessible* system parameter?”

When controlling goal is only to make small perturbation to the system to achieve regular dynamics then it is hard to create new orbits; generally they require stronger perturbations. A chaotic attractor typically embeds within it an infinite number of unstable periodic orbits. By proper control small perturbation can move the chaotic dynamics to one of the unstable periodic orbits. The parameter is controlled in time such that it stabilises the intended unstable periodic orbit (UPO). The method is very general and can be applied to variety of situations.

It is important to note that this method is more effective in the presence of chaos. As chaotic attractors embed infinite numbers of unstable orbits small parameter perturbation can stabilize one of the number of different orbits. For non-chaotic attractors the system improvement is limited as periodic orbits are limited to that specific system.

The prerequisite to apply this method to control chaos is that the dynamical equations of the system should be known.

$$\frac{d\mathbf{x}}{dt} = \mathbf{F}(\mathbf{x}, p) \tag{1.2.1}$$

p being the controlling parameter. Even if the dynamical equations describing the system are not known, but the time series of some scalar dependent variable $z(t)$ can be measured the chaotic attractor can be reconfigured using delay coordinates.

$$\mathbf{X}(t) = [z(t), z(t-T), z(t-2T), \ldots, z(t-MT)] \tag{1.2.2}$$

As control of chaos often leads to making the system fall into periodic orbits $\mathbf{X}$ or Eq(1.2.1) is used to find out the Poincaré surface of section. Each rotation maps to a point in that section. From this map a number of unstable orbits can be determined (26). After that parameter p can be perturbed to stabilize the system to the intended UPO.

Let us start with the simplest period one orbit, higher dimensional orbits can be explained as a generalization of the same procedure. Period one orbit acts as a fixed point on the Poincaré section. Let λ_s and λ_u be the experimentally determined stable and unstable eigenvalues of the surface of section map at the chosen fixed point. Then $\mid \lambda_s \mid < 1 < \mid \lambda_u \mid$. Let $\mathbf{e}_s$ and $\mathbf{e}_u$ be the experimentally determined unit vectors in the stable and unstable directions. Without loss of generality we can take $p = 0$ for the fixed point. If ξ_i denotes the i$^{\text{th}}$ fixed point on the Poincaré surface then for fixed point $\xi = \xi_N = 0$. Then slight change of p to $\bar{p}$ we can approximate

$$\mathbf{g} \equiv \delta\xi_N(p)/\delta p|_p = 0 \cong \bar{p}^{-1}\xi_N(\bar{p}) \tag{1.2.3}$$

$$\xi_{n+1} \cong p_n\mathbf{g} + [\lambda_u\mathbf{e}_u\mathbf{f}_u + \lambda_s\mathbf{e}_s\mathbf{f}_s].[\xi_n - p_n\mathbf{g}] \tag{1.2.4}$$

p is rewritten as p_n to associate it with nth section. The choice of p_n is such that ξ_{n+1} falls on the stable manifold of $\xi = 0$, i.e. $\mathbf{f}_u.\xi_{n+1} = 0$. If ξ_{n+1} falls on the stable manifold then parameter perturbation can be set to zero, and the orbit for the subsequent time will approach the fixed point at a geometrical rate λ_s.

1.2.2 Control by feedback

The method suggested by OGY is very efficient and has been successfully applied to some experiments (27; 28). An experimental application of the OGY method requires a continuous computer analysis of the state of the system. The changes in parameter p are discrete in time since the method deals with Poincaré map. The parameter modulation is applied as the trajectory of the system crosses the Poincaré map. The OGY method can stabilize only those periodic orbits whose maximal Lyapunov exponent is small compared to the reciprocal of the time interval between parameter changes. Since the corrections of the parameter are rare and small, the fluctuation noise leads to occasional bursts of the system into the region far from the desired periodic orbit, and these burst are more frequent for large noise.

Pyragas (29) suggested the idea of a time-continuous control to overcome this problem. With small perturbation UPOs can be stabilized with continuous feedback control.

In the following two methods of continuous control in the form of feedback are suggested. Both methods are based on the construction of a special form of time-continuous perturbation,which does not change the form of the desired UPO, but under certain condition stabilize it. Feedback can be external as well as internal. In the first method a combined feedback with a periodic external force of a special form is used. The second method is based on self controlling delayed feedback.

External force control

Let for us consider dynamical system Eq(1.2.1). We imagine that the explicit form of the equation is unknown but some scalar variable $y(t)$ can be measured as a system output. If the system is available

for external input $f(t)$ then we can divide the system into following subsystems

$$\frac{d\mathbf{x}}{dt} = \mathbf{P}(\mathbf{x}, y) \tag{1.2.5}$$

$$\frac{dy}{dt} = Q(\mathbf{x}, y) + f(t) \tag{1.2.6}$$

The vector **x** describes the remaining variables of the dynamical system that are not of interest. For simplicity it can be taken that $f(t)$ disturbs only the first equation, corresponding to the output value. For no external force ($f(t) = 0$), let the system have a strange attractor. Dynamics of the system as well as large number of distinct UPOs can be found by constructing delay coordinates (1.2.2). From the experimental output signal $y(t)$ various periodic signal $y_i(t)$ can be determined. where $y_i(t + T_i) = y_i(t)$ and T_i is the time period for ith UPO.The difference $D(t)$ between the signal $y_i(t)$ and the output signal is used as control signal.

$$f(t) = K[y_i(t)] - y(t) = D(t) \tag{1.2.7}$$

where K is an experimentally adjustable weight. This perturbation feeds into the system a negative feedback for $K > 0$. The important feature of the perturbation is that it does not change the solution of Eq(1.2.5) corresponding to the UPO $y(t) = y_i(t)$. By selecting the weight K stabilization can be achieved. Near the stabilization weight only a small external force is required to stabilize the UPOs.

Delayed feedback control

The complexity of the experimental realization of the above method is mainly in the design of a special periodic oscillator. The second methods works pretty well to such systems. In this method the external signal $y_i(t)$ in Eq(1.2.7) is substituted for the delayed output signal $y(t - \tau)$, where τ is the delay time. The perturbation cam be written in the form

$$f(t) = K[y(t - \tau) - y(t)] = kD(t) \tag{1.2.8}$$

Now when the delay coincides with the period of the ith UPO $\tau = T_i$, then the perturbation becomes zero for the solution of system Eq(1.2.5) correponding to this UPO $y(t) = y_i(t)$. So perturbation in this form also does not change the solution of the system corresponding to i^th UPO. Like the earlier method choice of an appropriate K leads to stabilization of the desired UPO. As this method does not depend on the external signal it is much simpler to realize this system.

1.2.3 Control through periodic perturbation

The inherent irregularity of chaoic dynamics and its strong sensitivity to perturbation sometimes lead us to believe that such dynamics cannot be destroyed by means of weak external forcing. Moreover, the notion that the existence of three incommensurate frequencies in a system can generally lead to chaos hardly suggests that the addition of an externally produced frequency will have controlling effect on chaotic dynamics. In the previous section we saw external feedback control can tame chaos. Even without the presence of feedback chaos can be controlled with the presence of small external periodic forcing. Chaotic attractor embeds infinite numbers of UPOs. Like earlier section Poincaré surface of section can be generated for the surface of section. On the Poincaré section a D-dimensional continuous dynamics can be represented as a can be presented as a D-1 dimensional discrete dynamics. Colse to a UPO an unstable limit cycle can be modeled by

$$x_{n+1} = (\lambda + \varepsilon f_n)x_n \tag{1.2.9}$$

where $\lambda > 1$, $< f_n >= 0$, $< f_n^2 >= 1$; we can take f_n to be harmonic. Angular brackets denote the average over n. When $\varepsilon = 0$ the fixed point $x*$ is clearly unstable. For finite ε the Lyapunov exponent η corresponding to the map (1.2.9) is

$$\eta = Re < ln(\lambda + \varepsilon f_n) > \tag{1.2.10}$$

For small ε,

$$\eta = ln\lambda - \varepsilon^2/\lambda^2 + \emptyset(\varepsilon^3) \tag{1.2.11}$$

When $\lambda^2 ln\lambda < \varepsilon^2$ the Lyapunov exponent in negative which implies $x*$ is stable. Even when $\lambda^2 ln\lambda > \varepsilon^2$, the forcing has an effect of reducing the Lyapunov exponent. Resonant interactions can further affect the stability of these cycle.

1.2.4 Control through synchronization

Synchronization of two identical chaotic system has been proposed by Pecora and Carroll in 1990. Later many other processes of synchronization are proposed. Afraimovich *et al.* investigated the possibility of some different types of synchronization where the parameters does not match. The idea was developed further by the works of Rulkov *et al.* (30; 31) and Parlitz *et al.* (32). This generalization of synchronization of chaotic system leads us to control of chaos of response system. We consider an n-dimensional dynamical system

$$\dot{\mathbf{u}} = \mathbf{f}(\mathbf{u}) \tag{1.2.12}$$

the system can be divided into two subsystems [**u**=(**v**,**w**)]

$$\dot{\mathbf{v}} = \mathbf{g}(\mathbf{v}, \mathbf{w}); \quad \dot{\mathbf{w}} = \mathbf{h}(\mathbf{v}, \mathbf{w}) \tag{1.2.13}$$

where $\mathbf{v} = (u_1, \ldots, u_m)$, $\mathbf{g} = (f_1(\mathbf{u}), \ldots, f_m(\mathbf{u}))$, $\mathbf{w} = (u_{m+1}, \ldots, u_n)$ and $\mathbf{h} = (f_{m+1}(\mathbf{u}), \ldots, f_n(\mathbf{u}))$. Now a new subsystem $\mathbf{w}'$ can be created identical to the **w** system by substituting the set of variables **v** for the corresponding $\mathbf{v}'$ in the function **h** and the previous equation can be augmented with the new system

$$\dot{\mathbf{v}} = \mathbf{g}(\mathbf{v}, \mathbf{w}); \quad \dot{\mathbf{w}} = \mathbf{h}(\mathbf{v}, \mathbf{w}); \quad \dot{\mathbf{w}}' = \mathbf{h}(\mathbf{v}, \mathbf{w}') \tag{1.2.14}$$

The subsystem components **w** and $\mathbf{w}'$ synchronize only if $\mathbf{w}' \rightarrow \mathbf{w}$ as $t \rightarrow \infty$. In the infinitesimal limit this leads to the variational equations for the subsystem;

$$\dot{\xi} = D_w \mathbf{h}(\mathbf{v}, \mathbf{w})\xi \tag{1.2.15}$$

where $D_w\mathbf{h}$ is the Jacobian of the **w** subsystem vector field with respect to w only. This equation leads to the calculation of the Lyapunov exponents of the subsystem, referred in literature as conditional Lyapunov exponents. If the largest conditional exponent is negative both subsystems synchronize.

In this analysis parameters of both the subsystem are taken to be identical; which in practical systems are often not true. It can be shown that if the parameters of the subsystems differs slightly then also both system synchronizes.

The generalized version of synchronization suggests that for two non-identical systems (e.g. two Lorenz with different parameter values) there may exists a smooth functional dependence that connects the overall nature of both the system. If two chaotic dynamical systems are generally synchronized and the drive system is non-chaotic the response system can also be non-chaotic (for certain range of parameters) though it should be chaotic for its own parameter value (33).

1.3 Discussion

A nonlinear system with chaotic behavior is very sensitive to initial conditions, particularly in the system with large Lyapunov exponents (34). A tiny error may lead to failure of the control process when its errors are amplified exponentially with time. Such errors can be introduced by the linearization of a nonlinear system, the inaccuracy of experimental measurement, and the noisy environment. A number of presented methods modify control parameters once each period of Poincaré map (3; 38; 35; 36), and the stabilization can be realized only for such periodic orbits whose maximal Lyapunov exponent is smaller than the reciprocal of the time interval between parameter changes. For the control system with large Lyapunov exponent or high-order unstable periodic orbits, the tiny errors may ‘kick’ the system state out of its controllable region. The fluctuation noise leads to occasional bursts of the system into the region far from the desired periodic orbit, and these bursts are more frequent for a large noise. Therefore the idea of adjusting the system state more frequently than once each period T (35; 37), and the idea of a time-continuous control seems

attractive in this context (29).

Pyragas have proposed two methods of permanent chaos control with a small time-continuous perturbation in the form of linear feedback (29). The stabilization of unstable periodic orbits (UPOs) of a chaotic system is achieved either by combined linear feedback with the use of a specially designed external oscillator or by delayed self-controlling linear feedback without any external force. They have calculated the maximal Lyapunov exponent of the UPOs using the linearization of system to analyze the local stability of the system and to select suitable experimentally adjustable weight parameter K. Both methods are based on the construction of a special form of a time-continuous perturbation, which does not change the desired UPO, but can stabilize it under certain conditions.

Ushio proposed a method of chaos control for stabilizing a periodic orbit embedded in a discrete-time chaotic system based on contraction mappings in 1995 (40). The validity of the method is shown using a property of contraction mappings.

An open-plus-closed-loop (OPCL) method of controlling nonlinear dynamic systems was presented by Atlee Jackson and Grosu in 1995 (39). The input signal of their method is the sum of Hübler's open-loop control and a particular form of a linear closed-loop control, the goal of which can be selected as one of the UPOs embedded in chaotic attractor, or another possible smooth functions of time. The asymptotic stability of the controlled nonlinear system is realized by the linear approximation around the stabilized orbit. But the calculation of the closed-loop control signal is very difficult in some cases, especially for complex and high-dimension chaotic systems.

In recent years many more control algorithms have been proposed and like the previous methods they all have their own shortcomings. While feedback methods have large parameter controlling range, practical implementation becomes difficult for fast chaos. The feedback control chaos methods stabilize one of the unstable periodic orbits (UPOs) embedded in its chaotic attractor by applying small temporal perturbations to an accessible system parameter. For some high-speed systems such as chaotic circuits and fast electro-optical systems, there is difficulty in attaining real-time data of the system parameters and variables. Similarly non-feedback based control methods lacks energy optimization. Recent research (41) based on genetic algorithm are proposed to optimize the signal

strength. This approach can achieve the control goal with significantly lower power, ranging from one to three orders of magnitude in difference.

Bibliography

[1] F. Takens, *Dynamical Systems and Turbulence, Warwick 1980*, p. 366

[2] Li, T., And J.A. Yorke, *Amer. Math. Monthly*,**82**, 985, 1975.

[3] Edward ott, Celso Grebogi and James A. Yorke, Phys. Rev. Lett. **64**, 1196 (1990).

[4] Lindsay, W. *Synchronization Systems in Communications and control*, Prentice Hall (1972).

[5] Van der Pol, B. and Van der Mark, *Nature*,**120**

[6] Angeli, A., R. Genesio and A. Tesi,*IEEE Trans. on Circ, 363, 1927.. Sys. I.*, **42**, 54, 1995.

[7] Belskii, Dmitriev, A.S., *J. of Communication Technology and Electronics*,**39**, 1994.

[8] Carroll, T.L., *IEEE Trans. on Circ. Sys.*, **42**, 105, 1995.

[9] Dedieu, H., M.P. Kennedy and M. Hasler, *IEEE Trans. on Circ. Sys. II*,**40**, 634, 1993.

[10] Dedieu, H. and M.J. Ogorzalek, *Proc. of IEEE Int'l Symp. on Circ. Sys.*, Seattle WA, April29-May 3, 1191, 1995.

[11] Kocarev, L., K.S. Halle, K. Eckert, L.O. Chua and U. Parlitz,Int J. Bifurcation and Chaos **2**, 709 (1992).

[12] Roy, R., T.W. Murphy, T. D. Maier, Z. Gills and E.R. Hunt, Phys. Rev. Lett. **68**, 1259 (1992).

[13] Gills, Z., C. Iwata, R. Roy, I. Schwartz and I. Triandaf, Phys. Rev. Lett. **69**, 3169 (1992).

[14] Parisi, J., R. Badii, E. Brun, L.Flepp, C. Reyl, R. Stoop, O.E. Rössler, A. Kittel and R. Richter,*J. of Zeitschirift fur naturforschung, Teil A*, 48A, 627, 1993.

[15] Colet, P., R. Roy and K. Wiesenfeld, Phys. Rev. E **50**, 3453 (1994).

[16] Gavrielides,A., V. Kovanis and P.M. Alsing, *Proc. of the SPIE - The Int'l Society for Optical Engr.* 2039, 250, 1993.

[17] Soumitro Banerjee and Celso Grebogi,Phys. Rev. E **59**, 4052 (1999).

[18] Nature, **261**, 459 (1976).

[19] Brandt, M.E. and G. Chen, Int J. Bifurcation and Chaos **6**, 219 (1996).

[20] Garfinkel, A., M.L. Spano, W.L. DItto and J.N. Weiss, *Science***257**, 1230, 1992.

[21] Christini, D.J. and J.J. Collins, Phys. Rev. E **54**, 49 (1996).

[22] Glanz, J.,*Science*, August, 1174, 1994.

[23] Schiff, S.J., K. Jerger, D. H. Duong, T. Chang, M.L. Spano and W.L. Ditto, *Nature*, August, 615, 1994.

[24] Peters, E., *Chaos and Order on Capital Markets*, John Wiley and Sons, 1991.

[25] Peters,E., *Fractal Market analysis*, John Wiley and Sons, 1994.

[26] G.H. Ganaratne, P.S. Linsay and M.J. Vinson, Phys. Rev. Lett. **63**, 1 (1989).

[27] E.R. Hunt Phys. Rev. Lett. **67**, 1953 (1991).

[28] W.L. Ditto, S.N. Rauseo M.L. Spano Phys. Rev. Lett. **65**, 3211 (1990).

[29] K. Pyragas Phys. Lett. A **170**, 421 (1992).

[30] N. Rulkov, M.M. Sushchik, L.S. Tsimring *et al.*,Phys. Rev. E **51**, 980 (1995).

[31] H.D.L. Abarbanel, N.F. Rulkov and M.M. Sushchik Phys. Rev. E **53**, 4528 (1996).

[32] L. Kocarev and U. Parlitz, Phys. Rev. Lett. **76**, 1816 (1996).

[33] Sagar Chakrabarty and Debabrata Dutta,**arXiv**:nlin/0612020.

[34] B. Hübinger, R. Doerner, W. Martienssen, M. Herdering, R. Pitka, and U. Dressler, Phys. Rev. E **50**, 932 (1994).

[35] D. Xu and S. R. Bishop, Phys. Lett. A **210**, 273 (1996).

[36] M. A. Matias and J. Guemez, Phys. Rev. Lett. **72**, 1455 (1994).

[37] B. Hbinger, R. Doemer, and W. Martienssen, Z. Phys. B: Condens. Matter **90**, 103 (1993).

[38] T. Shinbrot, C. Grebogi, E. Ott and J. A. Yorke, Nature (London) 363, 411 (1993).

[39] E. Atlee Jackson and I. Grosu, Physica D **85**, 1 (1995).

[40] T. Ushio, Phys. Lett. A **198**, 14 (1995).

[41] C. Y. Soong,W. T. Huang, F.P. Lin and P. Y. Tzeng, Phys. Lett. E **70**, 016211 (2004).

Chapter 2

Anti-control of chaos in dynamical systems

2.1 Introduction

Most studies which attempt to control chaotic dynamical systems direct their efforts towards controlling the system to regular periodic orbits or to specific chaotic orbits (1; 2) . However, there have been few attempts at control directed towards enhancing the chaoticity of chaotic flows. This is an important problem for its own intrinsic interest and may have practical applications as well. An important example of a situation where enhancing chaos is useful, is the process of mixing (3; 4; 5) . Mixing is a consequence of the stretching and folding of chaotic flows. A system which has exponential stretching, as in a chaotic flow, can mix efficiently. Many mixing processes like fluid flows, combustion processes, chemical reactions, heat transfer processes etc., can be modeled by chaotic flows (3). An enhancement of the chaoticity of such systems can lead to an enhancement of the rate of mixing; an outcome which has desirable consequences in many of these contexts. In addition to enhancing the rate of mixing, the enhancement of chaos can be desirable and useful also in other situations. In the case of biological systems, there are several instances of situations where maintaining or enhancing chaos is desirable (6) . It has been suggested that the pathological destruction

of chaotic behavior may be responsible for heart failure (7) , and some types of brain seizures (8). Techniques which are capable of enhancing and maintaining chaos could be useful in such contexts (9).

2.2 Enhancing chaos with parametric modulation

An important parameter, which characterizes the degree of chaos in a chaotic flow is the Lyapunov exponent, which gives the average rate of stretching. However, the rate of stretching is not uniform over a chaotic attractor in the case of dissipative flows or over the phase space of a conservative flow. Thus the local Lyapunov exponent (LLE) , a measure of the local rate of stretching, is different in different regions of the phase space (10) . The nonuniform nature of the spatial distribution of the LLEs can be exploited to construct a mechanism that can enhance chaos and, hence, the rate of chaotic mixing.

Let us consider an autonomous nonlinear dynamical system $\mathbf{x}$ of dimension n, evolving via the equations

$$\dot{\mathbf{x}} = \mathbf{F}(\mathbf{x}, \mu) \tag{2.2.1}$$

where the set of parameters μ takes values such that the trajectory shows chaotic behavior. Let $\mathbf{w}(\mathbf{x}, t)$ be the tangent vector to the trajectory at the point $\mathbf{x}$ and time t. The evolution of $\mathbf{w}$ is given by

$$\dot{\mathbf{w}} = (\mathbf{w}.\nabla)\mathbf{F} \tag{2.2.2}$$

The Lyapunov exponent of the system is defined by

$$\lambda = \lim_{t\to\infty} \frac{1}{t} \frac{\| \mathbf{w}(\mathbf{x}, t) \|}{\| \mathbf{w}(\mathbf{x}(0), 0) \|} \tag{2.2.3}$$

where $\mathbf{x}(0)$ is the value of $\mathbf{x}$ at $t = 0$ and $\| \mathbf{w} \|$ is the norm of $\mathbf{w}$. Now define the local Lyapunov exponent $\lambda(\mathbf{x})$ as

$$\lambda(\mathbf{x}) = \lim_{\triangle t\to 0} \frac{1}{\triangle t} ln \frac{\| \mathbf{w}[\mathbf{x}(t+ \triangle t), t+ \triangle t] \|}{\| \mathbf{w}[\mathbf{x}(t), t] \|} \tag{2.2.4}$$

The quantity $\lambda(\mathbf{x})$ represents the local rate of stretching at the point **x**. This is, in general, not uniform over the attractor. Note that the Lyapunov exponent λ Eq[2.2.3] is the average value of the LLEs for a long orbit or can be obtainedby averaging the LLEs over the invariant density of the attractors in dissipative systems.

A control procedure can be set up to enhance chaos and insofar as this improves mixing, the mixing rate can be increased utilizing the distribution of the LLEs. The control procedure operates in regions where the LLEs fall substantially below the average value . If, at any time, the LLE of the system falls below its average value to the point where

$$\lambda(\mathbf{x}) < (\lambda - \gamma\sigma_k) \tag{2.2.5}$$

where σ_k is the standard deviation of the distribution of LLE and γ is some chosen factor, the control is activated so that the parameter μ is changed to $\mu + sd\mu$. Here $d\mu$ is a small increment and s takes values $+1$ or -1 depending on which choice enhances the LLE. The system is allowed to evolve with the new value of the parameter as long as the condition Eq(2.2.5) is satisfied. Thereafter the parameter is reset to its original value. To decide the sign s, we can write an equation for **w** in matrix notation in the form

$$\dot{W}^T = W^T M^T, \ \dot{W} = MW \tag{2.2.6}$$

where W^T is a row vector and the matrix M^T is given by $M^T = \nabla\mathbf{F}$. The equation for the norm of W can be written as

$$\| \dot{W} \|^2 = W^T(M^T + M)W. \tag{2.2.7}$$

Thus the rate of change in the norm of W due to change in the parameter is given by

$$\begin{aligned} \triangle \| \dot{W} \|^2 &= \| \dot{W}(\mu + d\mu) \|^2 - \| \dot{W}(\mu) \|^2 \\ &\simeq W^T(M_\mu^T + M_\mu)Wd\mu \end{aligned} \tag{2.2.8}$$

where the last step is obtained by expanding to lowest order in $d\mu$ and $M_\mu = \partial M/\partial\mu$. Clearly, for the local rate of stretching to increase $\triangle \parallel W \parallel^2$ must be positive . Thus the sign s is determined to ensure that $\triangle \parallel W \parallel^2$ is positive.

It must be noted that Eq(2.2.8) is written in the lowest order in $d\mu$. Actually, the effect of the perturbation is nonlinear since when the parameter changes the entire trajectory of the system changes. Hence, the effect on the LLE can be quite different from that given by Eq(2.2.8) due to the effect of the higher nonlinear terms. In many cases the enhancement in the Lyapunov exponent turns out to be substantially higher than that expected in the linear approximation.

The procedure used above to enhance chaos and the mixing rate can be easily modified to apply to the case of discrete maps. For maps, the evolution equation Eq(2.2.1) can be written as

$$x_{t+1} = \mathbf{f}(\mathbf{x}_t, \mu) \tag{2.2.9}$$

where $\mathbf{x}_t$ are the dynamical variables at time t. The evolution of the tangent vector $\mathbf{w}$ is given by

$$w_{t+1} = (w_t.\nabla)\mathbf{f} \tag{2.2.10}$$

The control procedure is the same as above. The parameter μ is changed to $\mu + sd\mu$ when condition (2.2.5) is satisfied. To decide the sign s we can write Eq(2.2.10) in matrix form as

$$W_{t+1} = MW_t \tag{2.2.11}$$

where $M^T = \nabla f$. The equation for the norm of W is

$$\parallel W_{t+1} \parallel^2 = W_t^T M^T M W_t \tag{2.2.12}$$

Thus the rate of change in the norm of W due to change in the parameter is given by

$$\triangle \parallel W \parallel^2 = \parallel W_{t+1}(\mu + d\mu) \parallel^2 - \parallel W_{t+1}(\mu) \parallel^2 \quad (2.2.13)$$

$$= W_t^T (M^T M_\mu + M_\mu^T M) W_t d\mu \quad (2.2.14)$$

where the last step is obtained by expanding to lowest order in $d\mu$ and $M_\mu = \partial M/\partial\mu$. For control to enhance chaos and rate of mixing, the sign s for the parameter change $d\mu$ must be such that $\triangle \parallel W_{t+1} \parallel^2$ is positive.

Briefly, one can enhance the average rate of stretching by introducing a small parameter perturbation which enhances the LLE whenever the system trajectory visits a region where the LLEs take values much smaller than their average value.

2.3 Enhancing chaos by periodic and quasi-periodic perturbation

Weak periodic perturbation has been used to suppress chaos in dynamical systems. However, Weak periodic or quasi-periodic perturbation can also be used to induce chaos in non-chaotic parameter ranges of chaotic maps, or to enhance the already existing chaotic state. If the perturbation is large enough then the system goes to chaotic state in a easier way.

Transition of periodic state to chaotic attractor under weak periodic perturbation is highly dependent on the local dynamics. Chaos is more likely to occur near bifurcation points. Different kinds of bifurcations lead to different routes to chaotic transition. Two dimensional chaotic maps can be expressed under periodic perturbation

$$x_{n+1} = f(x_n, y_n, \mu) + \varepsilon \cos(2\pi\omega n) \quad (2.3.1)$$

$$y_{n+1} = g(x_n, y_n, \mu)$$

where ε is the amplitude of perturbation and ω is the frequency of the signal. The perturbed map with period-p perturbation can be equivalently described by a set of p equations

$$\begin{aligned} x_{pn+i} &= f(x_{pn+i-1}, y_{pn+i-1}, \mu) + \varepsilon \cos(2\pi\omega n) \\ y_{pn+i} &= g(x_{pn+i-1}, y_{pn+i-1}, \mu) \end{aligned} \tag{2.3.2}$$

where $i = 1, 2, \ldots, p$ and $n = 0, 1, 2, \ldots$. These p maps are topologically conjugated and exhibit analogous behaviour. For period doubling bifurcation, transition of periodic orbit to chaos depends on perturbation amplitude and not on perturbation frequency. The lower period orbits gets multiplied by p and gives higher periods whereas higher periodic orbits transits to chaos. For Hopf bifurcation chaotic transition does depend on frequency of perturbation as the perturbation frequency breaks the frequency locking and hence the periodic state of the dynamical system.

The dynamics becomes more interesting as one applies quasi-periodic perturbation to periodic orbits. For very weak perturbation low period attractors become quasi-periodic or torus attractors. As the perturbation gets stronger torus attractors goes through fractalization and become strange non-chaotic attractors (SNA) (11; 12). With perturbation amplitude being large the dynamics of the system can oscillate between chaotic and SNA which for sufficiently large amplitude becomes uniformly chaotic. In period doubling bifurcation SNA undergoes a crises and becomes chaotic whereas for Hopf bifurcation there is a direct transition from SNA to chaotic attractor without any crisis. Quasi-periodic perturbation enacts band merging of separate chaotic attractor and hence generating robust chaos.

2.4 Enhancing chaos via time delay feedback

A a natural yet nontrivial question for anti-control of chaos is whether one can make an arbitrarily given system chaotic or enhance the existing chaos of a chaotic system by using small controls. A positive answer can be given by showing that any given discrete-time autonomous system of finite dimensionality, which can even be originally stable provided that it has a bounded Jacobian, can be driven to be chaotic by using small-amplitude state feedback controls (13; 14). However this effec-

tive anti-control method utilizes a full state feedback control, which may not be desirable in some applications. Therefore, one may sometimes resort to finding different methodologies as stated earlier.

A system with time delay is inherently infinite dimensional, so it is known to be able to produce complicated dynamics such as bifurcation and chaos, even in a very simple first-order system. In particular, chaotic behaviors are observed to exist in some delay-differential equations due to their associated difference equations (15; 16). As a generalization one can approximate relationship between an nth-order stable linear differential equation with a time-delay feedback and a suitable discrete map. This, in turn, suggests a small-amplitude time-delay feedback method for anti-control of chaos in an nth-order stable linear or nonlinear differential equation.

We consider an nth-order single-input single-output (SISO) linear time-invariant (LTI) system described by the following differential equation:

$$y^{(n)}(t) + \alpha_{n-1}y^{(n-1)}(t) + \ldots + \alpha_1 y^{(1)}(t) + \alpha_0 y(t) = \beta_0 u(t) \tag{2.4.1}$$

where $u(t)$ and $y(t)$ are the input and output of the system, respectively, $\{\alpha_j\}_{j=0}^{n-1}$ and β_0 are constatnts with $\alpha_0\beta_0 \neq 0$. The uncontrolled system (2.4.1) , with $u(t) = 0$ therein, is therefore stable in the sense that $\mathbf{z}(t) \to \mathbf{0}$ as $t \to \infty$, where

$$\mathbf{z}(t) = [z_1, z_2, \ldots, z_n]^T = [y, y^{(1)}, \ldots, y^{(n-1)}]^T$$

time delay feedback can be designed of the form

$$u(t) = w(y(t - \tau)) \tag{2.4.2}$$

where w is a continuous function and $\tau > 0$ is the delay time, satisfying

$$|u(t)| \leqslant \varepsilon, \ \forall t \geqslant 0 \tag{2.4.3}$$

for a prespecified amplitude $\varepsilon > 0$, such that the output $y(t)$ of the system is chaotic in a rigorous mathematical sense.

Eq(2.4.1) can be recast in the following n-dimensional state-space form:

$$\dot{\mathbf{z}} = A_c\mathbf{z} + \beta_0\, \mathbf{b}_c u \tag{2.4.4}$$

where A_c and b_c are in the controllable canonical form, namely,

$$A_c = \begin{pmatrix} 0 & 1 & 0 & \cdots & 0 \\ 0 & 0 & 1 & \cdots & 0 \\ \vdots & \vdots & \ddots & \ddots & \vdots \\ 0 & 0 & 0 & \cdots & 1 \\ -\alpha_0 & -\alpha_1 & -\alpha_2 & \cdots & -\alpha_{n-1} \end{pmatrix}$$

$$b_c = \begin{pmatrix} 0 \\ 0 \\ \vdots \\ 0 \\ 1 \end{pmatrix}$$

Clearly, the functional form for the map w is not unique. One simple choice is

$$u(t) = w(y(t-\tau)) = \varepsilon \sin(\sigma y(t-\tau)) \tag{2.4.5}$$

which satisfies the requirement (2.4.3) . If the map

$$y_{k+1} = \frac{\beta_0}{\alpha_0} w(y_k) = \varepsilon_0 \sin(\sigma y_k) \tag{2.4.6}$$

is chaotic, then we may expect that the time-delay feedback Eq.(2.4.5) can make the output y(t) of system (2.4.1) chaotic provided that the delay time is sufficiently large and $\varepsilon_0 = \dfrac{\varepsilon\beta_0}{\alpha_0}$.

For any fixed nonzero value of ε_0 , the origin is a globally asymptotically stable fixed point of this map, if $0 < \sigma < \varepsilon_0$. As σ increases and passes through the value of ε_0 , the map (2.4.6) has one pair of nonzero conjugate, locally asymptotically stable, fixed points: $y^+ > 0$ and $y^- = y^+ < 0$. As σ continues to increase, each nonzero fixed point undergoes a cascade of period-doubling bifurcations leading to chaos. With an even further increase of the bifurcation parameter value σ, each chaotic attractor increases in size. Finally, at a critical value $\bar{\sigma} = \frac{\pi}{\varepsilon_0}$, the two chaotic attractors merge into one, still chaotic but with an almost unchanged size proportional to ε_0.

2.4.1 Enhancing chaos in stable nonlinear system

Let us consider a nonlinear SISO continuous-time synamical system of the form

$$y^{(n)} = \phi(\mathbf{y}) + \psi(y)u \tag{2.4.7}$$

where ϕ and ψ are smooth nonlinear functions of $\mathbf{y} = [y, \dot{y}, \ldots, y^{(n-1)}]^T$. Let $\mathbf{y} = \mathbf{0}$ is an asymptotically stable fixed point of the uncontrolled system [with $u(t) = 0$ therein] and $\psi(0) \neq 0$. There are two ways to transfer this system into a linear system of the form (2.4.1).

Approximate linearization approach

A typical way of system linearization is approximate linearization. Suppose that the maximum amplitude of the control input $u(t)$ of system (2.4.7) is $\varepsilon > 0$. Since the system is stable about its zero fixed point by assumption, for a sufficiently small ε, there exists a small neighborhood Ω of the origin such that if $\mathbf{y}(0)$ is in Ω then $\mathbf{y}(t)$ stays in Ω forever. In this small neighborhood Ω, Eq.(2.4.7) can be represented by its linearization, evaluated at the origin, as follows:

$$y^{(n)} + \alpha_{n-1}y^{(n-1)} + \ldots + \alpha_1 y^{(1)} + \alpha_0 y = \psi_0 u(t) \tag{2.4.8}$$

where

$$\alpha_i = -\frac{\partial \phi(y)}{\partial y^{(i)}}|_{y=0},\ i = 0, 1, \ldots, n-1$$

It follows from the analysis of the last section that the small amplitude time-delay feedback

$$u(t) = w(y(t-\tau)) = \varepsilon \sin(\sigma y(t-\tau)) \tag{2.4.9}$$

can make $y(t)$ chaotic within the bounded region .

Exact linearization approach

Another method for system linearization is the feedback exact linearization. Let the controller be

$$u = \frac{1}{\psi(y)}(-\phi(y) - \gamma_{n-1}y^{(n-1)} - \cdots - \gamma_1 y^{(1)} - \gamma_0 y + v(t)) \tag{2.4.10}$$

where $\{\gamma_i\}_{i=0}^{n-1}$ are n constants with $\gamma_0 \neq 0$, such that

$$s^n + \gamma_{n-1}s^{n-1} + \cdots + \gamma_1 s + \gamma_0 \tag{2.4.11}$$

is a Hurwitz stable polynomial. Then Eq.(2.4.7) becomes

$$y^{(n)} + \gamma_{n-1}y^{(n-1)} + \cdots + \gamma_1 y^{(1)} + \gamma_0 y = v(t) \tag{2.4.12}$$

which is in the same form as (2.4.1). Therefore, controller (2.4.11) with $v(t) = \varepsilon \sin(\sigma y(t-\tau))$ can make system (2.4.7) chaotic.

Clearly, controller (2.4.11) actually cancels the nonlinearity of the original system and renders it linear. As it stands, the controller is more complicated than the given system, which is physically impractical in most cases. However,the main purpose is simply to reformat the given system into an appropriate form by this ‘controller’ and then to create chaos by using the time-delayed feedback controller $v(t)$ in the suitable form. Therefore, if we consider the u in (2.4.11) as a coordinate transform rather than a controller, while the controller is v , then this approach is reasonable for anti-control of chaos.

2.5 Discussion

In applications of feedback control schemes it is generally necessary to measure the system state variables, thereby generating a control signal that is then applied to the signal to an accessible system parameter. In practice, it is relatively difficult to implement this class of schemes to some high-speed systems such as chaotic circuits and fast optoelectrical systems. Compared to feedback control techniques for inducing and enhancing chaotic behavior of nonlinear systems of small time scales, nonfeedback methods have the advantages of speed and flexibility. Furthermore, on-line monitoring and processing are not required. Of course, in order to find appropriate signals for control, the nature of the system dynamics must be understood a priori. This class of control approaches is suitable for cases in which no real-time data or only highly limited measurements of the system state are available. A number of studies on nonfeedback anticontrol of chaos have been carried out with various control signals, for example, constant perturbations (17; 18) , weak noise signals (19; 20) , and weak periodic perturbations (21; 23) . A few studies have also demonstrated the dual function of suppressing and inducing chaos with applications of weak periodic perturbations to the nonlinear dynamic systems (24; 25).

The non-feedback methods proposed in literature used control signals that had been assigned somewhat intuitively or arbitrarily rather than sought out based on optimization of the signal parameters. In the case of using a periodic perturbation as the control signal, with the frequency fixed a priori, the amplitude for achieving the control goal can be found by simply varying its value within a range. The signal determined in this manner is not optimal in any sense. Additionally, for a multi parameter control signal, the method for determining the proper combination of the parameter values is a problem. The approach used in finding a signal able to work efficiently in achieving a preset control target seems significant.

Power consumption for chaotification of non-chaotic orbits can be optimized by various methods (26). In use of periodic signals of high harmonics, the power of the optimized signal is not necessarily reduced with an increasing number of harmonic modes, while using quasi-periodic signals of multiple incommensurable frequencies has the trend of reducing signal power with an increase

in the number of the modes. However, the Genetic Algorithm-optimized signals of low-mode are favorable for their simplicity and effectiveness.

Although the differences are within one order of magnitude, the power of a quasi-periodic signal needed to reach the control goal is generally lower than a periodic one with the same number of modes.

To destabilize an ordered fixed-point or periodic state, the power required for chaotification varies relatively slowly at comparatively lower LLEs but increases drastically as the preset value of the target LLE reaches a certain critical value. In the case of enhancing the chaoticity of a chaotic state, required control power increases as preset target LLE increases. Unlike that for triggering chaos in ordered states however, here is no obvious slow-varying region appearing in the correlation of minimum power versus target LLE. Performing chaotification with GA-optimized weak perturbations demonstrates that further enhancing the chaoticity of a chaotic state needs more control power than triggering chaos in an ordered state, either fixed-point or periodic state.

Bibliography

[1] E. Ott, C. Grebogi, and J. A. Yorke, Phys. Rev. Lett. **64**, 1196 (1990) .

[2] L. M. Pecora and T. L. Caroll, Phys. Rev. Lett. **64**, 821 (1990) ; Phys. Rev. A **44**, 2374 (1990) .

[3] J. M. Ottino, *The Kinematics of Mixing, Stretching, Chaos and Transport* Cambridge University Press, Cambridge, (1989) .

[4] Y . Wang, J. Singer, and H. H. Bau, J. Fluid Mechanics **237**, 479 (1992).

[5] J. M. Ottino, Sci. Am. **260** (1) , 40 (1989) ; J. M. Ottino, F. J. Muzzio, M. Tjahjadi, J. G. Franjione, S. C. Jana, and H. A. Kusch, Science **253**, 755 (1995) ; J. M. Ottino, G. Metcalfe, and

S. C. Jana, in *Proceedings of the Second Experimental Chaos Conference* (World Scientific, Singapore, 1995) , pp. 3-20.

[6] E. Ott and M. Spano, Phys. Today **48** (5) , 34 (1995) , and references therein.

[7] M. A. Woo, W. G. Stevenson, D. K. Moser, R. M. Harper, and R. Trelease, Am. Heart J. **123**, 704 (1992) ; A. Goldberger, Ann. Biomed. Eng. **18**, 195 (1990) .

[8] S. J. Schiff, K. Jenger, D. H. Duong, T. Chang, M. L. Spano, and W. L. Ditto, Nature **370**, 615 1994 .

[9] W. Yang, M. Ding, A. Mandell, and E. Ott, Phys. Rev. E **51**, 102 1995 .

[10] H. D. I. Abarbanel, R. Brown, J. J. Sidorowich, and L. Sh. Tsimring, Rev. Mod. Phys. **65**, 1331 (1993) .

[11] Grebogi, C., Ott, E., Pelikan, S. and Yorke, J. A. Physica D **13**, 261268 (1984).

[12] Nishikawa, T. and Kaneko, K. Phys. Rev. E **54**, 61146124 (1996).

[13] X. F. Wang and G. Chen, IEEE Trans. Circuits Syst., I: Fundam. Theory Appl. **47**, 410415 (2000).

[14] X. F. Wang and G. Chen, Int. J. Bifurcation Chaos Appl. Sci. Eng. **10**, 549570 (2000).

[15] K. Ikeda and K. Matsumoto, Physica D **29**, 223235 (1987).

[16] P. Celka, Physica D **104**, 127147 (1997) .

[17] Xu and S. R. Bishop, Phys. Rev. E **54**, 6940 (1996) .

[18] Z. M. Ge and T. N. Lin, J. Sound Vib. **259**,585 (2003).

[19] D. J. Christini and J. J. Collins, Phys. Rev. Lett. **75**, 2782 (1995).

[20] D. J. Christini and J. J. Collins, Phys. Rev. E **52**, 5806 (1995).

[21] S. T. Vohra, L. Fabiny, and F. Bucholtz, Phys. Rev. Lett. **75**,65 (1995).

[22] R. Chacón, Phys. Rev. Lett. **86**, 1737(2001).

[23] I. B. Schwartz, I. Triandaf, R. Meucci, and T. W. Carr, Phys. Rev. E **66**, 026213 (2002).

[24] Y. Lei, W. Xu, Y. Xu, and T. Fang, Chaos, Solitons Fractals **21**, 1175 (2004).

[25] Q. S. Li and R. Zhu, Chaos, Solitons Fractals 1**9**, 195 (2004).

[26] C. Y. Soong and W. T. Huang, Phys. Rev. E **75**, 036206 (2007).

Chapter 3

Control end enhancement of chaos through memory dependent feedback

Chaos is omnipresent in nature. For a nonlinear system of more than two degrees of freedom, it is chaotic whenever its evolution sensitively depends on the initial conditions. Mathematically, there must be an infinite number of unstable periodic orbits embedded in the underlying chaotic set and the dynamics in the chaotic attractor is ergodic. Physically, chaos can be found in nonlinear optics (laser), chemistry (Belouzov-Zhabotinski reaction), electronics (Chua-Matsumoto circuit), fluid dynamics (Rayleigh-Bénard convention), meteorology, solar system, and the heart and brain of living organisms. As chaos is intrinsically unpredictable and its trajectories diverge exponentially in the course of time evolution, controlling chaos is apparently of great interest and importance. Ott, Grebogi and Yorke (1) proposed a successful technique to control low-dimensional chaos. The basic idea is to take advantage of the sensitivity to small disturbances of chaotic systems to stabilize the system in the neighborhood of a desirable unstable periodic orbit naturally embedded in the chaotic motion. Pyragas (2) proposed a more efficient method which makes use of a time-delayed feedback to some dynamical variables of the system. Control of spatiotemporal chaos in partial differential equations was also considered (3; 4). As an alternative method of control, chaos synchronization was pioneered by Pecora and Carroll (5). The theory and application of chaotic synchronization has

been extensively studied (6) in various research directions, for instance, electronic circuits, laser experiment, secure communication, biological and chemical systems, shock capturing (7), and wake turbulence (8). Synchronous stability was studied by Pecora and Carroll (9) and Yang et al. (10). The stability of the synchronous state can be understood from the eigenvalue distribution of the coupling matrix of a nonlinear system.

As opposed to the mainstream of controlling or eliminating chaos in dynamical systems, anti-control of chaos, which means creating chaos when it is beneficial, has also attracted some growing interest. This is due to some desirable features of chaos in some time- and/or energy-critical applications where chaos can provide a system designer with a variety of special properties, richness of flexibility, and a cornucopia of opportunities. Recent studies have shown that chaos can be used for a variety of applications such as information transmission with high power efficiency (11), generating truly random numbers (12; 13), and novel spread spectrum (14), ultrawide bandwidth (15; 16), and optical (17) communication schemes. Examples also include liquid mixing, human brain and heartbeat regulations (18; 19). It is expected that chaos research in engineering will eventually reach the point where it will lead to improved and refined design procedures, enabling a designer to design a system to be either chaotic or nonchaotic at will.

Numerous methods have been suggested to control and enhance chaos of the dynamical systems. OGY method is one of the most popular methods to control chaos. However this method has some drawbacks as it deals with the Poincaré map. The method can stabilize only those periodic orbits whose maximal Lyapunov exponent is small compared to the reciprocal of the time interval between parameter changes. A more effective method of time continuous control was suggested later by Pyragas. Pyragas suggested two alternative methods of chaos control. Chaotic systems can be stabilized to a periodic orbit by the application of small additive external drive. As an alternative method it was suggested that this external drive can also be taken as a delay feedback.

Here we present an different method for chaos control. In general delay feedback depends on the difference in state variable in different times. It is applied with some external coupling. We show this delay can also be memory dependent to control chaos.

Poincaré maps and stroboscopic maps are quite useful tool to analyse chaos. Chaos is possible only in systems which have dimensions more than two. However stroboscopic mapping enables us to make a time slice of equal interval and the effective system is a discrete time dynamical system of lower dimension. This low dimensional discrete systems retains the main aspects of chaotic dynamics and are easier to analyse. For this reason analysis of this discrete time dynamical systems or maps are very important in the study of nonlinear dynamics.

In the fourth chapter we discuss the effect of memory dependent feedback in one dimensional quadratic maps. In discrete system delay feedback is translated as n-step memory dependent feedback. We are interested in one step memory dependent feedback as maps are generated by stroboscopic mapping and the step width can be adjusted by estimation of return time of the system. In the fourth chapter we show the change of dynamics in logistic map with the application of memory dependent modulation of the system parameter r. The system not only becomes periodic for a larger range of the system parameter it also depicts richer dynamical structures. Crises and period incrementing bifurcation are among the new features in the bifurcation diagram. A period five window emerge through intermittent transition which lead to non-standard type-I intermittency with exponent 0 [in stead of the standard exponent $-\frac{1}{2}$]

In chapter five we look into the interplay of chaotic and periodic dynamics in view of memory modulated control. Under memory modulation one dimensional system effectively behave as a two dimensional one. We take logistic map again as our model system but control the system such that one part of the dynamics always remain chaotic; the other part move from periodic to chaotic state. The most interesting dynamics of this system is period adding bifurcation. This scenario is also different from border collision dynamics which is very common underlying dynamics for period adding bifurcation. We show an elaborate analysis to explain period adding bifurcation and a a universal period adding exponent δ is calculated for quadratic map. We apply the negative algorithm to the system to show that the same formulation with positive feedback can enhance chaos to a great extent.

We move to higher dimensional discrete system in chapter Six. In ecology, there are some species whose population goes from generation to generation, for example, gypsy moths or any of many other species of insects. These topics are usually modelled by difference equations, iteration map or discrete dynamical systems. Instead of looking to stroboscopic maps of higher dimensional chaotic systems we take the discrete version of famous Lotka-Volterra population model. We examined the fixed point dynamics and bifurcations of this dynamical system and investigate the effect of memory dependent feedback on it. The system undergoes Neimark-Sacker bifurcation, fold bifurcation and flip bifurcation as different stability relation is satisfied between the system parameters. Interestingly we find such memory dependent feedback can lead to period adding dynamics also in two dimensions. Further investigation confirms our speculation that interplay of chaos with periodic dynamics leads to period incrementing bifurcation.

As a natural progress we move from two dimensional discrete dynamical systems to three dimensional continuous time system. In chapter seven we analyse the system with time continuous delay feedback. Keeping analogy with memory dependent feedback we modify the parameter with memory dependent continuous time delay. We first apply it to damped harmonic oscillator and show that the damped oscillator can be modified to a limit cycle with memory delay feedback. Limit cycle only occurs for some discrete values of delay. This effective method is applied to three dimensional rössler system and we analyse and predict the values of the delay needed for the formation of limit cycle.

Bibliography

[1] E. Ott, C. Grebogi, and J. A. Yorke, Phys. Rev. Lett. **64**, 1196 (1990).

[2] K. Pyragas, Phys. Lett. A **170**, 421 (1992).

[3] G. Hu and K. He, Phys. Rev. Lett. **71**, 3794(1993).

[4] S. Boccaletti, G. Grebogi, Y. C. Lai, H. Mancini, and D. Maza, Phys. Rep. **329**, 103197 (2000).

[5] L. M. Pecora and T. L. Carroll, Phys. Rev. Lett. **64**, 821 (1990).

[6] L. M. Pecora, T. L. Carroll, G. A. Johnson, D. J. Mar, and J. F. Heagy, Chaos **7**, 520 (1997).

[7] G.W. Wei, Phys. Rev. Lett. **86**, 3542 (2001).

[8] B. S.V. Patnaik and G.W. Wei, Phys. Rev. Lett. **88**, 054502 (2002)

[9] L. M. Pecora and T. L. Carroll, Phys. Rev. Lett. **80**, 2109 (1998).

[10] J. Yang, G. Hu, and J. Xiao, Phys. Rev. Lett. **80**, 496 (1998).

[11] V. Dronov, M. R. Hendrey, T. M. Antonsen, Jr., and E. Ott,Chaos **14**, 30 (2004).

[12] J. T. Gleeson, Appl. Phys. Lett. **81**, 1949 (2002).

[13] T. Stojanovski, J. Pihl, and L. Kocarev, IEEE Trans. Circuits Syst. I **48**, 382 (2001).

[14] M. P. Kennedy, G. Kolumba n, G. Kis, and Z. Ja ko , IEEE Trans. Circuits Syst. I **47**, 1702 (2000).

[15] N. F. Rulkov, M. M. Sushchik, L. S. Tsimring, and A. R. Volkovskii, IEEE Trans. Circuits Syst. I **48**, 1436 (2001).

[16] G. M. Maggio, N. F. Rulkov, and L. Reggiani, IEEE Trans. Circuits Syst. I **48**, 1424 (2001).

[17] G. D. VanWiggeren and R. Roy, Science **279**, 1198 (1998).

[18] S. J. Schiff, K. Jerger, D. H. Duong, T. Chang, M. L. Spano, and W. L. Ditto, “Controlling chaos in the brain,” Nature London **370**, 615620 (1994) .

[19] M. E. Brandt and G. Chen, IEEE Trans. Circuits Syst., I: Fundam. Theory Appl. **44**, 10311034 (1997).

Chapter 4

The phase–modulated logistic map

4.1 Introduction

Chaos control has been an ongoing theme of research in nonlinear dynamics since the early 1990's (1) when it was realized that small parametric perturbations could stabilize periodic orbits embedded within chaotic attractors. The sensitivity to initial conditions that is characteristic of chaotic dynamics can, depending on the circumstance, be either wanted or an undesirable dynamical feature. Thus both theoretical and practical considerations have been responsible for the interest in the area, resulting in a large body of work on different methods for ensuring a desired (usually periodic or stable) motion in a nonlinear dynamical system. A variety of techniques have been employed, many of which have been realized in practical applications; several of these have been reviewed in detail (2).

One of the most powerful methods for chaos control is through feedback stabilization (3). It is widely recognized that feedback, as a general principle, is an efficient means of ensuring stable behaviour; this has been widely used (4; 5). (Linear feedback systems have also been studied in the context of dynamical systems theory (6).) Another common technique for controlling chaotic motion is by modulation of the system parameters: by judiciously varying parameters, it is often possible to drive a nonlinear system into a desired dynamical state (2).

By combining both delayed feedback and parametric modulation it is possible to devise versatile methods for chaos control and in the present paper we study a simple dynamical system wherein both these aspects are included. This is the logistic map where the nonlinearity parameter is modulated by linear feedback,

$$x_{n+1} = (\alpha + \varepsilon \, \mathrm{sgn}(x_{n-1} - x_n))x_n(1 - x_n). \tag{4.1.1}$$

The quantity $\phi = \mathrm{sgn}(x_{n-1} - x_n)$, termed an instantaneous phase (7), has been used in previous work to detect order within chaotic dynamics (7; 8; 9). The use of time–delays has the well–known effect of increasing the dimensionality of the problem. Thus, the above driven dynamical system can be rewritten as a two–dimensional map,

$$x_{n+1} = (\alpha + \varepsilon \, \mathrm{sgn}(y_n - x_n))x_n(1 - x_n) \tag{4.1.2}$$

$$y_{n+1} = x_n, \tag{4.1.3}$$

although, as we argue in Section 4.2 below, the dynamics is effectively 1–dimensional, and the system can be more easily studied as the mapping(s)

$$x_{n+1} = f_{\pm}(x_n) \equiv (\alpha \pm \varepsilon)x_n(1 - x_n) \tag{4.1.4}$$

with f_+ or f_- being chosen dynamically, namely in a history–dependent manner. This makes the dynamics *non Abelian*, since $f_+(f_-(x)) \neq f_-(f_+(x))$ for nonzero ε.

This non–Abelian character gives rise to novel dynamical behaviour which is described in detail in Section 4.3 of this paper. In the following Section 4.2, we first discuss the model, and argue that analysis in terms of 1-dimensional maps can adequately explain the different dynamical regimes. We obtain a phase diagram of the system under variation of the parameters α and ε; its main features can be understood through a generalization of the kneading theory for unimodal maps developed by Metropolis, Stein and Stein (MSS) (10). This theory, which takes into account itinerary shifts

between maps f_+ and f_-, is presented in Section 4.4. Because of the history dependent nature of the dynamics, the intermittency found near specific tangent bifurcations exhibits nonstandard scaling exponents, the origin of which lies in the details of the dynamics (11), as discussed in Section 4.4.

One additional motivation for studying the specific form of modulation which switches the nonlinearity parameter between different values is that it can be implemented quite easily using digital outputs (6; 12). In the concluding Section 4.5 we outline a simple circuit-based experimental realization of the proposed feedback modulation. There have been related earlier studies of the logistic map where similar parametric modulation has been studied both for periodic (14; 13) and stochastic (13) drives, although without feedback or delay. The analysis used here could find application for other similar forms of driving, and we conclude this paper with a discussion and summary of our results.

4.2 Phase–diagram under modulation

We examine the behaviour of typical orbits of Eqs. (4.1.2-4.1.3) as a function of the parameters. The dynamics for the case of $\varepsilon = 0$, when the system reduces to the unmodulated logistic map is well understood. For small ε, the nonlinearity parameter undergoes slight variation, and the dynamics can be either periodic or chaotic, depending on the parameters α and ε. The motion is confined to the unit square, but since the Jacobian corresponding to Eqs. (4.1.2-4.1.3) is singular, the resulting orbits are further constrained. For all orbits with period $\neq 1$, there is an eigenvalue which is zero; thus they are either a set of points (when the orbit is periodic), or lie on *one dimensional* curves in the (x, y) plane when the orbit is chaotic. This feature of the motion, which is particular to the form of modulation that we have considered here, allows for considerable simplification in the analysis.

In order to get a global view of the dynamics of the modulated system, we obtain the phase–diagram of the different dynamical regimes as a function of $3 \leq \alpha \leq 4$, and for $\varepsilon > 0$. In a single logistic map, the motion can become unbounded when the nonlinearity parameter α exceeds 4, and

in order to focus on dynamics that remains globally bounded, we rescale Eq. (1) as

$$x_{n+1} = [\alpha + (4 - \alpha)\varepsilon' \mathrm{sgn}(x_{n-1} - x_n)]x_n(1 - x_n), \tag{4.2.1}$$

and examine the parameter regime $0 \leq \varepsilon' \leq 1$. The dynamics can be bounded even for $\varepsilon' > 1$, depending on the value of α, but we do not consider this region here. The case of negative ε is also not studied here since this latter system has additional features that are consequent on initial state sensitivity; this will be discussed elsewhere.

Of the two Lyapunov exponents, one is zero, while the other is given by

$$\lambda = \lim_{N\to\infty} \frac{1}{N} \sum_{i=1}^{N} \ln |\frac{\partial x_{i+1}}{\partial x_i}|. \tag{4.2.2}$$

Shown in Fig. 4.1 are regions in the (α, ε') plane where the motion is periodic or chaotic. The regions of stability in Fig. 4.1 have the characteristic and canonical shape of "swallows" or "shrimps" for two–parameter maps as has been discussed earlier (15; 16; 17). The organization of such stable regions is around superstable orbits (17) as will be discussed in the next section.

The magnetization (7; 8) is the average phase along the trajectory,

$$\Phi = \lim_{N\to\infty} \frac{1}{N} \sum_{i=1}^{N} \mathrm{sgn}(x_{i-1} - x_i), \tag{4.2.3}$$

which, in the present case, is also the averaged, scaled driving. This quantity, which has been examined in a number of recent studies (7; 8), has been shown to provide a different measure of detecting ordering in chaotic dynamics (7; 9). Together, λ and Φ provide a classification of the different types of motion in nonlinear dynamical systems (7; 18). Fig. 4.2 displays the different phases, namely regions where the magnetization takes distinct values. Note that for periodic motion of period M or for chaotic motion in M bands, the magnetization takes values $\Phi = K/M$, where $K(< M)$ depends on the itinerary of the orbit.

Along the axis $\varepsilon' = 0$, the system degenerates to the single logistic mapping $x \to \alpha x(1 - x) \equiv$

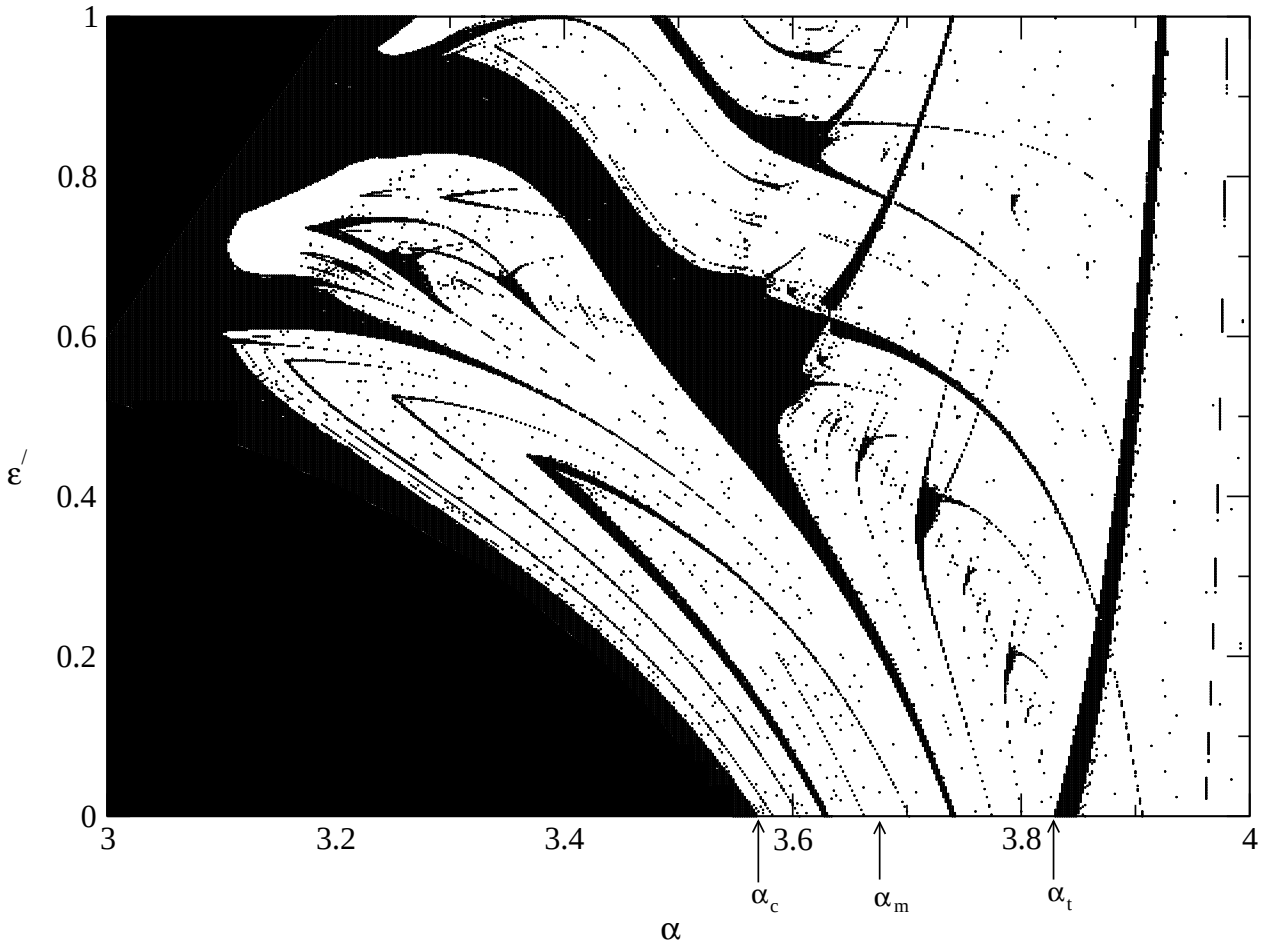

Figure 4.1: Regions of chaotic dynamics (white) and periodic motion (black) in the α, ε' plane. The system reduces to the single logistic map on the line $\varepsilon' = 0$. There can be stable motion for particular α above $\varepsilon' = 1$ but we do not consider this here.

$f(x)$, for which the entire phenomenology, both qualitative and quantitative, are very well known (19). We recall some of the main features that are of relevance in the modulated system.

- The cascade of period–doubling bifurcations accumulates at $\alpha_c = 3.569946\ldots$.
- A band–merging crisis occurs at $\alpha_m = 3.678857..$, when there is a transition from a two–band attractor to a single–band chaotic attractor. This occurs when

$$f^{(3)}(\frac{1}{2}) = 1 - \frac{1}{\alpha} \tag{4.2.4}$$

  namely when the unstable period–1 orbit coincides with the third iterate of the map maximum, and signifies the end of the inverse period–doubling cascade.
- All the purely odd periods occur in the range $\alpha_m < \alpha \leq \alpha_t \equiv \sqrt{8} + 1$, the period–3 orbit being created at the tangent bifurcation that occurs at α_t. Below α_m, the periodic windows have periods of the form $k = m \cdot 2^j\, j = 1, 2\ldots$.
- In each periodic window of period k, there is a superstable orbit, namely one where the map maximum is an element:

$$f^{(k)}(\frac{1}{2}) = \frac{1}{2}.$$

  The itineraries of the superstable periodic orbits can be described symbolically through the U-sequences (10), which encodes the iterates of the map maximum falling on the right (R) or left (L) of the maximum.
- Below $\alpha = \alpha_m$ the magnetization Φ is zero while above α_m, in each periodic window of period k the magnetization takes a value that is an integral multiple of $\frac{1}{k}$. The fractional nature of the magnetization is unrelated to the nature of the dynamics (which can be chaotic or periodic), but relates to the geometry of the attractor, the number of distinct bands on which the dynamics occurs and the order in which they are visited.

With modulation, many of the above features are preserved, at least for small ε'. Thus periodic windows continue into the phase plane for $\varepsilon' > 0$, although as can be seen in Fig. 4.1, there are

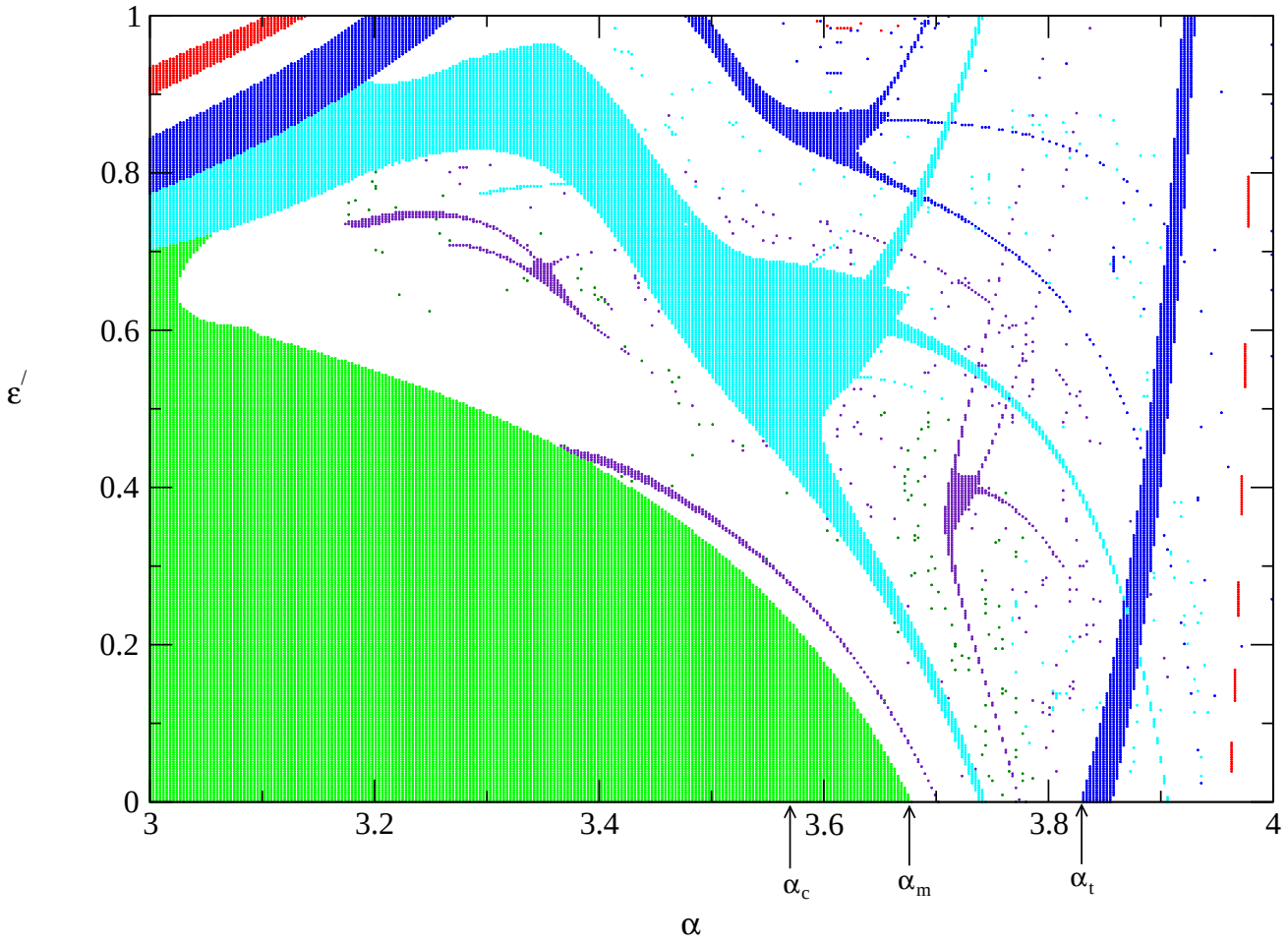

Figure 4.2: The magnetization Φ in different regions of the phase plane. When the motion is periodic with period k or in k bands, the magnetization takes the value j/k. Regions with different values of k are coloured distinctly.

many mergings of the periodic windows, as well as the creation of entirely new regimes of stability. Most notable (see Fig. 4.2) is the creation of a large stable zone of period 5, as also, in comparison to the width of the periodic windows at $\varepsilon' = 0$, large zones of other odd periods.

Thus one major effect of the modulation appears to be the *stabilization* of periodic dynamics. Application of an appropriate amplitude of modulation can stabilize any desired period (within a range), and thus this is a technique for the control of chaos. Our interest here, however, extends to the actual nature of the dynamics and the bifurcations that occur in the system. These are discussed in Section 4.3.4.

4.2.1 One–dimensional analysis

Since one eigenvalue of the Jacobian is always zero, it is possible to analyse the present system in terms of the theory of 1–d unimodal maps. Note that each orbit of Eq. (1),

$$O : x_0, x_1, x_2, \ldots, x_i, \ldots \tag{4.2.5}$$

can be additionally characterised by the 'sign-sequence', namely the sequence of the signs (±) of the modulation,

$$\mathcal{S} : s_0, s_1, s_2, \ldots, s_i, \ldots \quad s_i = \mathrm{sgn}(x_{i-1} - x_i) \tag{4.2.6}$$

A periodic orbit will necessarily have a periodic sign sequence. The correspondence is not 1-1: many different orbits could have the same sign sequence, and chaotic orbits can also have periodic sign sequences. Not all sign sequences will be permitted since the map f is unimodal (see below).

Keeping in mind the limit $\varepsilon \to 0$, where the symbolic dynamics for all orbits is well known, it is useful to consider the present system as the effective "1–dimensional" mapping

$$x_{n+1} = f_{\pm}(x_n), \tag{4.2.7}$$

with the functions $f_+(x) = (\alpha+\varepsilon)x(1-x)$ or $f_-(x) = (\alpha-\varepsilon)x(1-x)$ chosen according to the permitted sign-sequence. The advantage of using this 1-dimensional description is that the allowed periodic orbits of the dynamical system, Eq. (1) can be well understood and characterized by extending the kneading theory for unimodal maps (10) to take into account the switching between the two different logistic maps. This is discussed in the next section.

4.3 Periodic Orbits and Crises

When the dynamics is governed by a single map f, a point x is said to belong to a periodic orbit or cycle of period k if

$$f^{(k)}(x) = x. \tag{4.3.1}$$

In the present system, this needs to be generalized since the maps f_- and f_+ are applied in a history dependent manner. Thus a periodic orbit of period k is determined by the condition

$$f^{(k)}_{s_1 \ldots s_k}(x) \equiv \; f_{s_k}(f^{(k-1)}_{s_1 \ldots s_{k-1}}(x)) = x \tag{4.3.2}$$

where s_i is either + or -, and the sequence $s_1 s_2 \ldots s_k$ corresponds to a *valid* or *permitted* sign sequence, namely a dynamically consistent sequence of the maps $f_\pm$. The orbit is stable if, for a neighbourhood of x_1, the condition

$$\mu = \left| \prod_{i=1}^{k} f'_{s_i}(x_i) \right| < 1 \tag{4.3.3}$$

is satisfied.

One class of valid itineraries can be deduced from the MSS (10) sequences. Along the line ε'=0, the system reduces to a single logistic mapping, and the sequence of periodic orbits that occur can be completely described. For unimodal maps, periodic orbits where the map maximum is an element of the cycle can be symbolically coded by whether iterates fall to the left (L) or right (R) of the maximal point (C). MSS described how to construct the symbolic itinerary of any periodic orbits lying between any other pair of periodic orbits by a simple algebraic procedure (10). An extension of this algebra which takes into account the dynamical alternation between the maps f_- and f_+ is applicable here. As can be seen from Fig. 1, periodic dynamics on the line $\varepsilon' = 0$ carries over for nonzero (but small) ε'. To use the MSS procedure here, it should be recognsied that since the dynamics uses different maps based on the itinerary, the symbols R, L and C carry subscripts + or - to denote which of the maps is used to determine the subsequent dynamics. Thus, the period–3 orbit, which has the U-sequence

$$\text{RL} \tag{4.3.4}$$

on the line $\varepsilon' = 0$ now necessarily becomes

$$\text{C\_R\_L}_+. \tag{4.3.5}$$

For a single unimodal map, there are distinct period–5 orbits with MSS sequences RLR^2 and RL^2R respectively. These generalize to $C_+R_-L_+R_-R_-$ and $C_+R_-L_+L_-R_-$. Listed in Table I are all possible U-sequences that can exist for periodic orbits with period less than 9 between these two period–5 orbits (cf. the Table in Ref. (10) Appendix). Similiar kind of constructions can be carried out for higher period orbits with additional rules governing permitted symbol (R,L,C) and valid sign sequences (20).

In addition to the generalizations of the MSS sequences, new sequences become possible which do not arise in the unimodal system. Such "non-MSS" periodic orbits naturally do not extend from the $\varepsilon' = 0$ line and can therefore be identified easily from Fig. 4.1. We discuss these briefly below.

4.3.1 Superstable and doubly superstable orbits

An orbit of period k is termed *superstable* if (cf. Eq. (4.3.3)) $\mu = 0$ and corresponds to parameter values (α, ε') for which the critical point of the map belongs to the orbit. In the present system, the critical point of either f_- or f_+ being part of the cycle makes the orbit superstable. This imposes one constraint, and thus the condition for superstability is met along a line (namely codimension 1) in the (α-ε') parameter plane. Such lines are denoted M_j^k in Fig. 4.3, the subscript j indexing the several different such orbits that can occur. It can happen that the critical point of both maps are elements of the cycle, in which case we term the orbit *doubly superstable* (DSS). Such orbits occur at isolated points (of codimension 2) in the phase plane, and play a crucial role in determining the nature of the MSS and non MSS sequences that occur in this system.

This is most easily illustrated by the example of period 5 orbits.

4.3.2 Example: Orbits of period $k = 5$

The logistic map has 3 MSS itineraries for period 5 orbits at different values of α. These are, respectively RLR^2, RL^2R and RL^3.

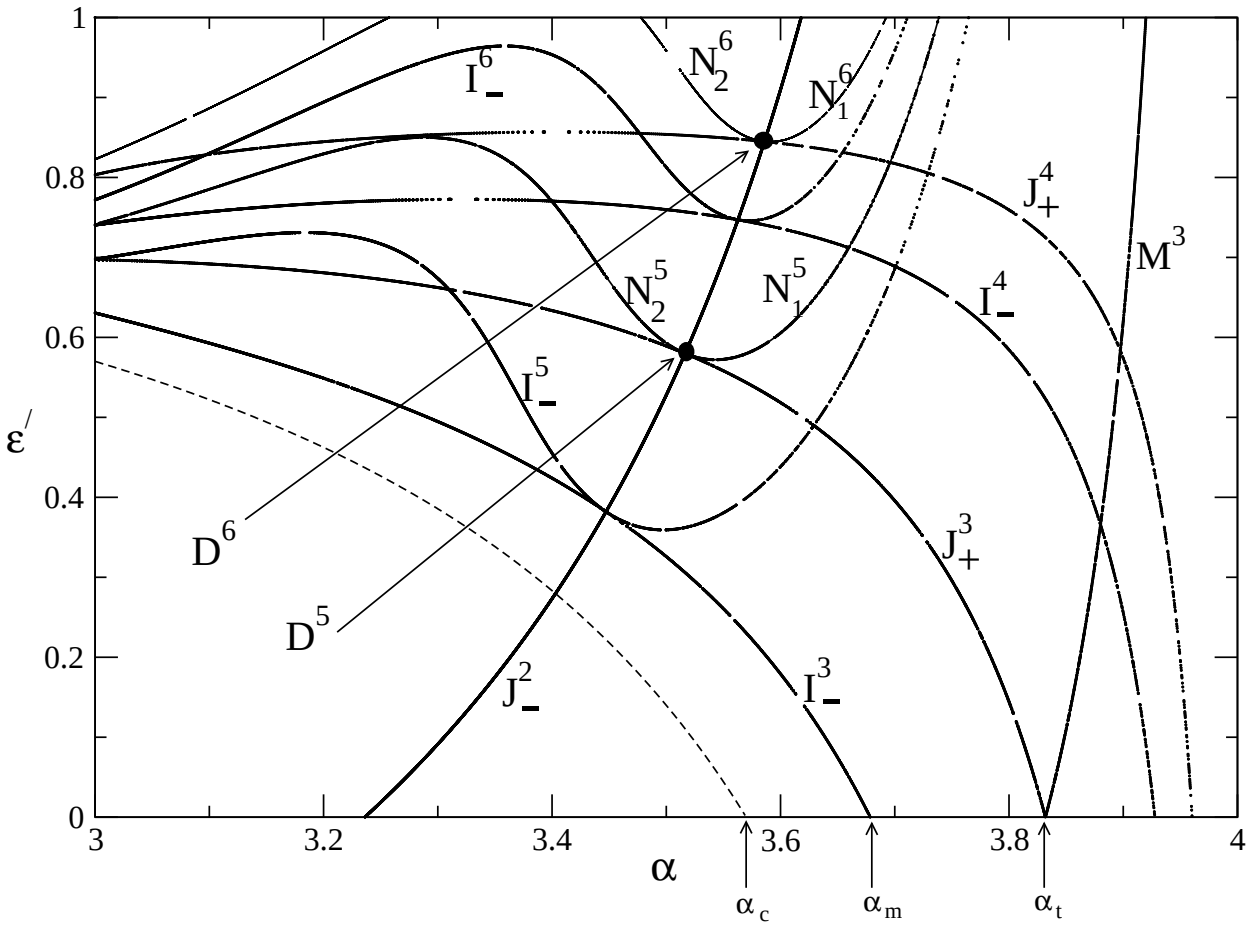

Figure 4.3: Lines of organization of the superstable orbits in parameter space. Only the low order periodic orbits are shown: some of these have been described in the text and in Table II. A few DSS points are also indicated, as are the crisis lines I_-^3 and I_-^5.

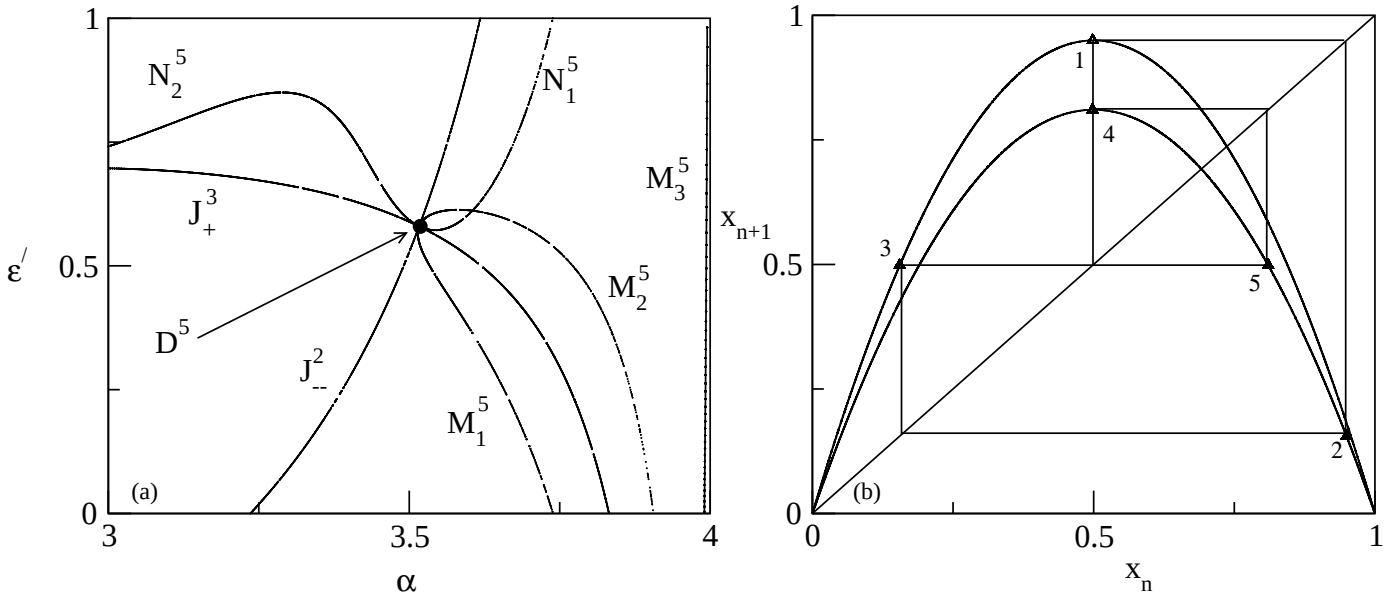

Figure 4.4: (a) Locus of points in the parameter plane relevant to the period–5 orbits, namely M_j^5, $j = 1, 3$, N_k^5, $k = 1, 2$,D^5, and J_+^3, J_-^2. (b) The orbit diagram for the doubly superstable period 5 orbit, showing the itinerary of points and the hopping between the two maps f_+ and f_-.

In the modulated system these become (see Fig. 4.4(a))

$$M_1^5 \ : \ \mathrm{C_+R_-L_+R_-R_-} \tag{4.3.6}$$

$$M_2^5 \ : \ \mathrm{C_+R_-L_+L_-R_-} \tag{4.3.7}$$

$$M_3^5 \ : \ \mathrm{C_+R_-L_+L_-L_+} \tag{4.3.8}$$

and they start on the lower boundary of the phase plane, namely at $\varepsilon' = 0$. With increasing ε', the locus of M_1^5 and M_2^5 move toward each other (as a function of α, ε') and merge at (3.52,0.58), giving rise to a DSS orbit (Fig. 4.4(b)) with itinerary

$$D^5 : \mathrm{C_+R_-L_+C_-R_-C_+}. \tag{4.3.9}$$

In effect, the DSS orbit is created when the fourth iterates of C_+, namely R_- in M_1^5 or L_- in M_2^5 move gradually to the left and right respectively, until the points coincide at C_-.

Non-MSS sequences are created out of the DSS point, D^5 by the reverse process, namely by permitting the C_+ element to go either to the right or the left, thereby making the itineraries (Fig. 4.4(a))

$$N_1^5 \quad : \quad L_+R_-L_+C_-R_- \equiv C_-R_-L_+R_-L_+ \tag{4.3.10}$$

$$N_2^5 \quad : \quad R_+R_-L_+C_-R_- \equiv C_-R_-R_+R_-L_+ \tag{4.3.11}$$

Note that both these would be forbidden in a single unimodal map (in MSS notation, they are RLRL and R^3L).

For the DSS point, D^5, we observe that

$$C_- \to R_- \to C_+ \tag{4.3.12}$$

which gives the condition

$$f_-(f_-(\frac{1}{2})) = \frac{1}{2} \tag{4.3.13}$$

which is satisfied along the *joining* line, J_-^2. A family of DSS points (see Fig. 4.3) occur at the intersections of this and lines J_+^k which connect C_+ and C_- in k steps, as for instance J_+^3,

$$C_+ \to R_- \to L_+ \to C_- \tag{4.3.14}$$

which is specified by

$$f_+(f_-(f_+(\frac{1}{2}))) = \frac{1}{2}. \tag{4.3.15}$$

DSS points of order $m + k$ occur at intersections of either J_+^k and J_-^m lines (see Fig. 4.3 for the point D^6) or J_+^m and J_-^k.

4.3.3 Crisis lines

The band–merging crisis in the logistic map occurs when the third iterate of the map maximum coincides with the unstable period–1 fixed point; see Eq. (4.2.4). Since the maps f_- and f_+ are used

in a history dependent manner for nonzero ε', this generalizes to

$$f_+(f_-(f_+(\frac{1}{2}))) = 1 - \frac{1}{\alpha - \varepsilon} \tag{4.3.16}$$

and this condition is satisfied along the line denoted I^3_- in the (α, ε') plane; see Fig. 4.3. (The subscript - is indicative of the fact that the third iterate of the maximum coincides with the fixed point of the map f_-, and the letter I denotes that this is an interior crisis line). In an analogous manner, one can have other crisis lines, say when the pth iterate of the map maximum coincides with the period–1 fixed point of the map f_-,

$$I^p_\pm : f^{(p)}_{s_1 s_2 \ldots s_p}(\frac{1}{2}) = 1 - \frac{1}{\alpha \pm \varepsilon}, \tag{4.3.17}$$

$s_1 \ldots s_p$ being a valid sign sequence as discussed earlier.

The crisis lines and the DSS points, along with the MSS and non MSS orbits organize the dynamical behaviour of this system. Table II lists (the lowest order) lines that form the skeleton of the pattern present in the parameter space.

4.3.4 Period incrementing bifurcations

At fixed α, when ε' increases, the nonlinearity parameter in the map f_+, namely $\alpha + \varepsilon$, increases, while that in f_- decreases. These can lead to competing effects of stabilization through f_- and destabilization through f_+. Chaotic motion can only occur if $\alpha + \varepsilon$ exceeds α_c= 3.569946...(the lower left region of stability in Fig. 4.1 is defined by $\alpha + \varepsilon \leq \alpha_c$) but whether the dynamics is stable or unstable will depend crucially on the history of a given orbit. In the present system we have not observed any dependence of the asymptotic dynamics on the initial conditions.

An expanded view of the region $3.1 \leq \alpha \leq 3.7$, $0 \leq \varepsilon' \leq 0.6$ is shown in Fig. 4.5. The prominent feature of this region of the phase diagram is the merging of periodic windows at nonzero ε'. At these window mergings, there is a *period incrementing* bifurcation: the windows that merge correspond to periods $p-1$ and p, where p is odd. Since all odd periods in the logistic map (namely

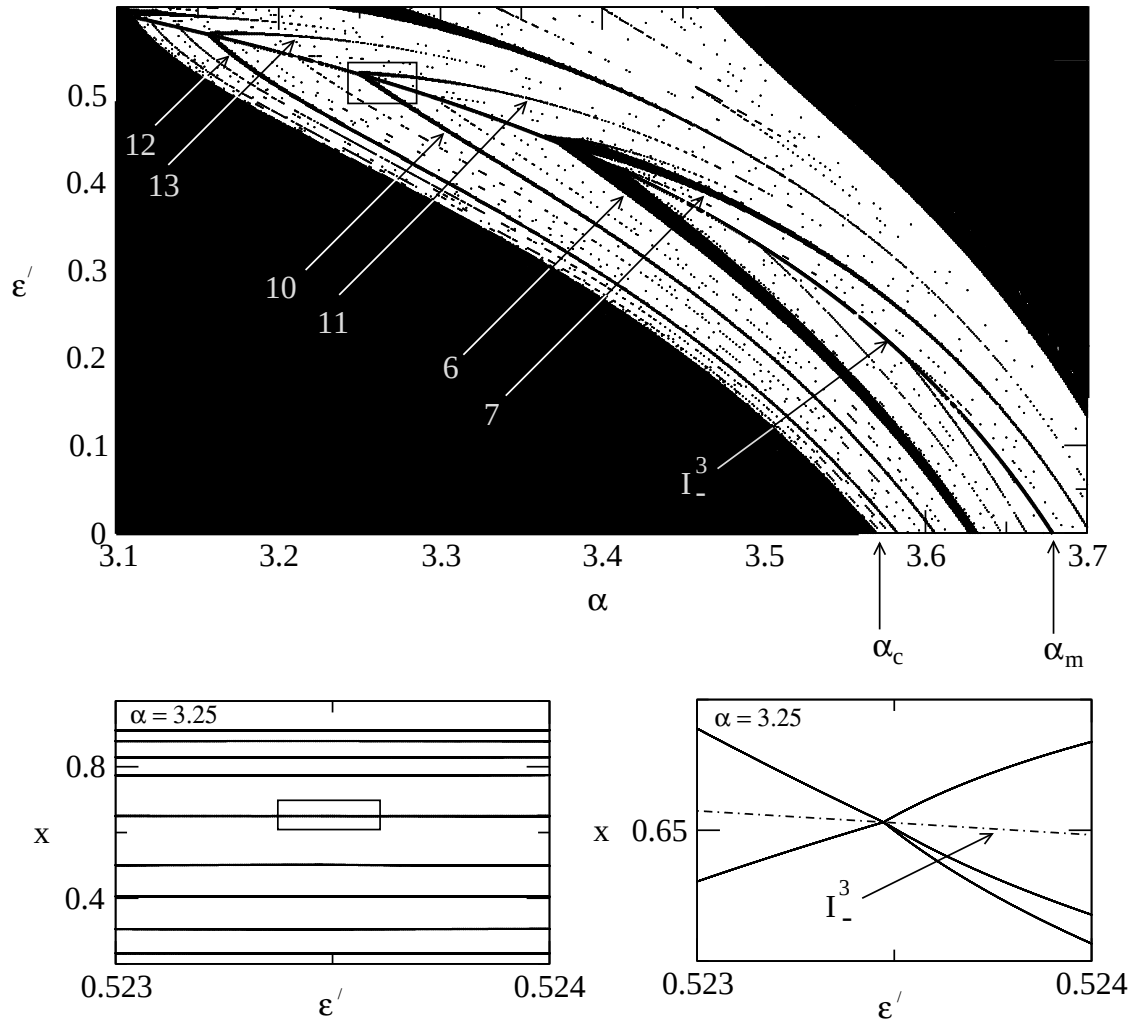

Figure 4.5: Period incrementing-bifurcations (a) Expanded view of a portion of Fig. 4.1 showing the merging of periodic windows that cause period incrementing bifurcations, (b) Bifurcation diagram for period 10 to 11 bifurcation (region inside the box in (a)) and (c) Blow up of the region inside the box in (b) showing the period incrementing phenomena.

on the line $\varepsilon' = 0$) can occur only to the right of α_m, and even periods which are of the form $2^m \cdot j$ can occur only to the left, the respective windows in the modulated system originate to the right and left of α_m. The merging of these periodic windows occurs, as can be seen, along the crisis line I_-^3. In each of the windows, there are superstable orbits and for these we can write the condition for the period incrementing bifurcation as the simultaneous occurrence of

$$f_+(f_-(f_+(\frac{1}{2}))) = 1 - \frac{1}{\alpha - \varepsilon} \tag{4.3.18}$$

and

$$f^{(p)}_{s_1 \ldots s_p}(\frac{1}{2}) = \frac{1}{2} \tag{4.3.19}$$

where the valid sign sequence is such that $s_1 s_2 s_3 \equiv +-+$. At the merging of the period 6 and period 7 orbits, for instance, the respective orbit itineraries are

$$\mathrm{C_+R_-L_+R_-R_+R_-} \quad \text{and} \quad \mathrm{C_+R_-L_+R_-R_-R_+R_-}. \tag{4.3.20}$$

In Table III the extended MSS sequence for orbits in a period–incrementing bifurcation are listed. This is for the main families of windows (with periods less than or equal to 9) that merge along the line I_-^3. There are many families of period incrementing bifurcations, all of which occur along the lines I_-^m for different m; I_-^3 and I_-^5 are indicated on Fig. 4.3. At the merging of the period p and $p+1$ windows on the crisis line I_-^m, the superstable orbit has the condition

$$f^{(p-m)}_{s_{m+1} \ldots s_p}(1 - \frac{1}{\alpha - \varepsilon}) = \frac{1}{2}. \tag{4.3.21}$$

The reverse bifurcation, where the period decreases by one, can also occur, and does so by the reverse of the above mechanism. It should be mentioned that this bifurcation differs from period–adding (21) as well as from the border–collision bifurcation (22). In the latter case, there is a transition from period p to period m, all points of the periodic orbits collapsing onto an stable periodic point at the border (22). The period incrementing (or decrementing) bifurcation is *locally*

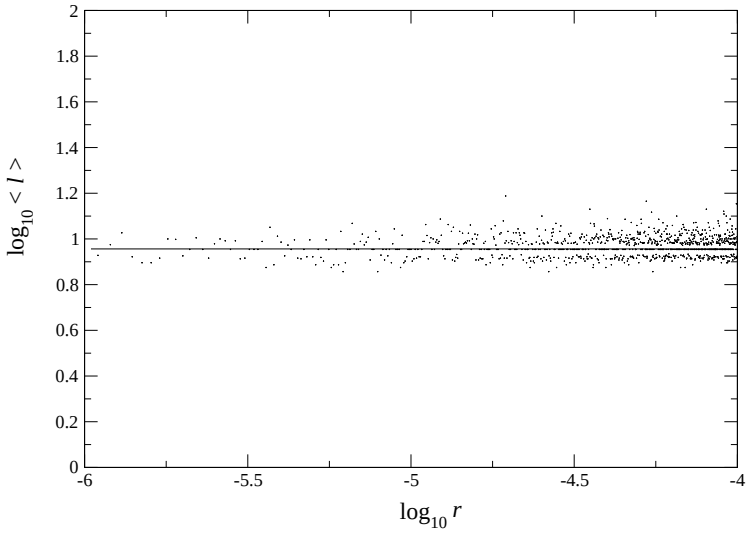

Figure 4.6: Log-log plot of $\langle \ell \rangle$ versus r. The straight line passing through the data has slope $\theta \approx 0.08$.

similar to border–collision in that two elements of the periodic orbit become three (or vice–versa),

$$\mathrm{R\_R_+} \rightarrow \mathrm{R\_R\_R_+}.$$

4.4 Intermittency

Here we examine the characteristics of the intermittent dynamics that is observed in this model. As has been noted already, compositions of the maps are non–Abelian since $f_+(f_-(x)) \neq f_-(f_+(x))$ and this can give rise to nonstandard dynamical behaviour. We study the tangent bifurcation that gives rise to the period 5 orbit at α=3.25 though our observations hold for other ranges of parameter values as well.

At $\alpha = 3.25$, one regime of intermittent motion occurs for ε' just below $\varepsilon'_c \approx 0.8225\ldots$ while above ε'_c, there is a period–5 cycle. A characteristic of any intermittent dynamics is the scaling behaviour of the average length of the laminar region, ℓ, namely

$$\langle \ell \rangle \sim \frac{1}{r^\theta} \tag{4.4.1}$$

where $r \equiv (\varepsilon_c' - \varepsilon')$ is the parametric distance from the tangent bifurcation. For the standard Type I intermittency (23) the exponent $\theta = \frac{1}{2}$.

For the present system we find that the average length of the laminar region does not vary with r, and instead (see Fig. 4.6) follows the law

$$\langle \ell \rangle \propto \frac{1}{r^{\mu}}, \qquad \mu \simeq 0. \tag{4.4.2}$$

Such lack of sensitivity to the tangent bifurcation is unexpected, especially since the return map for the dynamics appears to have the canonical Type-I form in the neighborhood of the tangency, namely

$$y_{n+1} = y_n + p{y_n}^2 + qr \tag{4.4.3}$$

where p and q are constants and y_n is the distance of x_n from the tangency point. This map can be viewed as the differential equation

$$\frac{dy}{d\ell} = ay^2 + r \tag{4.4.4}$$

and the length of the laminar region is the number of steps (ℓ) taken to cross the bottleneck near $y = 0$ and is found from

$$\ell = \int d\ell = \int_{-\Delta}^{c} \frac{dy}{ay^2 + r} \tag{4.4.5}$$

$$= \sqrt{\frac{1}{ar}}[\tan^{-1}\sqrt{\frac{a}{r}}c + \tan^{-1}\sqrt{\frac{a}{r}}\Delta] \tag{4.4.6}$$

If r is sufficiently small and $\Delta > 0$, with $\sqrt{\frac{a}{r}} \gg 1$, then

$$\ell = \frac{\pi}{\sqrt{ar}} \tag{4.4.7}$$

This argument can be generalized to the case of the nonlinear term in Eq. (6.0.1) being $y_n^{2\delta}$, when one obtains $\ell \propto r^{-(1-\frac{1}{2\delta})}$.

This reasoning breaks down in the present case due to the nature of the detailed dynamics and

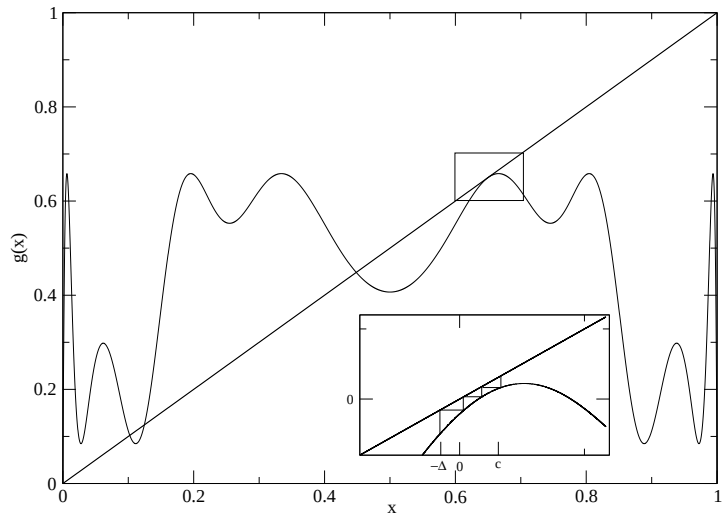

Figure 4.7: Plot of the composite function $g(x)$ (see Eq. (4.4.8) on the interval. The single point of tangency here is at $x = 0.6514$; the other points can be seen by examining other composite functions which can be obtained from $g(x)$ by cyclic permutation of the constituent $f_{\pm}$. Shown in the inset is the canonical form in the vicinity of the tangency with a schematic trajectory that passes through the tangency bottleneck from Δ to c.

indeed to the unique features of the history dependent dynamics. When considering a period k tangent bifurcation in a single mapping, f, it is obvious that the graph of $f^k(x)$ will be tangent to the diagonal at the k points of the periodic orbit. Here, on the other hand, each of the k points is a point of tangency for a *different* effective mapping. Thus, in the 5-cycle for α=3.25 and $\varepsilon' = \varepsilon'_c$, the five points of tangency each arise from a different history and are points of tangency for five separate maps, each of which is a combination of 2 f_+'s and 3 f_-'s. One of these, namely

$$g(x) = f_-(f_+(f_-(f_+(f_-(x))))). \tag{4.4.8}$$

is shown in Fig. 4.7. As can be seen, there is a single point of tangency; note that the overall dynamics is *not* governed by $g(x)$ except in the neighborhood of the tangency since the dynamics is history dependent. Nevertheless, as we argue, the effect of residual fixed points in such combination maps crucially affects details such as the reinjection probabilities and thereby the scaling exponents. (It should be clarified that tangency occurs simultaneously in the five different combination maps at

$\varepsilon' = \varepsilon'_c$.) The fixed point adjoining the tangency point in Fig. 4.7 can have stable cycles around it. This is different from the intermittency in the standard logistic map.

In the standard Type-I intermittency scenario, for ε' below ε'_c the periodic orbit is itself unstable, but points cycle through the neighborhoods of the fixed points in a consistent manner: iterates leave the neighbourhood of one point of tangency to go to a second and then to a third and so on. In the composed map $f^{(k)}$, points traverse the tangency bottleneck in its entirety.

This need not be the case when the orbit reinjects into the tangency bottlenecks at different points, as was first noted by Kim, Kwon, Lee and Lee (11). If there is a distribution $\mathrm{P}(y_{\mathrm{in}})$ of points y_{in}, where the trajectory enters the neighbourhood of the tangency then the laminar length would have to be

$$\langle \ell \rangle = \int_{-\Delta}^{c} \ell(y_{\mathrm{in}}, c) P(y_{\mathrm{in}}) dy_{\mathrm{in}} \tag{4.4.9}$$

with the normalization

$$\int_{-\Delta}^{c} P(y_{\mathrm{in}}) dy_{\mathrm{in}} = 1 \tag{4.4.10}$$

For every y_{in}, Eq. (7.1.1) yields

$$\ell(y_{\mathrm{in}}, c) = \frac{1}{\sqrt{ar}} [\tan^{-1} \sqrt{\frac{a}{r}} c - \tan^{-1} \sqrt{\frac{a}{r}} y_{\mathrm{in}}] \tag{4.4.11}$$

With a flat distribution $P(y_{\mathrm{in}}) = \frac{1}{c+\Delta}$, we have from Eq. (7.1.3)

$$\begin{aligned} \langle \ell \rangle &= \frac{1}{2a(c+\Delta)} \ln \left[\frac{r + ac^2}{r + a\Delta^2} \right] \\ &+ \frac{\Delta}{\sqrt{ar}(c+\Delta)} [\tan^{-1} \sqrt{\frac{a}{r}} c + \tan^{-1} \sqrt{\frac{a}{r}} \Delta]. \end{aligned} \tag{4.4.12}$$

In Eq. (4.4.12), for small r, the first term on the right has no r dependence. When reinjection occurs from below, $\Delta > 0$ and the tangency bottleneck is fully traversed; the second term gives the leading

$r^{-1/2}$ dependence. However, when Δ is negative, then the two inverse tangents cancel each other for very small r (each is equal to $\pi/2$ in magnitude, but the signs differ) resulting in behaviour observed in Fig. 4.6.

From Figs. 1 and 2 it is apparent that period–5 intermittency occurs over a range of α around 3.25. We have observed that for higher α the exponent θ eventually becomes $\frac{1}{2}$, the crossover being controlled by the details of the reinjection dynamics (24). The nonstandard reinjection behaviour is not maintained at all tangent bifurcations in this system; the exponents can revert to the standard Type I case upon variation of parameters.

4.5 Discussion and summary

The parametrically modulated logistic map has been extensively studied for specific forms of driving which include the cases of periodic (26), quasiperiodic (27; 28), as well as stochastic forcing (29). The different dynamical phenomena that obtain in the logistic map are modified under the influence of driving in interesting ways, leading frequently to novel bifurcations and attractors with unexpected dynamical and structural properties (30). Our choice of delayed feedback modulation makes the dynamics non–Abelian, and since the choice of (noninvertible) map depends on the history, the system is deterministic and also non-Markovian. These new features give rise to novel dynamical features.

The zones of dynamical stability have a complicated and hierarchically organized structure. These are well–understood, having the canonical shape for stability regions in two–parameter mappings (15; 16; 17). Our main method for understanding the organization of periodic orbits in such driven systems is through a generalization of the results of MSS (10) for the organization of periodic orbits in unimodal maps, and we show how this scheme helps in rationalizing the different periodic orbits that can arise in the driven system. In addition, we find that there are non–MSS periodic orbits, namely the stabilization of “forbidden” itineraries for periodic orbits which results from the choice of delayed feedback forcing.

There also appear to be regions in parameter space where there are no periodic windows and

our preliminary studies of the dynamics here have revealed a peculiar characteristic of the attendant tangent bifurcations. Although they are still of Type-I, owing to the interplay of two different mappings in determining the dynamics, the actual mechanics of the re-injection process (11) leads to the scaling exponents being quite different from $\frac{1}{2}$.

Dynamics in the case of additive forcing,

$$x_{n+1} = \alpha x_n(1 - x_n) + \varepsilon \, \mathrm{sgn}(x_{n-1} - x_n), \tag{4.5.1}$$

is also very similar. The phase diagram in this latter case (not shown here) has identical features—period incrementing bifurcations, stable shrimp regions, superstable and doubly–superstable orbits, etc. Much of the analysis presented for multiplicative modulation carries over. Note, however, that an analogy can be made between Eq. (4.5.1) and a globally coupled map lattice with delay–feedback, as has been done in other cases of driven dynamical systems (32). Interest in the study of emergent ordered collective behaviour in coupled maps with delays (33) suggests that this analogy should be explored systematically.

Delay feedback modulation of the form studied here can be easily realized in experiment, particularly in electronic circuits (34). There are standard procedures for introducing time-delays, and the Schmitt trigger provides a simple means of comparing two signals to obtain a digital output with the desired phase (12); this can then be fed back into the system as in Eq. (4.5.1).

However, the motivation to examine driven dynamical systems arises from a variety of contexts. For instance, modulated mappings arise in specific population models, particularly when migration or other exogenous effects need to be considered (25). Indeed, there have been studies of a variety of forced systems with dichotomous (13; 14) drives, as well as more complicated driving terms (31). The analysis presented in this paper can be extended to other pulsed driven systems. In particular, quasiperiodic driving can be approached systematically as the limit of periodic pulses of increasing period; studies of such modulation are presently under way (20).

Bibliography

[1] E. Ott, C. Grebogi and J. A. Yorke, Phys. Rev. Lett. **64**, 1196 (1990).

[2] For a review, see T. Shinbrot, Adv. Phys. **44**, 73 (1995); *Handbook of Chaos Control : Foundations and Applications*, edited by H. G. Schuster (Wiley-VCH, Berlin, 1999).

[3] K. Pyragas, Phys. Lett. A **170**, 421 (1992).

[4] R. Roy, T. W. Murphy Jr, T. D. Maier, Z. Gills and E. R. Hunt, Phys. Rev. Lett. **68**, 1259 (1992).

[5] B. Peng, V. Petrov and K. Showalter, J. Phys. Chem., **95**, 4957 (1991)

[6] N. Gershenfeld and G. Grinstein, Phys. Rev. Lett. **74**, 5024 (1995).

[7] W. Wang, Z. Liu and B. Hu, Phys. Rev. Lett. **84**, 2610 (2000).

[8] B. Hu and Z. Liu, Phys. Rev. E **62**, 2114 (2000).

[9] M. D. Shrimali and R. Ramaswamy, Phys. Lett. A **295**, 273 (2002).

[10] M. Metropolis, M. L. Stein and P. R. Stein, J. Combin. Theor. **15**, 25 (1973).

[11] C. M. Kim, O. J. Kwon, E. K. Lee and H. Lee Phys. Rev. Lett. **73**, 525 (1994).

[12] N. Gershenfeld, *The physics of information technology*, (Cambridge University Press, UK, 2000).

[13] J. Rössler, M. Kiwi, B. Hess and M. Markus, Phys. Rev. A **39**, 5954 (1989).

[14] Sanju and V. S. Varma, Phys. Rev. E **48**, 1670 (1993).

[15] J. A. C. Gallas, Phys. Rev. Lett. **70**, 2714 (1993); Physica A **202**, 196 (1994).

[16] E. Barreto, B. R. Hunt, C. Grebogi and J. A. Yorke, Phys. Rev. Lett. **78**, 4561 (1997).

[17] B. R. Hunt, J. A. C. Gallas, C. Grebogi and J. A. Yorke, Physica D **129**, 35 (1999).

[18] C. Grebogi, E. Ott, F. Romeiras and J. A. Yorke, Phys. Rev. A **36**, 5365 (1987).

[19] W. de Melo and S. van Strien, *One-dimensional dynamics*, (Springer Verlag, Berlin, 1993)

[20] A. Nandi and R. Ramaswamy, to be published.

[21] S. Coombes and A. H. Osbaldestin, Phys. Rev. E **62**, 4057 (2000).

[22] H. E. Nusse, E. Ott and J. A. Yorke Phys. Rev. E **49**, 1073 (1994).

[23] Y. Pomeau and P. Manneville, Comm. Math. Phys. **74**, 189 (1980).

[24] D. Datta, J. K. Bhattacharjee, A. Nandi, and R. Ramaswamy, in *Proceedings of the National Conference on Nonlinear Science and Dynamics*, IIT Kharagpur, 2003.

[25] S. Parthasarathy and S. Sinha, Phys. Rev. E **51**, 6239 (1995).

[26] Sanju and V. S Verma, Int J. Bifurcation and Chaos **13**, 2699 (2003).

[27] J. F. Heagy and S. M. Hammel, Physica D **70**, 140 (1994).

[28] A. Prasad, V. Mehra, and R. Ramaswamy, Phys. Rev. E **57**, 1576 (1998).

[29] S. J. Linz and M. Lücke, Phys. Rev. A **33**, 2694 (1986).

[30] C. Toniolo, A. Provenzale and E. A. Spiegel, Phys. Rev. E **66**, 066209 (2002).

[31] A. Venkatesan, S. Parthasarathy and M. Lakshmanan, Chaos, Solitons & Fractals **18**, 891 (2003).

[32] A. Parravano and M. G. Cosenza, Phys. Rev. E **58**, 1665 (1998)

[33] S. Lepri, Phys. Lett. A **191**, 291 (1994).

[34] A. P. Malvino, *Electronic Principles*, (Mc Graw-Hill, New York, 1999).

Table I: Extended MSS sequences for periodic orbits with period ≤ 9 between the period 5 orbits M_1^5 and M_2^5.

Period k	Itinerary	Notation
5	$R_-L_+R_-R_-$	M_1^5
9	$R_-L_+R_-R_-L_+R_-L_+R_-$	M_1^9
7	$R_-L_+R_-R_-L_+R_-$	M_1^7
9	$R_-L_+R_-R_-L_+R_-R_+R_-$	M_2^9
8	$R_-L_+R_-R_-L_+R_-R_-$	M_1^8
3	R_-L_+	M^3
6	$R_-L_+L_-R_-L_+$	M_1^6
9	$R_-L_+L_-R_-L_+R_-R_-L_+$	M_3^9
8	$R_-L_+L_-R_-L_+R_-R_-$	M_2^8
9	$R_-L_+L_-R_-L_+R_-R_+R_-$	M_4^9
7	$R_-L_+L_-R_-L_+R_-$	M_2^7
9	$R_-L_+L_-R_-L_+R_-L_+R_-$	M_5^9
8	$R_-L_+L_-R_-L_+R_-L_+$	M_3^8
5	$R_-L_+L_-R_-$	M_2^5

Table II: Notation used to describe lines in parameter space along which the phase diagram is organized. The subscripts on C, R and L indicate which map, $f_\pm$, determines the dynamics and $\mathrm{F}_\pm = 1 - \frac{1}{\alpha \pm \varepsilon}$.

M^k is indicative of superstable period k orbits which follow the MSS pattern.

$I_\pm^k$ denotes interior crisis analogues where the map maximum iterates to the period-1 point of the map $f_\pm$ in k steps.

$J_\pm^k$ orbits connect C_+ (or C_-) to C_- (or C_+) in k steps.

N^k orbits are superstable period k orbits which are Non-MSS.

	Itinerary	Orbit equation
I_-^3	$\mathrm{C}_+\mathrm{R}_-\mathrm{L}_+\mathrm{F}_-$	$f_+(f_-(f_+(\frac{1}{2}))) = (1 - \frac{1}{\alpha-\varepsilon})$
I_-^5	$\mathrm{C}_-\mathrm{R}_-\mathrm{R}_+\mathrm{R}_-\mathrm{L}_+\mathrm{R}_-\mathrm{F}_-$	$f_+(f_-(f_+(f_-(f_-(\frac{1}{2}))))) = 1 - \frac{1}{\alpha-\varepsilon}$
I_-^6	$\mathrm{C}_-\mathrm{R}_-\mathrm{R}_+\mathrm{R}_-\mathrm{L}_+\mathrm{L}_-\mathrm{R}_-\mathrm{F}_-$	$f_-(f_+(f_-(f_+(f_-(f_-(\frac{1}{2})))))) = 1 - \frac{1}{\alpha-\varepsilon}$
I_-^4	$\mathrm{C}_-\mathrm{R}_-\mathrm{L}_+\mathrm{L}_-\mathrm{R}_-\mathrm{F}_-$	$f_-(f_+(f_-(f_+(\frac{1}{2})))) = 1 - \frac{1}{\alpha-\varepsilon}$
J_+^3	$\mathrm{C}_+\mathrm{R}_-\mathrm{L}_+\mathrm{C}_-$	$f_+(f_-(f_+(\frac{1}{2}))) = \frac{1}{2}$
J_+^4	$\mathrm{C}_+\mathrm{R}_-\mathrm{L}_+\mathrm{L}_-\mathrm{C}_-$	$f_-(f_+(f_-(f_+(\frac{1}{2})))) = \frac{1}{2}$
J_-^2	$\mathrm{C}_-\mathrm{R}_-\mathrm{C}_+$	$f_-(f_-(\frac{1}{2})) = \frac{1}{2}$
M^3	$\mathrm{C}_-\mathrm{R}_-\mathrm{L}_+$	$f_+(f_-(f_-(\frac{1}{2}))) = \frac{1}{2}$
N_2^5	$\mathrm{C}_-\mathrm{R}_-\mathrm{R}_+\mathrm{R}_-\mathrm{L}_+$ $\mathrm{C}_-\mathrm{R}_-\mathrm{L}_+\mathrm{R}_-\mathrm{L}_+$	$f_+(f_-(f_+(f_-(f_-(\frac{1}{2}))))) = \frac{1}{2}$
N_2^6	$\mathrm{C}_-\mathrm{R}_-\mathrm{R}_+\mathrm{R}_-\mathrm{L}_+\mathrm{L}_-$ $\mathrm{C}_-\mathrm{R}_-\mathrm{L}_+\mathrm{R}_-\mathrm{L}_+\mathrm{L}_-$	$f_-(f_+(f_-(f_+(f_-(f_-(\frac{1}{2})))))) = \frac{1}{2}$

Table III: Extended MSS sequences for periodic orbits with period ≤ 9 about the interior crisis line I_-^3. The windows for period p and $p+1$ orbits merge at the period–incrementing bifurcation; these share identical extended MSS itineraries in the first 3 and last $p-4$ positions, with the higher period orbit having an additional R_- point.

Period k	Itinerary	Notation
8	$R_-L_+R_-R_+R_-L_+R_-$	M_4^8
6	$R_-L_+R_-R_+R_-$	M_2^6
8	$R_-L_+R_-R_+R_-R_+R_-$	M_5^8
9	$R_-L_+R_-R_-R_+R_-R_+R_-$	M_6^9
7	$R_-L_+R_-R_-R_+R_-$	M_3^7
9	$R_-L_+R_-R_-R_+R_-L_+R_-$	M_7^9

Chapter 5

Period adding bifurcation in a one dimensional map

In a strikingly simple experiment(1) performed recently, a sequence of period adding bifurcations were observed. Period adding bifurcations have been seen quite frequently of late but these systems have been of the neurobiological variety (2)-(4), electrical circuits (5) and pulsing lasers(6)-(7). In the work of Colli *et al.*, it is bubble formation in a liquid which was studied. The bubbles were caused by a constant airflow into the liquid. It is the time interval x_n between consecutive bubbles which was of interest. Empirically one could write $x_{n+1} = f(x_n)$. A map was actually suggested for the process. The experiment was done as follows:

A cylindrical tube is used as the bubble column.The bubbles are issued by injecting air through a metallic nozzle submerged in a viscous fluid and the liquid is maintained at a fixed height. The nozzle is placed with its tip well below the liquid surface to avoid wall effects on the forming bubble. The nozzle is attached to a small air chamber. Air from a compressor is injected to a capacitive reservoir and a proportionating solenoid valve controlled by a PID controller sets the air flow to the chamber under the nozzle. The flow rate is measured by a flow-meter.[Fig5.1]

In order to study the influence of the pneumatic system in the bubble formation dynamics, a hose is connected from the solenoid valve to the chamber under the nozzle, keeping fixed the influence of

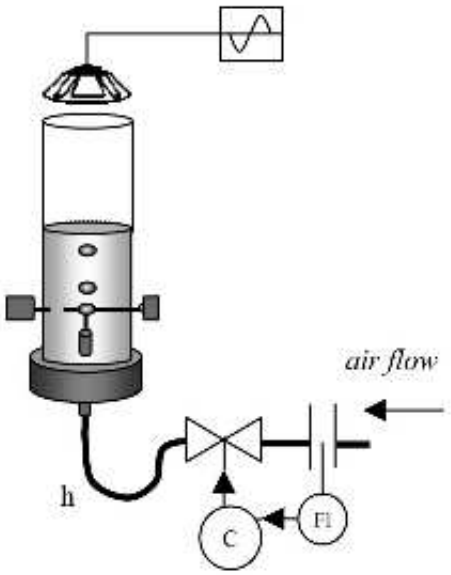

Figure 5.1: Experimental apparatus for bubble formation with the flow-meter (Fl), the controller (C) and the solenoid valve, representing the control loop of the air flow rate, and the hose (h) between the valve and the chamber under the nozzle.

the other elements of the pneumatic system. Four different hose lengths were used to see the effect of change of hose length on bubble formation. The detection system is based on a laser-photodiode with a horizontal He-Ne laser beam focused on the photodiode placed above the nozzle. The time interval between successive bubbles is measured by time circuitry inserted in a PC slot.

E. Colli looked at the time series of time intervals x_n between successive bubbles and investigated the correlation between two successive time intervals. Experimental results have shown that the sequence x_n is not necessarily constant. Stable periodic regimes of high period and chaotic regimes appeared. Period adding bifurcation was also observed for certain hose lengths with varying air flow rates.

By looking at the period adding sequence obtained in the experiment and the proposed map, we thought that it should be possible to explore this sequence in a different fashion. Considering the fact that a long pipe length and a high air flow rate are necessary for the period adding process, we noticed that the Reynold's number would be high in this region and accordingly, we thought that a

fully chaotic map could be relevant to start with. The fact that the system is dissipative implies that a low order system would be reasonable to describe the dynamics. Period doubling or intermittency in a Navier Stokes fluid were modeled by the logistic map with the general control parameter r [*ie.* $x_{n+1} = rx_n(1 - x_n)$], which is a good choice for studying the universal features associated with the phenomena. In this particular case the phenomenon is period adding and this simple map cannot show period adding bifurcation. We thought a variation of the logistic map should be a good candidate to generate and explain this phenomenon. Accordingly, we propose to model the system by

$$x_{n+1} = 4x_n(1 - x_n) \text{ if } x_n < x_{n-1}$$

$$x_{n+1} = rx_n(1 - x_n) \text{ if } x_n > x_{n-1}$$

This particular choice gives us an added advantage. Recently much work has been devoted to neurobiologically motivated relaxation oscillators. These oscillators almost always show a sequence of period adding phenomena in their very rich bifurcation patterns. In all such cases the period adding comes from piecewise smooth maps (8)-(10). In fact the map proposed by Colli et al. to describe their system, namely

$$f_{l,\phi}(T) = -\phi + \{ \text{ greatest root of t}\rightarrow\text{T} + m[t - d(T)]^3 - l[t - d(T)]\} \qquad (5.0.1)$$

also has the feature of piecewise continuity because the chosen root of the cubic equation switches in a discontinuous manner. We have tried to show in this chapter that similar scenarios (8)-(10) can also be achieved by modulating the control parameter in a 1-D map.

5.1 The model

With this in mind, we have introduced a logistic map (11)-(12) where the non-linearity parameter is modulated by a history dependent feedback. We can introduce modulation in the general form:

$$x_{n+1} = [r_0 - (4 - r_0)\tanh(\frac{x_n - x_c}{\varepsilon})]x_n(1 - x_n) \tag{5.1.1}$$

where we can take x_c as

(i) some definite predefined value. or

(ii)$x_c = x_{n-1}$, so that the next step of the dynamics depends on the previous step. This way the dynamics of the map becomes history dependent.

We explored in detail the limit $\varepsilon \to 0$. In that limit the hyperbolic tangent function becomes a step function. We note that the limits $x_n \to x_c$ followed by $\varepsilon \to 0$ and $\varepsilon \to 0$ followed by $x_n \to x_c$ do not commute. For our practical purpose, we need the order $\varepsilon \to 0$ followed by $x_n \to x_c$. In this case the limit of the hyperbolic tangent can be ± 1. We chose the value $+1$, keeping in mind that control of chaos is what we are after.

In the following bifurcation diagrams x_n is plotted against r_0 and not against r as the bifurcation diagram with respect to r_0 captures the r=4 dynamics explicitly.

For case (i) $x_c = 0.5$ [Fig 7.1(a)] is a reasonable cut-off though a vast range of x_c can be used to achieve period adding bifurcation [Fig 7.1(b)-7.1(d)]. It shows the strength of our model.

Case (ii) shows period adding cascade in a more elegant way. It seems to be a better model for bubble formation dynamics as there is no predefined cut-off in the experiment.

In this scenario, Eq(6.0.1) takes the form:

$$x_{n+1} = 4x_n(1 - x_n) \text{ if } x_n < x_{n-1}$$
$$x_{n+1} = rx_n(1 - x_n) \text{ if } x_n \geq x_{n-1} \tag{5.1.2}$$

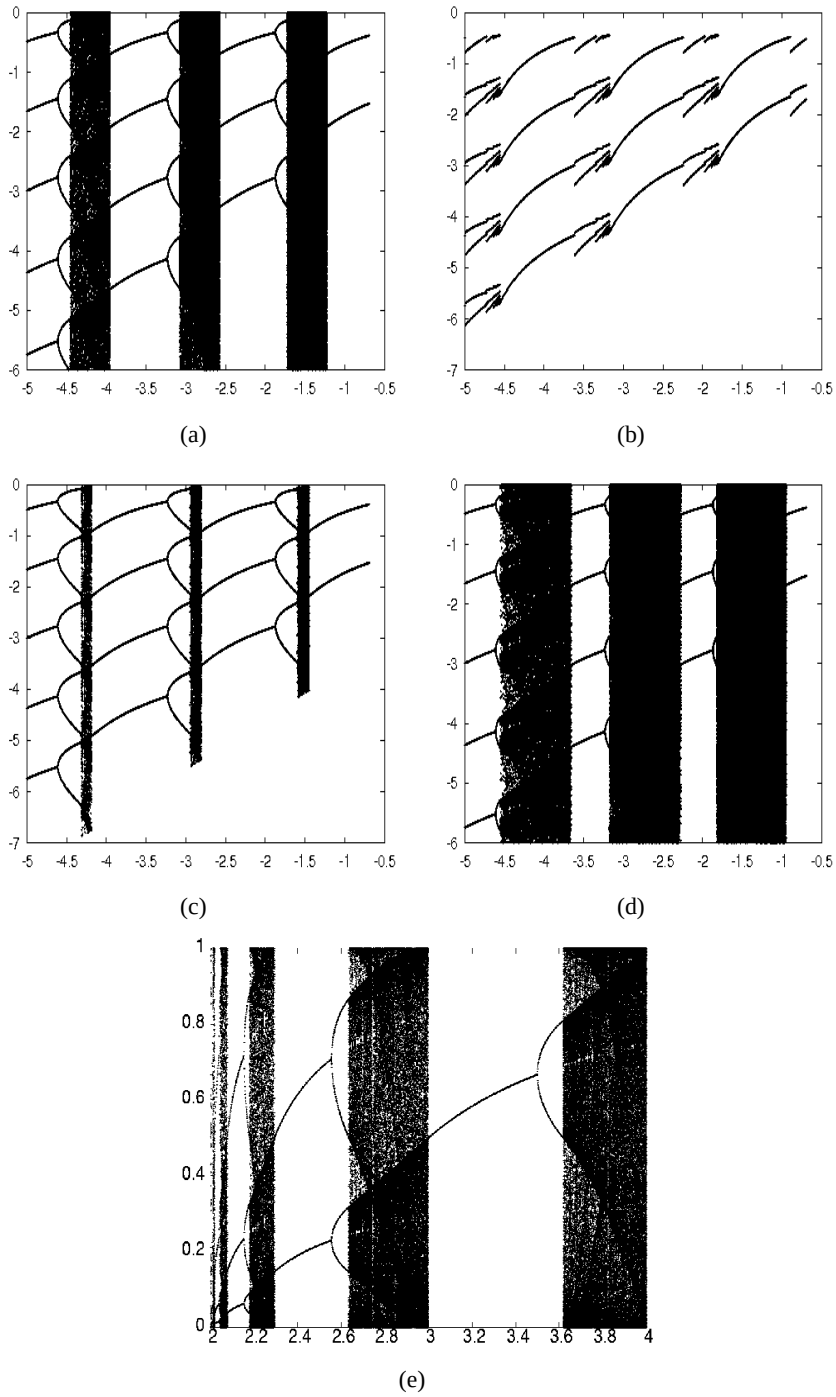

Figure 5.2: (a)Bifurcation diagram of the memory coupled logistic map with predefined cutoff $x_c = 0.5$ in the limit $\varepsilon \to 0$. (b-d)Bifurcation diagram for case(i) for different values of cutoff; x_c=0.2, 0.4 and 0.6 respectively. Both axes are plotted in log scale. x axis is plotted as log(r_0-2) and y axis as log(x_n). (e)Bifurcation diagram with $x_c = \frac{1}{2}$, axes are in natural scale.

where $r = (2r_0 - 4)$. For r=4, the logistic map is fully chaotic while for $r < 3$, it shows a stable fixed point. We want to point out that the system that has been much studied is

$$x_{n+1} = (r_0 + g_n)x_n(1 - x_n))$$

where $r_0 + g_n$ is never greater than four and g_n can have various complicated forms but it has always been local (13)-(14). Our departure from the usual practice is that our g_n is memory dependent(12).

5.2 Exploration of dynamics

We begin by exploring the dynamics of the map

$$x_{n+1} = f_1(x_n) = 4x_n(1 - x_n) \text{ if } x_n < x_{n-1} \quad (5.2.1)$$

$$x_{n+1} = f_2(x_n) = rx_n(1 - x_n) \text{ if } x_n > x_{n-1} \quad (5.2.2)$$

with $0 < r < 4$. Without the memory dependence, the logistic map $x_{n+1} = 4x_n(1 - x_n)$ is fully chaotic with a Lyapunov index of ln(2) and an invariant density distribution which is continuous in $0 \leq x \leq 1$. The map $x_{n+1} = rx_n(1 - x_n)$, by itself shows fixed points for $r < 3$ followed by cycles of period 2^n and so on. In the presence of memory, the above map does not begin with a fixed point but with a 2-cycle. We can qualitatively see the existence of it by noticing that for $r < 1$, x_{n+1} will be smaller than x_n if we use Eq(7.1.2) and then Eq(7.1.1) will have to be used at the next step and $x_{n+2} > x_{n+1}$ which forces the use of Eq(7.1.2) at the next step. Thus, we have a possible 2-cycle x_1,x_2 with

$$x_2 = 4x_1(1 - x_1) \quad (5.2.3)$$

$$x_1 = rx_2(1 - x_2) \quad (5.2.4)$$

We see immediately that

$$x_2 = 4rx_2(1-x_2)(1-rx_2(1-x_2)) \quad \text{and} \tag{5.2.5}$$

$$x_1 = 4rx_1(1-x_1)(1-4x_1(1-x_1)) \tag{5.2.6}$$

Thus x_1 and x_2 are the fixed points of two iterated functions F(x) and G(x) given by

$$F(x) = 4rx(1-x)(1-4x(1-x)) \tag{5.2.7}$$

$$G(x) = 4rx(1-x)(1-rx(1-x)) \tag{5.2.8}$$

These functions have zero as the stable fixed point for $r < \frac{1}{4}$. The two cycle elements will be non zero for $r > \frac{1}{4}$ and can be found from Eq(5.2.7) and Eq(5.2.8) and the cycle will be stable so long as the slopes of F(x) and G(x) at the fixed point are greater than -1. Destabilization through a pitchfork bifurcation occurs at (using F(x))

$$-1 = 4r_c[1-8x_c(1-x_c)][1-2x_c]$$

which leads to

$$1-2x_c = \frac{1-2r_c+\sqrt{4r_c^2+4r_c-9}}{2(4r_c-5)}$$

using Eq(5.2.7) at x_c and r_c, we substitute for x_c from above and find $r_c = \frac{\sqrt{160}-4}{8} \simeq 1.113$. Above $r = r_c$, the 2-cycle bifurcates to a 4-cycle and then to 8-cycle. These bifurcations are supported by a numerical analysis. Near r=1 there is another possible fixed point solution. For restricted basin of attraction we get a stable solution of $f_2(x) = x$. This solution is stable for $r < 3$ and at $r_0 = 2.7460$ the basin of attraction for this fixed point collides with that of the period 8-cycle and crisis occurs. After that we see only the fixed point attractor.

5.3 Period adding bifurcation

We note that r=2 is going to be interesting. At r=2, The map of Eq(7.1.2) has the feature that all initial conditions less than $x_n = \frac{1}{2}$ are going to yield $x_{n+1} > x_n$ but will not cross $x_{n+1} = \frac{1}{2}$. This means that such points will be repeatedly iterated by the map of Eq(7.1.2) and will reach the fixed point $x = \frac{1}{2}$. However, initial conditions starting at $x_n > \frac{1}{2}$ will yield $x_{n+1} < x_n$ and the next iteration will use the map of Eq(7.1.1) which will obviously yield an iterate $x_{n+2} > x_{n+1}$ forcing the map of Eq(7.1.2) at the next stage. The new input may or may not be less than $\frac{1}{2}$ and hence a fixed point may not be reached. Thus exactly at r=2 some initial conditions lead to a fixed point and some initial conditions do not. This opens up the possibility that for $r = (2 - \varepsilon)$, we may have a fixed point as the sole outcome of the iteration by Eqs(7.1.1) and (7.1.2).

Beyond $r = 2$, we need to refer to the complete numerical results shown in Fig 5.3(a). As we go slightly beyond $r = 2$, a periodic window of very large period emerges. The period decreases very rapidly for $r = 2 + \varepsilon$, with $\varepsilon \ll 1$. The period decrement is through the inverse of a period adding bifurcation. At every decreasing point, three branches come and meet and two emerge. This gives rise to a ribbon like structure which is shown in Fig 5.3(b).

Period adding phenomena was extensively studied in the context of switching circuits through border collision bifurcation(15)-(18). This is a common form of bifurcation when the dynamical system can be modelled by a set of piecewise smooth maps. One dimensional piecewise smooth maps can be defined in the following way

$$x_{n+1} = f(x_n;\mu) = \begin{cases} g(x_n;\mu) & \text{if } x_n \geq \lambda \\ h(x_n,\mu) & \text{if } x_n \leq \lambda \end{cases} \tag{5.3.1}$$

In the limit $\varepsilon \to 0$ our model Eq(6.0.1) can be cast in this form if x_c is taken to be some predefined constant. We can write down our system in the following form

$$x_{n+1} = f(x_n;\mu) = \begin{cases} g(x_n) = 4x_n(1-x_n) & \text{if } x_n < x_c \\ h(x_n;r_0) = (2r_0-4)x_n(1-x_n) & \text{if } x_n \geq x_c \end{cases} \tag{5.3.2}$$

Now border collision occurs when the fixed points of the smooth maps cross the border $x_n = x_c$. For first map $x_L^* = \frac{3}{4}$ and it cannot cross the border, although the fixed point of the second map $(x_n > x_c)$ $x_R^* = \frac{2r_0-5}{2r_0-4}$ can cross the border as r_0 is varied. When x_R^* collides with the border $x_n = x_c$ bifurcation occurs. The fixed point gets stabilized and a chaotic band emerges. For $x_c = \frac{1}{2}$ the collision occurs at

$$x_R^* = x_c = \frac{1}{2}\,;\, \frac{2r_0-5}{2r_0-4} = \frac{1}{2}\,;\, r_0 = 3$$

Which we can verify by Fig[7.1(e)]. The higher periods also gets unstable by the same process. For $x_L^* > x_c$ no fixed point is possible and only a chaotic band is possible.

Two dimensional piecewise smooth maps can be expressed as

$$g(x_n;y_n;\mu) = \begin{cases} g_1(x_n;y_n;\mu) & \text{if } x_n, y_n \in R_A \\ g_2(x_n;y_n;\mu) & \text{if } x_n, y_n \in R_B \end{cases} \tag{5.3.3}$$

where the border divides the map into two regions R_A and R_B. In the limit $\varepsilon \to 0$ and $x_c = x_{n-1}$ our

system can also be represented as a set of two dimensional piecewise smooth maps.

$$\begin{aligned} y_{n+1} &= x_n \\ x_{n+1} &= 4x_n(1-x_n) \text{ if } x_n < y_n \end{aligned} \tag{5.3.4}$$

and

$$\begin{aligned} y_{n+1} &= x_n \\ x_{n+1} &= (2r_0-4)x_n(1-x_n) \text{ if } x_n \geq y_n \end{aligned} \tag{5.3.5}$$

where the border is $y_n = x_n$. Now the fixed points of the first map as well as second map are $x_n = x_{n-1} = y_n$. All the fixed points lie on the border, so border collision does not happen.
As we move towards $r = 2$ from above, the distance between two consecutive nodes decreases. If we define the quantity

$$\delta = \lim_{n\to\infty} \frac{r_n - r_{n-1}}{r_{n+1} - r_n} \tag{5.3.6}$$

where r_n is the value of r at which an (n-1) cycle goes to an n-cycle, then δ converges to 1.414. We now explain how this happens.

In the ribbon like structure, every node is a fixed point of the return maps $f_2^{n-6}(f(f_2(x_m)))$ and $f_2^{n-6}(f_2(f(x_m)))$, where n denotes the number of cycles executed at that particular value of r and $f(x_m)$ is a composite function of $f_1(x_m)$ and $f_2(x_m)$. Convergence of the fixed point from left to right at the nodes ensures that these nodes are also fixed points of $f_2(x_m)$. So for each node

$$f_2^{n-6}(f_2(f(x_m^*))) = f_2(x_m^*) = x_m^* \tag{5.3.7}$$

i.e. $x_m^* = 1 - \frac{1}{r}$, and hence

$$f_2^{n-6}(f_2(f(1-\frac{1}{r}))) = 1 - \frac{1}{r} \tag{5.3.8}$$

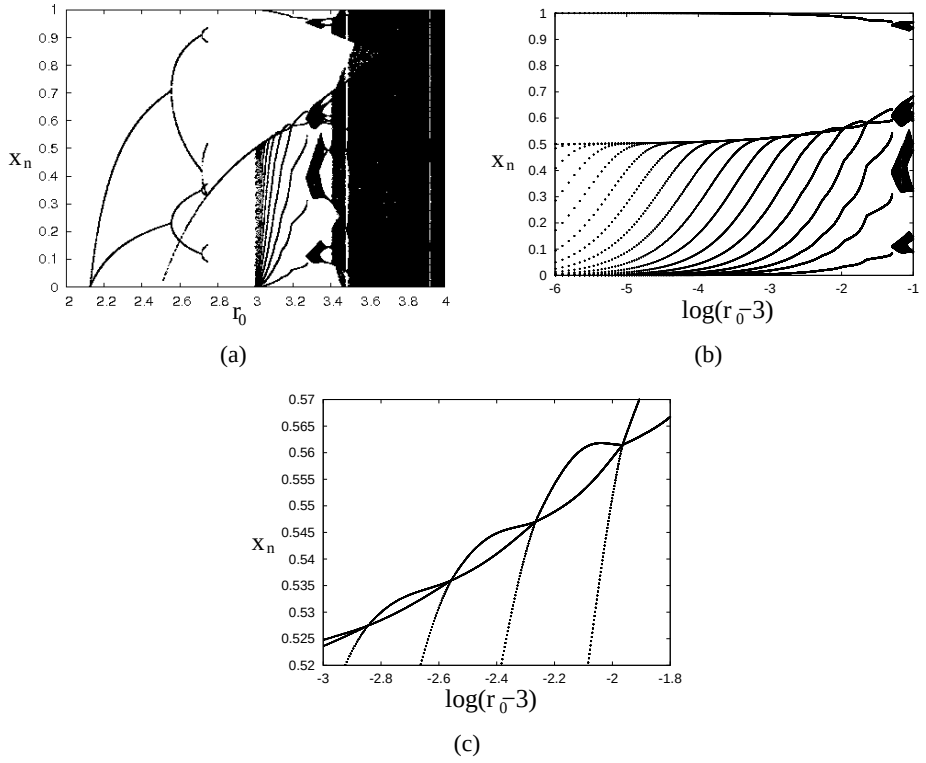

Figure 5.3: (a)Bifurcation diagram of the memory coupled logistic map. (b)Near $r_0 = 3$ (i.e. r=2) we see the ribbon like structure. The box is enlarged in the next (c) figure.

gives the r-value for the node r_n at the n^{th} cycle. But Eq(5.3.8) can be decomposed as

$$\left[f_2^{n-7}(f_2(f(1-\frac{1}{r}))) - (1-\frac{1}{r}) \right] \left[r f_2^{n-7}(f_2(f(1-\frac{1}{r}))) - 1 \right] = 0 \tag{5.3.9}$$

where the first factor gives the solution for the n-1 cycle and the second produces the new (n^{th}) node.

So Eq(5.3.8) gives all the nodes up to the nth order.

We get the value of r for the nth node (r_n) from

$$r f_2^{n-7}(f_2(f(1-\frac{1}{r}))) = 1 \tag{5.3.10}$$

If for n=N the period adding phenomenon stops, then

$$r f_2^{N-6}(f(1-\frac{1}{r})) = 1 \tag{5.3.11}$$

and also

$$r f_2^{N-5}(f(1-\frac{1}{r})) = 1 \tag{5.3.12}$$

when period adding stops $r_N \rightarrow r_{N+1}$, then Eq(6.3.5) and (6.3.6) give

$$r_N f_2(\frac{1}{r_N}) = 1 \tag{5.3.13}$$

which gives $r_N = 2$. So at $r = 2$ the period addition phenomenon stops. It clarifies the bifurcation diagram.

By finding the roots r_n we can find the ratio δ of Eq(5.3.6). Also we can find δ in the following way; Near r=2 let $r_n = 2 + \Delta_n$,then

$$r_n^n \Delta_n^2 = 1 \tag{5.3.14}$$

$$r_{n+1}^{n+1} \Delta_{n+1}^2 = 1 \tag{5.3.15}$$

where $r_n \approx r_N$. This gives

$$\delta_n = \frac{\Delta_n - \Delta_{n-1}}{\Delta_{n+1} - \Delta_n} \tag{5.3.16}$$

So $\delta_n = \sqrt{r_N} = \sqrt{2}$. For a large n, our numerical result supports this analysis.[Fig 5.4]

Beyond $r = 2.5427$, there is a chaotic band with the emergence of a periodic window at $r = 2.7244$ [Fig 5.5(a)]. For $2.7564 \leq r \leq 2.7876$, we see a cycle of period 11. Each element of the eleven cycle exhibits a sequence of period doubling bifurcation for $r < 2.7564$ and $r > 2.7876$. For one particular element of the 11-cycle the two sets of bifurcations on either side is shown in Fig 5.5(b).

As we further increase the value of r, there are two large periodic windows. At $r = 2.9499$, a 6-cycle is formed. Period-6 fixed points bifurcate and take the period doubling route to chaos.

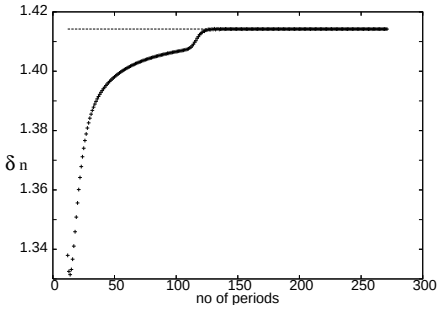

Figure 5.4: Numerical measure of δ_n. for large n it merges with the solid line $\delta_n = \sqrt{2}$.

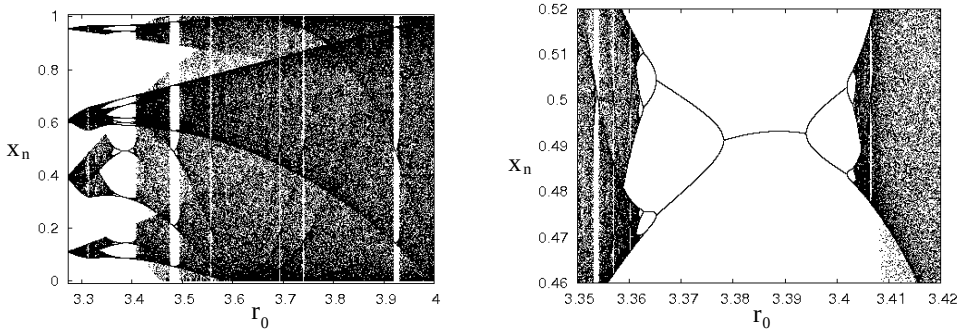

(a) (b)

Figure 5.5: (a)Rich dynamical structure after inverse period adding stops.(b)Period doubling route to chaos in 11-cycle.

Like in a logistic map a period 3-cycle is formed and takes intermittent route (19)-(21) to chaos. At $r = 3.8384$ period-3 becomes stable and goes through period doubling bifurcation. In between various other periodic windows can be seen.

We applied static as well as random perturbation to the system. Under static perturbation;

$$x_{n+1} = r x_n(1-_n) + \eta \tag{5.3.17}$$

the map still remains at a fixed point of $f_2(x_n)$ for $r < 2$ as the perturbation decreases quadratically over the iteration. For dynamic noise the map depends on the perturbations of two consecutive steps linearly and the equality condition ($x_{n+1} = x_n$) fails for $r < 2$. We get a replica of period adding bifurcation for $r < 2$. [Fig. 5.6]

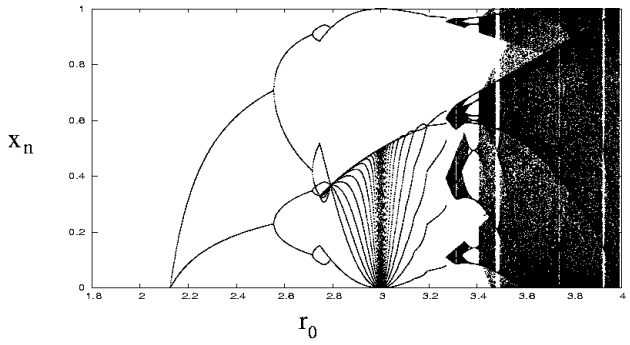

Figure 5.6: Bifurcation diagram with dynamic noise.

5.4 Disscussion

In closing we note that if we introduce a memory dependence on the logistic map, then it is possible to reduce the completely chaotic behavior of the first map $[x_{n+1} = 4x_n(1 - x_n)]$ to a controlled periodic orbit for low values of r. We also note that many scenarios that are generally modeled by piecewise smooth maps (8)-(10) can also be done by this method. With recent experiment (22) it is possible to simulate a logistic map exactly and hence this class of systems. As r is increased [Eq(6.0.2)] there are bifurcations in the memory dependent map with two striking features in the course of the bifurcations. One is the sudden collapse of a eight cycle to the fixed point which continues to be stable as r approaches from below and the other is the sequence of period adding bifurcations for $r > 2$ which approaches the infinite period limit as r approaches 2 from above. The mechanism of period adding bifurcation for the system under memory modulation is quite different from border collision. We note that the number expressing the bunching of r as successive period-adding occurs is distinctly different from the corresponding number for the period adding route of Yin Shui Fan and Teresa Ree Chay (23). This difference is because of the different mechanisms for the period adding in the two cases.

Bibliography

[1] E. Colli ,V. S. M. Piassi ,A. Tufaile and J. C. Sartorelli , Phys. Rev. E **70** 066215 (2004).

[2] Yang M. , Gu H., Li Li, Liu Z. , Ren Wei CACA, Neuroreport, **14(17)** 2153 (2003).

[3] Mosekilde E., Lading B., Yanchuk S. and Maistrenko Y., Biosystems, **63** 2 (2001).

[4] Gu H. ,Yang M. , Li Li, Liu Z. and Ren Wei, Phys. Lett. A, **319** 89 (2003).

[5] E. A. Jackson, *Perspective of Nonlinear Dynamics* (CUP,Cambridge,England,1989).

[6] A. N. Pisarchik, R. Meucci and F. T. Arecchi, Eur. Phys. J. D **13** 385 (2001).

[7] R. Roy , T. W. Murphy , T. D. Maier , Z. Gills and E. R. Hunt , Phys. Rev. Lett. **68** 1259 (1992).

[8] Pisarchik A.N. and Jaimes-Retegui R., Journal of physics:Conference Series, **23** 2005.

[9] S. Coombes and A. H. Osbaldestin , Phys. Rev. E, **62** 4057 (2000).

[10] Holden A. V.and Fan Y. S, Chaos,Solitons & Fractals, **2** 4 (1992).

[11] Dutta D., Bhattacharjee J. K., Nandi A. and Ramaswamy R., Proceedings of the National Conference on Nonlinear Science and Dynamics, (2003).

[12] Nandi A., Dutta D., Bhattacharjee J. K. and Ramaswamy R., chaos, **15** 023107 (2005).

[13] N. Gershenfeld and G. Grinstein , Phys. Rev. Lett., **74** 5024 (1995).

[14] J. Rössler ,M. Kiwi ,B. Hess and M. Markus , Phys. Rev. A, **39** 5954 (1989).

[15] Soumitro Banerjee, M.S. Karthik, Guohui Yuan and J.A. Yorke, *IEE Trans. Circuits Syst.-I*, **47** 3 (2000)

[16] H.E. Nusse and J.A. Yorke, *Int. J. Bifurcat. Chaos*, **5** 1 (1995)

[17] H.E. Nusse and J.A. Yorke, Physica D,**57**, 39-57

[18] G.H. Yuan,S. Banerjee, E. Ott and J.A. Yorke,*IEE Trans. Circuits Syst.-I*,**45**, 7, 707-716

[19] Sanju and V. S. Varma , Phys. Rev. E, **48** 1670 (1993).

[20] J. E. Hirsch , B. A. Huberman and D. J. Scalapino , Phys. Rev. A, **25** 519 (1982).

[21] Chil-Min Kim, O. J. Kwon, Eok-Kyun Lee and Hoyun Lee, Phys. Rev. Lett., **73** 525 (1994).

[22] Madhekar S., Electronic Circuit Realization of the Logistic Map,*SÄDHANA* **31** 69 (2006).

[23] Yin Shui Fan and Teresa Ree Chay, Phys. Rev. E ,**51** 1012 (1995).

Chapter 6

Two dimensional discrete dynamical systems under memory modulation

In ecology, there are some species whose population goes from generation to generation, for example, gypsy moths or any of many other species of insects. These topics are usually modelled by difference equations, iteration map or discrete dynamical systems. A famous discrete model (1) is the following logistic difference equation

$$x_{n+1} = r x_n (1 - x_n) \tag{6.0.1}$$

which describes evolution of the population of a single species in discrete time, where r is a number describing the fertility rate of the species and x_n denotes the population density of the n-th generation of the species. This can be expressed by saying that the population in any generation depends only on the population in the previous generation. This discrete model shows much richer dynamics than its continuous counterpart

$$\frac{dx(t)}{dt} = r x(t)(1 - x(t)) \tag{6.0.2}$$

The logistic map of Eq(6.0.1) shows rich dynamical structures such as chaos, intermittency and various bifurcation which cannot be observed in lower dimensional continuous systems. Simplicity

of difference equations helps us to understand the dynamical systems in a greater depth. These difference equations also serve as important models for modulation of chaos, ie. control and enhancement of chaos. In our present work we study the two dimensional predator prey dynamics (2)-(6) suggested by the famous Lotka-Volterra equations

$$\frac{dx(t)}{dt} = \varepsilon x(t)[1 - y(t)] - \alpha x(t)^2 \tag{6.0.3}$$

$$\frac{dy(t)}{dt} = -\varepsilon y(t)(1 - x(t)) \tag{6.0.4}$$

where x(t) is the population density of the prey and y(t) is the population density of the predator at time t. The dynamics of the prey population is logistic growth and the intrinsic growth rate is ε in the absence predators.The functional response, the number of prey individuals consumed per unit area per unit time by an individual predator, is the function αx. The natural death rate of predator is ε. In the above ε , α both are positive constants.

6.1 Discrete Lotka Volterra dynamics

We are interested in the discrete form of this equation as the discrete dynamics is much richer and can lead to chaotic dynamics (2). In Euler scheme, taking the step size to be unity we can discretize the differential form as

$$x_{n+1} = (1 + \varepsilon)x_n - \alpha x_n^2 - \varepsilon x_n y_n \tag{6.1.1}$$

$$y_{n+1} = (1 - \varepsilon)y_n + \varepsilon x_n y_n \tag{6.1.2}$$

From the point of view of biology the dynamics of the predator-prey system should be confined within the first quadrant of x_n, y_n phase plane. To ensure that the initial conditions are taken in such

a way that the iterates always remain positive; we need to impose

$$x_0 > (1 - \frac{1}{\varepsilon}) \tag{6.1.3}$$

$$y_0 < 1 + \varepsilon - \alpha x_0 \tag{6.1.4}$$

6.1.1 Fixed points and their stability

The fixed points (x,y) of the discrete Lotka Volterra model can be obtained from the following equations

$$x = (1 + \varepsilon)x - \alpha x^2 - \varepsilon xy \tag{6.1.5}$$

$$y = (1 - \varepsilon)y + \varepsilon xy \tag{6.1.6}$$

Apart from the trivial fixed point (x=0,y=0) there are two more fixed points, $(x = \frac{\varepsilon}{\alpha}, y = 0)$ and $(x = 1, y = 1 - \frac{\alpha}{\varepsilon})$. From biological requirement the third fixed points does not exist for $\alpha > \varepsilon$. Now from linear stability analysis we can predict their stability. The eigenvalues (λ) for the stability matrix can be obtained from the following determinant

$$A_c = \begin{pmatrix} (1 + \varepsilon - 2\alpha x - \varepsilon y) - \lambda & -\varepsilon x \\ \varepsilon y & (1 - \varepsilon + \varepsilon x) - \lambda \end{pmatrix} = 0$$

For the trivial fixed point (0,0) $\lambda_{1,2} = 1 + \varepsilon, 1 - \varepsilon$ which makes it a saddle point, as we are interested in $\varepsilon > 0$. For $\varepsilon > 2$ it becomes a unstable fixed point. $\lambda_{1,2} = 1 - \varepsilon, 1 - \varepsilon + \frac{\varepsilon^2}{\alpha}$ for the fixed point $x = \frac{\varepsilon}{\alpha}, y = 0$. As long as $\varepsilon < 2$ the fixed points are stable for $\varepsilon < \alpha$. For $\varepsilon > 2$ it becomes a saddle as $\lambda_1 < -1$ but the other eigenvalue becomes stable for $\varepsilon^2 > (\varepsilon - 2)\alpha$.

The stability analysis of the third fixed point leads to interesting dynamics. $\lambda_{1,2} = 1 - \frac{\alpha}{2} \pm \frac{\sqrt{\alpha^2 + 4\varepsilon\alpha - 4\varepsilon^2}}{2}$. For $\alpha > 2(\sqrt{2} - 1)\varepsilon$ the square-root term becomes positive and the eigenvalues become real. The fixed point becomes stable for $\varepsilon > \alpha$. The fixed point becomes a stable spiral for $\alpha = 2(\sqrt{2} - 1)\varepsilon$ and remains stable until $\alpha = \frac{\varepsilon^2}{\varepsilon + 1}$.

6.2 Bifurcation analysis

At $\varepsilon = \alpha$ stability of the fixed point changes. For $\varepsilon < \alpha$ ($x = \frac{\varepsilon}{\alpha}, y = 0$) is stable but as $\varepsilon > \alpha$ this point loses its stability and the other fixed point ($x = 1, y = 1 - \frac{\alpha}{\varepsilon}$) becomes stable. So at $\varepsilon = \alpha$ the system goes through a fold bifurcation.
We come across an important bifurcation at $\alpha = \frac{\varepsilon^2}{\varepsilon + 1}$, at this point the amplitude of the eigenvalue [$re^{i\phi}$] becomes unity and the stable spiral undergoes a Neimark-Sacker bifurcation and invariant closed curve stabilizes for $\alpha < \frac{\varepsilon^2}{\varepsilon + 1}$. These invariant circles collapse to periodic points through formation of smaller islands Fig 6.1(d) which then form smaller invariant curves Fig 6.1(e). For larger values of ε (smaller α) the system leads to chaos Fig 6.1(f).

Under certain parameter constraints the system can also goes through flip bifurcation. We can find the condition for flip bifurcation taking into account the dynamics in centre manifold. As we are interested in the local dynamics near the fixed point $x_n = 1, y_n = 1 - \frac{\alpha}{\varepsilon}$, we make a coordinate transform to consider this fixed point to be our new origin.

$$u_n = x_n - 1$$
$$v_n = y_n - 1 + \frac{\alpha}{\varepsilon}$$

then Eq(7.1.3) can be rewritten as the following

$$u_{n+1} = (1 - \alpha)u_n - \varepsilon v_n - \alpha u_n^2 - \varepsilon u_n v_n \tag{6.2.1}$$
$$v_{n+1} = (\varepsilon - \alpha)u_n + v_n + \varepsilon u_n v_n \tag{6.2.2}$$

we find out the eigenvalues $\lambda_{1,2} = \frac{1}{2}[\frac{2 - \alpha \pm \sqrt{\alpha^2 + 4\varepsilon\alpha - 4\varepsilon^2}}{2}]$, and rewrite Eqs(6.2.1-6.2.2) in terms of the eigenvectors (p_n, q_n) of the linear part. By the center manifold theory, we know that the stability of (0, 0) near $\alpha = f(\varepsilon)$ can be determined by studying at a one-parameter family of

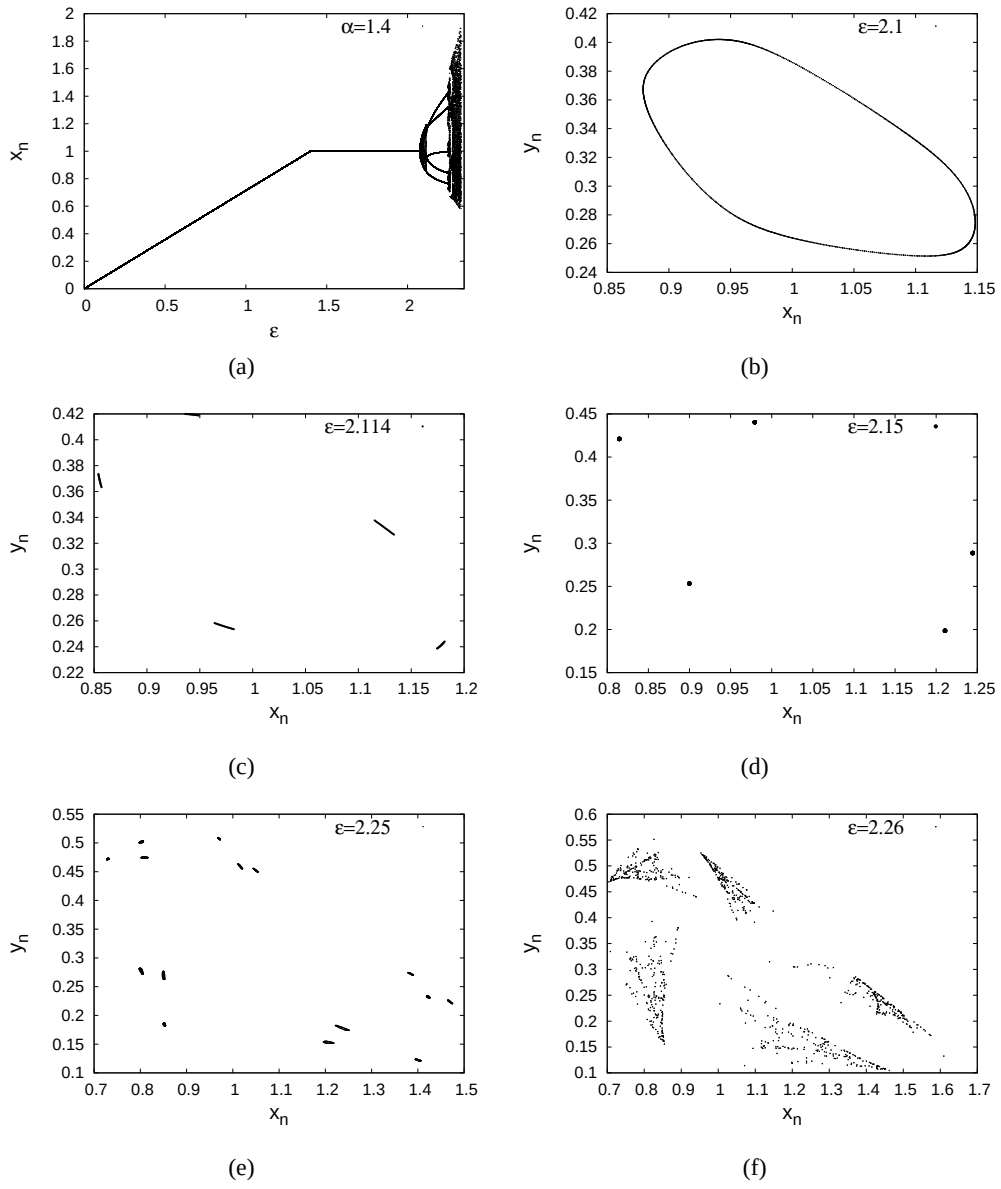

Figure 6.1: (a)Bifurcation diagram for $\alpha = 1.4$. We can see a fold bifurcation at $\alpha = \varepsilon$. For $\varepsilon = 2.0747$ Neimark bifurcation occurs and invariant circles can be seen (b) after that. Different dynamics are illustrated in (b,c,d,e,f) for corresponding values of $\varepsilon = 2.1, 2.114, 2.15, 2.25, 2.26$. Breaking of invariant circle to small island is clear from (d,e). After this the band is chaotic intermittently separated by few periodic bands. Invariant circles undergoes different bifurcations and the dynamics becomes chaotic.

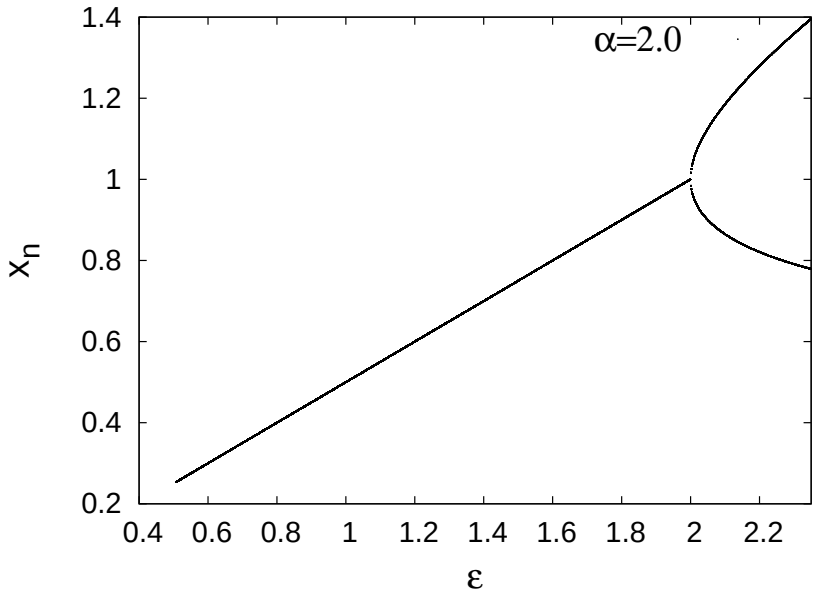

Figure 6.2: Bifurcation diagram when ε is varied with x_n. The value of α is kept fixed at 2.0. A fold bifurcation can be observed also at $\varepsilon = 2.0$.

equations on a center manifold, which can be represented as follows

$$W^c(0) = \{(p_n, q_n, r) \in \mathbf{R}^3 | p_n = h(p_n, r), h(0,0) = 0, Dh(0,0) = 0\}.$$

Now the coefficient of p_n is equal to '-1' for flip bifurcation, which leads to the following condition to be satisfied.

$$4\varepsilon^4 - 8\varepsilon^3\alpha + (3\alpha^2 + 4)\varepsilon^2 + \alpha^3\varepsilon - 4\varepsilon\alpha = 0 \tag{6.2.3}$$

For $\alpha = 2$ this condition is satisfied and we get flip bifurcation for $\varepsilon = 2$ Fig 6.2.

6.3 Control of invariant circles to periodic orbits

Memory modulation is an effective way to control chaos and lowering the value of Lyapunov exponents. Though control of chaos has been in the literature the memory modulation technique is quite of late (8; 9). In earlier works (10; 11) we have shown that one dimensional quadratic maps can be controlled effectively with feedback algorithm using one step memory. One dimensional logistic

map shows chaotic dynamics for $r = 4$, Control of chaos emerges through following memory delay feedback which also leads to additional phenomena.

$$x_{n+1} = 4x_n(1 - x_n) \text{ if } x_n < x_{n-1} \tag{6.3.1}$$

$$x_{n+1} = rx_n(1 - x_n) \text{ if } x_n \geq x_{n-1} \tag{6.3.2}$$

this modulation leads to suppression of chaos for a large range of parameters and is effective in lowering the local Lyapunov exponent (LLE). We looked at the dynamics of this discrete predator-prey model under similar memory modulation. Under memory feedback Eq(7.1.1) and Eq(7.1.2) gets modified to the following equations;

$$x_{n+1} = \begin{cases} (1+\varepsilon)x_n - (\alpha_0 + \beta)x_n^2 - \varepsilon x_n y_n \text{ if } (x_n, y_n) > (x_{n-1}, y_{n-1}) \\ (1+\varepsilon)x_n - (\alpha_0 - \beta)x_n^2 - \varepsilon x_n y_n \text{ if } (x_n, y_n) < (x_{n-1}, y_{n-1}) \end{cases} \tag{6.3.3}$$

$$y_{n+1} = (1 - \varepsilon)y_n + \varepsilon x_n y_n \tag{6.3.4}$$

At $\alpha = \varepsilon$ the unmodulated system goes through a fold bifurcation. It would be interesting to see the dynamics if we take this bifurcation point to be the starting point of modulation, ie. $\alpha_0 = \varepsilon$. Now according to the control algorithm when the system becomes more unstable the dynamics will push the system towards more controlled dynamics as for $\alpha > \varepsilon$ the system has stable fixed point. Now for small values of ε we get ordered dynamics of period four. With the increase of ε we see more interesting dynamics Fig 6.5(f). The system shows period adding dynamics which is quite different from the one we analysed in (11). Here with β period increases in a continuous manner but there is no fixed ratio like Feigenbaum constant. In reality the ratio $\frac{\Delta_n}{\Delta_{n-1}}$ of the corresponding width (Δ_n) of consecutive two period n and $n-1$ increases slowly Fig[6.3(a),6.3(b)].

We can as well take α_0 to be some other point. Another possibility to take α_0 to be in the periodic point region of Fig 6.1(a). Then the dynamics is an outcome of the interplay between chaotic

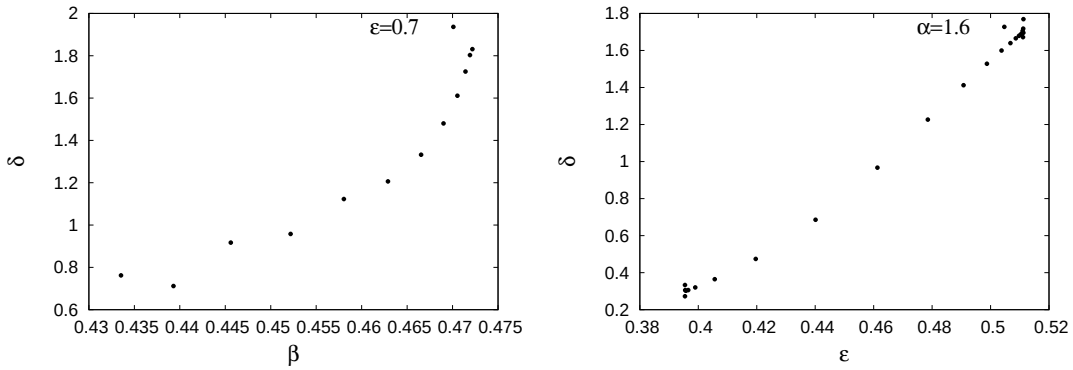

(a) (b)

Figure 6.3: calculation of $\delta = \frac{\Delta_n}{\Delta_{n-1}}$. (a) δ is calculated when period adding occurs by varying α. (b) Numerical values of δ as period adding happens when ε is changed. In both cases the ratio increases with higher period.

dynamics and invariant orbits. As the invariant orbits are feeble attractors (Lyapunov exponents nearly zero) chaotic dynamics supersedes the periodic dynamics and invariant circles only retains their signature when they are modulated with periodic dynamics Fig 6.3. We can as well control the dynamics by modulating the value of ε. Then the system takes the form;

$$x_{n+1} = (1 + \varepsilon^{'})x_n - \alpha x_n^2 - \varepsilon^{'} x_n y_n \tag{6.3.5}$$

$$y_{n+1} = (1 - \varepsilon^{'})y_n + \varepsilon^{'} x_n y_n \tag{6.3.6}$$

where $\varepsilon^{'} = \varepsilon_0 - \gamma sgn(x_n - x_{n-1})$. Now from previous analysis Fig 6.1(a) we know when we vary ε at $\varepsilon = \alpha$ fold bifurcation occurs and as we increase ε the system undergoes Neimark-Sacker bifurcation and eventually to chaos. So when the system moves further from periodic dynamics memory modulation gives negative feedback and maintains the system in periodic state for larger range of ε. This modulation also leads to period adding bifurcation for higher values of ε. For smaller values system shows periodic dynamics of period four Figs[6.5(e),6.5(f)].

The memory dependent control method is very efficient in controlling chaos and also for putting the systems from higher periodic state to a lower periodic one. But period adding phenomena is a outcome of the interplay between the chaotic dynamics and periodic state. Period adding bifurca-

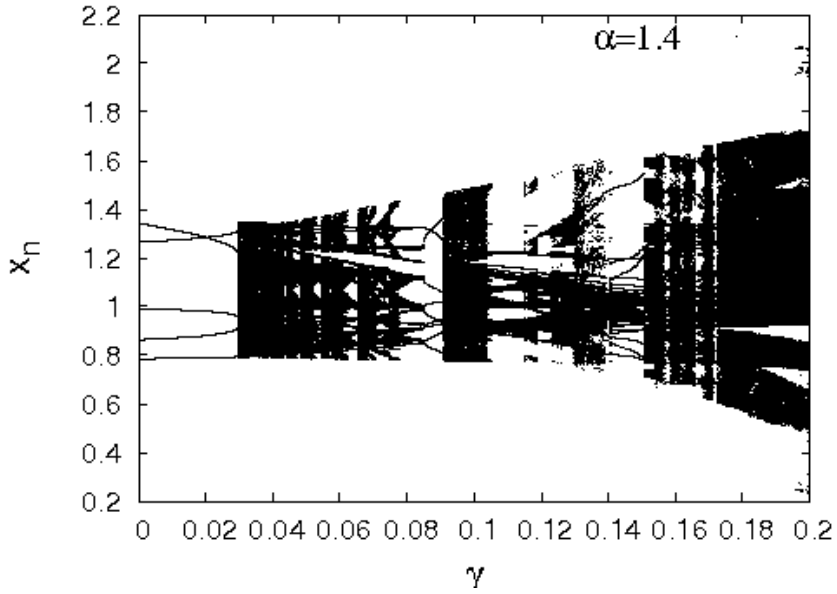

Figure 6.4: Interplay between chaotic bands and invariant orbits. From unmodulated case Fig 6.1(a) x_0 is taken to be 2.2. This consideration mixes invariant circles with chaotic as well as periodic point-bands. This mixing leads to chaotic bands separated by small periodic windows.

tion does not happen when we control non-chaotic attractors. From the corresponding Lyapunov exponents in Figs[6.5(c),6.5(d)] we can verify our statement.

6.4 Discussion

In this chapter we studied the the dynamical behaviors of the discrete-time prey-predator model, which is obtained by using the scheme of Euler's method with step one. We can see that there exist some parameter values such that the discrete model has a stable invariant cycle. However, the continuous model does not have limit cycles. We would like to point out that some continuous predator-prey model with functional response has limit cycles. There have been a great amount of literature on this topics ((6; 7; 12; 13) and references therein). On the other hand, it should be recognized that the discrete model is derived from the continuous model by Euler's method, and not from actual population growth laws. For some parameter values or initial values, this model can have negative values of $x(n)$ or y_n, which have no biological meaning. Therefore, it is a further

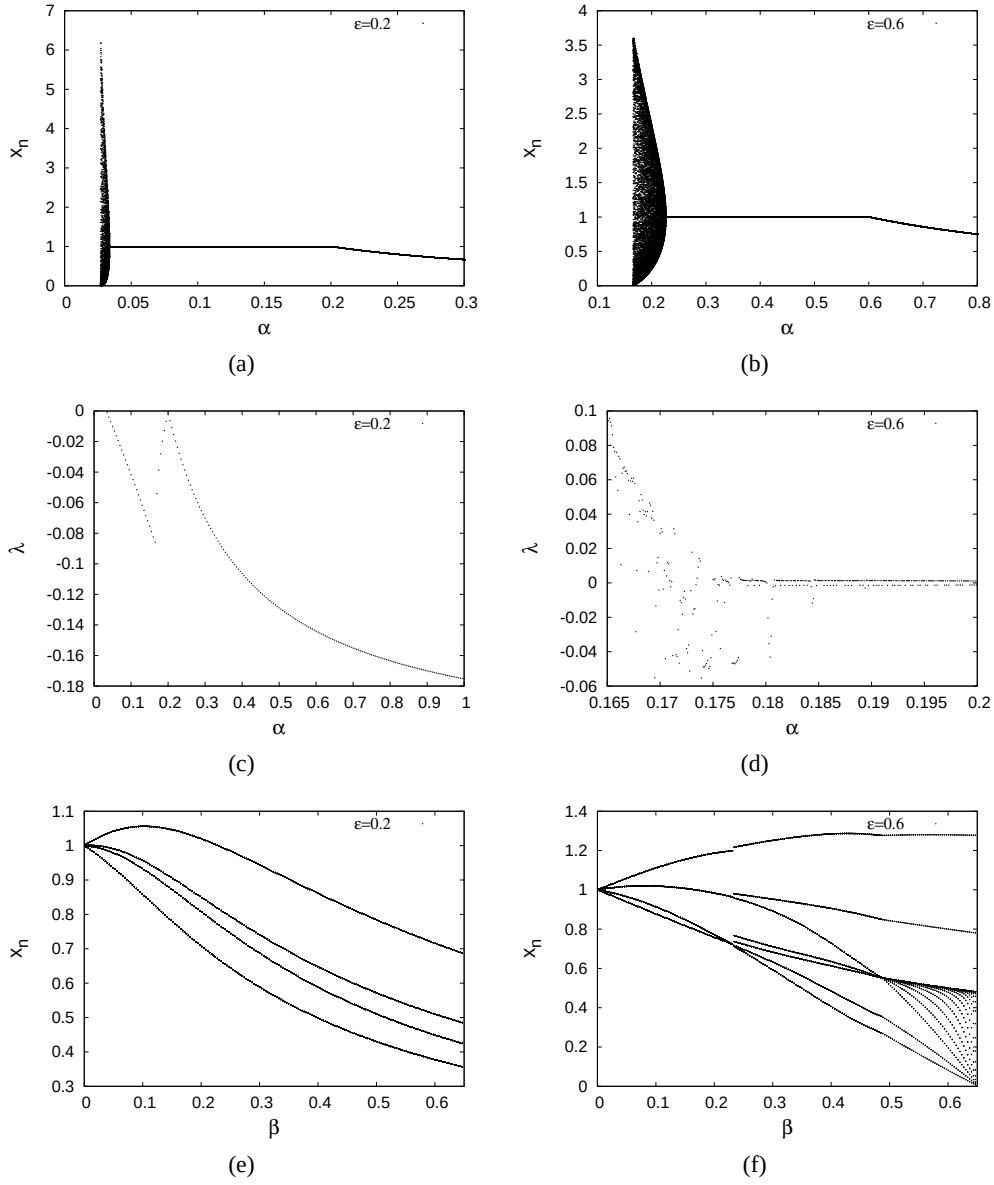

Figure 6.5: Period adding occurs when a strong chaotic attractor interacts with periodic dynamics.Bifurcation diagrams(a,b) and Lyapunov exponents (c,d) of unmodulated discrete Lotka-Volterra system for two different values of ε is plotted [(c)$\varepsilon = 0.2$,(d)$\varepsilon = 0.6$] with α. Bifurcation diagrams (e,f) for the modulated system for the same values of ε show that interplay of periodic state with strong chaotic one leads to period adding.

study topic in future how propose a reasonable discrete-time predator prey model.

Control of invariant cycle can be done with the same method as with controlling chaos. We showed memory modulation of the system parameter leads to interesting dynamics such a period adding which is generally seen where border collision occurs. As discussed in last chapter memory modulation dynamics is different from border collision dynamics and hence worth greater understanding. Unlike previous chapters we have shown memory modulation method is effective for higher dimensional systems.

Bibliography

[1] R. M. May, *Stability and Complexity in Model Ecosystems* (Princeton University Press,Princeton, 1973).

[2] A.J Lotka, J. Am. Chem Soc. **42**, 1595 (1920).

[3] V. Volterra, Atti R. Accad, Naz. Lincei, Mem. Cl. Sci. Fis,. Mat. Nat. **2**, 31 (1926).

[4] H. Haken, *Synergetics*, 3rd ed. (Springer-Verlag, New York, 1983).

[5] D. Neal, *Introduction to Population Biology* (Cambridge University Press,Cambridge, U.K. 2004).

[6] J. Maynard Smith, *Models in Ecology* (Cambridge University Press,Cambridge, U.K. 1974).

[7] J. D. Murray, *Mathematical Biology*, 3rd ed. (Springer-Verlag, New York, 2002), Vols. I and II.

[8] D. Dutta, J. K. Bhattacharjee, A. Nandi, and R. Ramaswamy, in *Proceedings of the National Conference on Nonlinear Science and Dynamics*, IIT Kharagpur, 2003.

[9] A. Prasad, V. Mehra, and R. Ramaswamy,Phys. Rev. E **57**, 1576 (1998).

[10] Nandi A., Dutta D., Bhattacharjee J. K. and Ramaswamy R., chaos, **15** 023107 (2005).

[11] Debabrata Dutta, J.K. Bhattacharjee, Physica D, *in press*

[12] K. Gopalsamy and X.Z. He, Physica D **76**, 344 (1994).

[13] M. Mobilia, T. Goeorgiev, U. C. Täuber, Phys. Rev. E, **73**, 040903(R) (2006)

Chapter 7

Controlling dynamical systems by memory dependent switching: a variation on the Pyragas scheme

The earliest proposal for control of chaos was prescribed by Ott, Grebogi and Yorke (OGY)(1). They exploited the presence of an infinite number of unstable periodic orbits (UPO) in the chaotic state. The idea of OGY was to stabilize a UPO by a small time dependent change in the control parameter. The advantage of stabilizing a UPO lies in that it can be done by a small change in the control parameter (2; 3; 4). However the OGY technique is not efficient for large Lyapunov numbers and hence a variation was introduced by Pyragas (5). In the two schemes suggested by Pyragas (5) one requires an external force and the other does not. The one which requires the external force calls for a complex experimental realization and so we discuss the second scheme. This scheme introduces a feedback into the dynamical system written as

$$\begin{aligned} \frac{dy}{dt} &= P(y, \mathbf{x}) \\ \frac{d\mathbf{x}}{dt} &= \mathbf{Q}(y, \mathbf{x}) \end{aligned} \tag{7.0.1}$$

where $(y, \mathbf{x})$ is a (n+1) dimensional dynamical system and y is the variable that we are focusing on. The y-equation is modified in the Pyragas scheme by a term $F(t)$, where $F(t) = K[y(t-\tau) - y(t)]$, where τ is a delay time and we have

$$\frac{dy}{dt} = P(y, \mathbf{x}) + F(t) \tag{7.0.2}$$

clearly if τ happens to be period T_i of the i^{th} UPO, the system is unperturbed. The primary effort in the implementation of the Pyragas scheme is the determination of τ and K that would stabilize the chaotic orbit. We show the results of this condition For the Rössler system in Fig 7.4(a) .

In the present work we use a variation on the Pyragas scheme. We couple the prescription suggested by Pyragas with the literature on switching in dynamical systems. Our goal is to set up a technique for controlling the output of dynamical system. Our approach is not restricted to chaotic dynamics and in reality does not have any significant overlap with the standard switching dynamics because we use switching in an irregular manner by making it memory dependent. Our prescription is quite similar with that of Pyragas in using a delay time τ (though we do not link it to UPO). However unlike Pyragas we do not use it as a drive. In the spirit of OGY we rather use the delay and switching to perturb the control parameter. We first exhibit our scheme by using it to control the dynamics of a damped linear oscillator.

7.1 Memory modulated harmonic oscillator

Periodic orbits (1; 5) arise in both Hamiltonian systems and dissipative ones. The simplest Hamiltonian system with a periodic orbit is the simple harmonic oscillator. The frequency of motion is determined by the constants of the restoring force and the amplitude is determined by initial conditions. For the nonlinear oscillator, the frequency depends on the amplitude and thus on the initial conditions. If we now add a damping (dissipative system) which in the usual phenomenology is

proportional to the velocity (linear damping), then the oscillations die out. A negative damping, on the other hand, would cause the oscillation amplitudes to grow exponentially. If we follow the phase space nomenclature, then the fixed point at the origin ($x = \dot{x} = 0$) is a centre for the conservative system. It is a stable spiral for a mildly damped oscillator and unstable spiral for the corresponding negative damping. For the dissipative system to exhibit periodic orbits, the damping needs to be nonlinear. Such periodic orbits are called limit cycles and the amplitude of the limit cycles are generally independent of initial conditions. The periodic orbit can also be formed in the dissipative systems provided the nonlinear dissipation is such that the damping is positive over part of the cycle and negative over the remainder. This gives an energy balance over the complete cycle. From the linear to nonlinear oscillator, there is a change in the nature of the fixed point at the origin when the motion changes at the origin. This is well exemplified in the Van der Pol oscillator

$$\ddot{x} + k\dot{x}(x^2 - 1) + \omega^2 x = 0$$

where the nonlinear damping makes the fixed point $x = \dot{x} = 0$ an unstable spiral as opposed to the stable spiral for $\ddot{x} + k\dot{x} + \omega^2 x = 0$.

We introduce a memory dependent switching (6; 8) to write

$$\ddot{x} + k\dot{x}\Theta[x(t) - x(t-\tau)] + {\omega_0}^2 x = 0 \tag{7.1.1}$$

In the above $\Theta(y)$is the step function which is +1 if y is positive and -1 if y is negative and τ is a preassigned time. The switching is apparent if we write Eq(7.1.1) as

$$\ddot{x} + k\dot{x} + {\omega_0}^2 x = 0 \qquad if \qquad x(t) > x(t-\tau) \tag{7.1.2}$$

$$\ddot{x} - k\dot{x} + {\omega_0}^2 x = 0 \qquad if \qquad x(t) < x(t-\tau) \tag{7.1.3}$$

The switching condition makes it clear that the switching is memory dependent. We note immedi-

ately that the stable spiral in the absence of Θ-function becomes a centre in its presence. This is the indication of the existence of something different and accordingly we write down the solutions for the two segments Eqs(7.1.2,7.1.3) as $x_1(t) = Ae^{-\frac{k}{2}t}\cos(\omega t + \phi_1)$, $x_2(t) = Be^{\frac{k}{2}t}\cos(\omega t + \phi_2)$ where A, ϕ_1, B, ϕ_2 are determined by initial conditions and $\omega = \sqrt{{\omega_0}^2 - \frac{k^2}{4}}$. A periodic solution of period T would imply that there is at least one switch in the interval $0 < t < T$. Investigating solutions with one switch only, we require $x_1(t') = x_2(t')$ and $\dot{x_1}(t') = \dot{x_2}(t')$ for a smooth solution and periodicity implies $x_1(0) = x_2(T)$ with $\dot{x_1}(0) = \dot{x_2}(T)$. It is straight forward to see that a solution can be found for $T = \frac{2\pi}{\omega}$ and $t' = \frac{T}{2}$. The actual existence of a switch is controlled by the "memory time " τ. We note that if $\omega\tau << 1$, then the theta function can be written as $\Theta(\dot{x}\tau)$. It is the sign of the velocity that controls the switch in this case and it is easy to see that a periodic orbit will result. The same argument holds for $\tau = T$, the orbit is now simply inverted with respect to the previous one. We show the numerical evidence of the periodic orbits in Fig 7.1. While the orbit has some limit cycle characteristics in that it is a periodic orbit. In a non conservative system, the size of the orbit depends on initial condition Fig 7.2(a) which is a hallmark of a conservative system. We note that while the limit cycle of $\tau = 0$ and $\tau = T$ are easily understandable, it is the closed orbit for $\tau = \frac{T}{2}$ which is nontrivial. In general, we find a quantisation of stabilising 'τ' in units of the half period $\frac{T}{2}$ Fig 7.2(b).

Limit cycle oscillations have practical applications in many nonlinear mechanical as well as electronic systems. Based on the above observations, we now propose a method to control chaotic dynamics by converting chaotic oscillators to limit cycles. We propose to exploit the known regular dynamics of these systems to flip the control parameter in the 'favourable' region when the dynamics seem to become irregular. This will help stabilize limit cycles in the following systems.

Let $\dot{x_i} = f_i(\bar{\mu}, \{x_j\})$, where $\bar{\mu}$ is a set of control parameters, represent a chaotic system. In what follows, we will take $\bar{\mu}$ to have only one component μ. We assume the system shows chaotic as well as non-chaotic dynamics for different values of control parameter. We make our parameter μ memory dependent so that the system can self-modulate its dynamics according to the controlling method. The dynamics will be governed by both chaotic as well as non-chaotic attractors. So, for

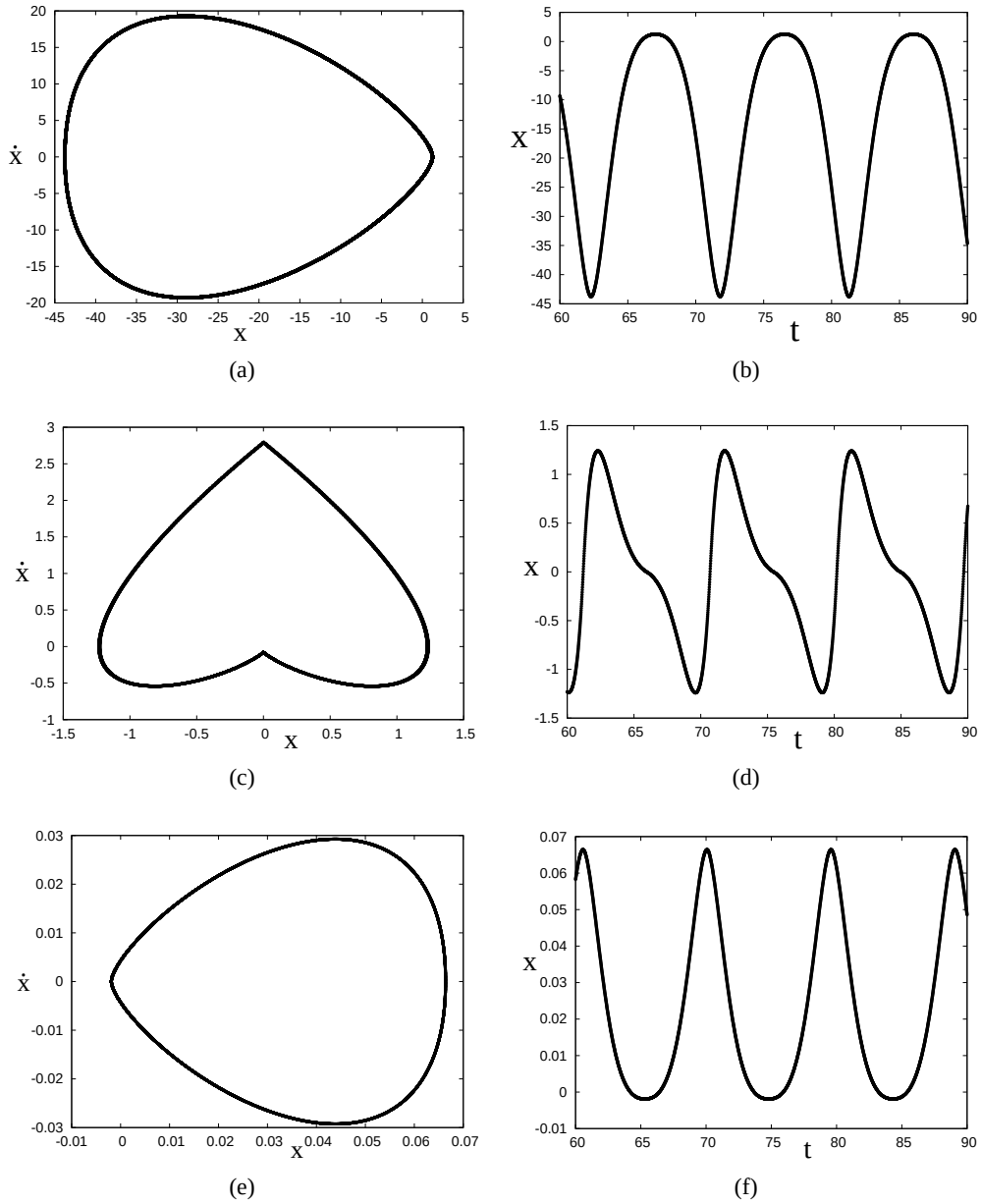

Figure 7.1: Limit cycle for (a)τ = 0.001 and the time series(b). (c) $\tau = 4.749 \approx \frac{T}{2}$ and time series (d). (e)$\tau = 9.45 \approx T$ and time series (f). Initial condition is taken as $x_0 = \dot{x_0}$. k=1.5 and $\omega_0 = 1.0$.

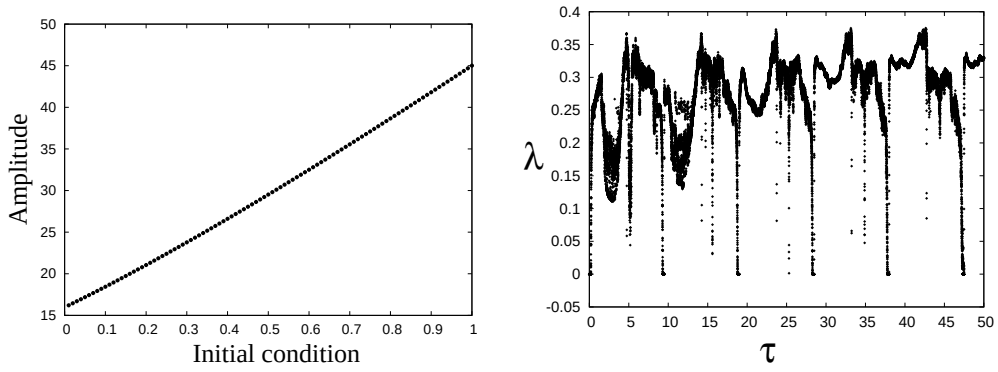

(a) (b)

Figure 7.2: Shape as well as amplitude of limit cycle depends on the initial condition. (a) width (for x axis) of the limit cycle is plotted with initial condition. $\dot{x}_0$ is taken constant in this figure. (b)Lyapunov exponents for the damped oscillator under memory modulation. Lyapunov exponents are plotted against the feedback time τ. the positive Lyapunov exponents in figure (b) indicates runaway solution for the oscillator.

certain choice of μ there can be a balance between both type of dynamics and the system can show limit cycle oscillation.

7.2 Modification of Pyragas scheme

We propose the following controlling method to modify dynamics of chaotic systems to limit cycle oscillations. We assume for $\mu < \mu_c$ the system dynamics is regular (fixed point or periodic orbit) and for $\mu > \mu_c$ the system is chaotic. We replace μ by $\mu + \varepsilon\Theta[x(t) - x(t-\tau)]$ where Θ is +1 for $x(t) > x(t-\tau)$ and -1 for $x(t) < x(t-\tau)$. τ is some predefined timescale. For small τ this control method restricts the dynamics from going very far from its initial points. For certain values of controlling parameter ε, the chaotic and fixed point dynamics balance each other and we see limit cycle oscillations.

7.3 Non phase coherent oscillators

We start with Lorenz oscillator. We modify the usual controlling parameter r. Without any loss of generality we can modify the system as following;

$$\begin{aligned} \dot{x} &= \sigma(y - x) \\ \dot{y} &= (r - \varepsilon\Theta[y(t) - y(t-\tau)])x - y - xz \\ \dot{z} &= xy - bz \end{aligned} \tag{7.3.1}$$

where b and σ have their usual values. If τ is small the Θ function is governed by the local dynamics. If the trajectory tries to move far from the initial points, r is changed to $r - \varepsilon$ and it induces a positive "damping" in the system. Thus the system tries to compensate its "energy" change over a cycle. For specific values of ε, change in energy over a complete cycle becomes zero and we observe limit cycle.

This mechanism is also applicable to many other chaotic oscillators. When τ is not small two cases

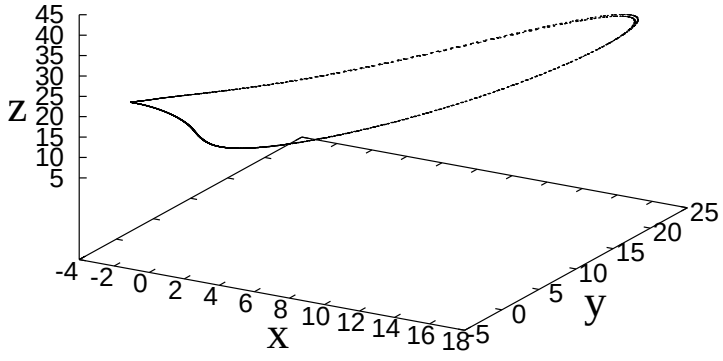

Figure 7.3: Limit cycle due to memory modulated parameter control of Lorenz system. Usual parameters are taken. σ = 10,b=$\frac{8}{3}$ and r=28. ε=10.0 and τ = 0.001 are taken for this figure.

can happen. For phase coherent attractors we can define an approximate value for the phase of the chaotic attractor. Memory modulation of governing parameter of those attractors leads to periodic dynamics. Those attractors show periodicity in limit cycle oscillations, ie. only for discrete values of τ we see limit cycles. For non phase coherent attractors we do not see periodicity in τ for its larger values though for smaller values of τ we do see periodic oscillations. Lorenz system under usual parameter regime shows double loop chaotic attractor which is a good example of a non phase coherent attractor.

7.4 Phase coherent oscillators

We demonstrate the first mechanism for a phase coherent chaotic system. Under certain parameter values (a=b=0.2,c=5.7) Rössler oscillator goes through chaotic motion and the chaotic attractor is a phase coherent one. We numerically calculate the approximate time period of the Rössler oscillator. Measurement of time period of more complicated attractors can be done by estimating Hilbert phase and measuring the corresponding time period.

Now we take $\tau \to 0, \frac{T}{2}, T$ and control the parameter 'b' with the same kind of prescription as before

$$\begin{aligned} \dot{x} &= -y - z \\ \dot{y} &= x + ay \\ \dot{z} &= b + \varepsilon\Theta[y(t) - y(t-\tau)] + z(x - c) \end{aligned} \tag{7.4.1}$$

Here a,b and c have their usual values. The Θ function can take the values either +1 or -1 and hence can lead to damped as well as undamped solution. The dynamical analysis resembles the earlier analysis for 1-D oscillator and we observe limit cycle oscillations as shown in Fig 7.4(b). This is to be compared with the corresponding limit cycle stabilization of Pyragas which is shown for reference in Fig 7.4(a). It should be noted that we do not use a feedback nor do we look for the UPOs.

To verify that the underlying dynamics is the same as with the 1-D model we calculated numeri-

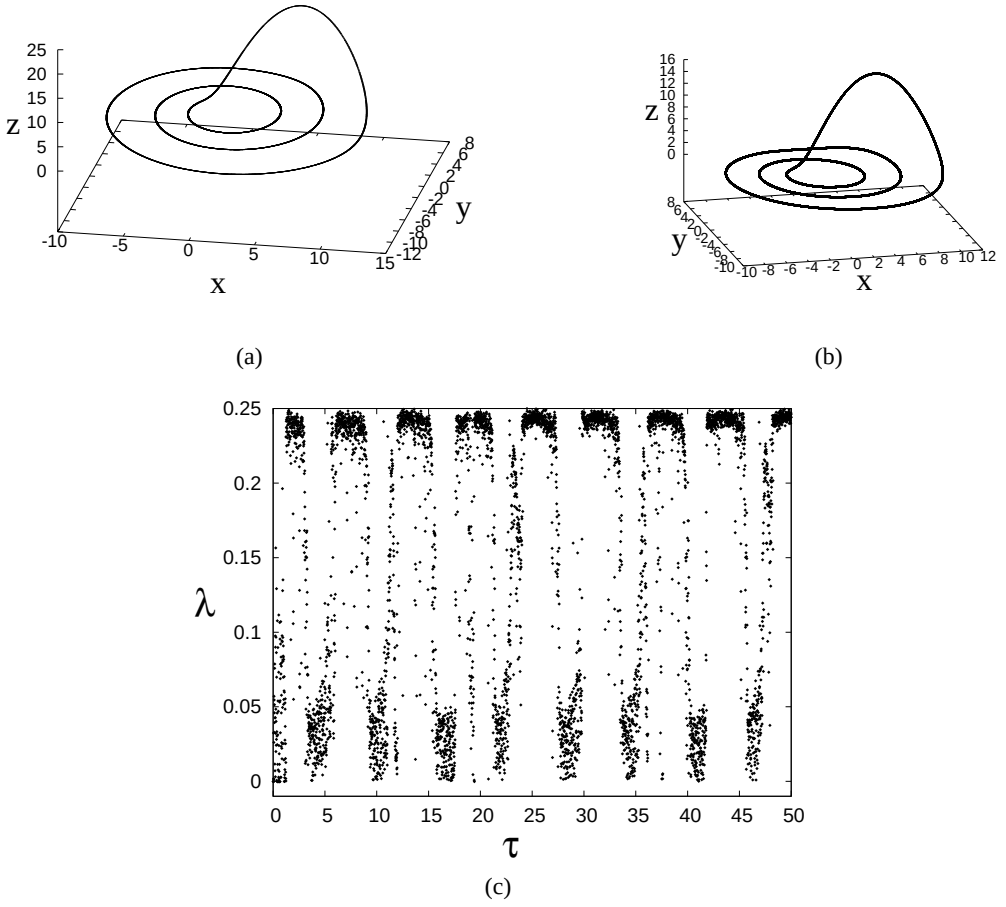

Figure 7.4: (a) Stabilization of period three cycle can be observed with external parametric modulation suggested by Pyragas . (K=0.2,τ=17.5) (b) limit cycle formed by controlling the parameter 'b' with memory modulation. Usual parameters (a=b=0.2,c=5.7) are taken for the figure. ε=0.23, τ=0.001 leads to this limit cycle.(c) Lyapunov exponent is plotted with τ. Limit cycle occurs for discrete range of feedback time τ periodically.

cally the average value of time period for the Rössler oscillator and found the Lyapunov exponents for different values of τ. From Fig 7.4(c) we can see $\tau \approx nT$ cases lead to more stable formation of limit cycle than $\tau \approx (n + \frac{1}{2})T$. In chaotic oscillators phase space points are revisited only approximately. We observe limit cycles only when $\tau \approx nT$, n=0,1,2,.... The Lyapunov spectrum with respect to τ shows a sharp fall. This result confirms our speculation that chaotic dynamics can be altered to limit cycle oscillations using memory dependent parameter modulation.

7.5 Discussion

we have shown that a memory dependent switching of a control parameter in a dynamical system can be very effective in altering the dynamics. With the prescription given Pyragas it is possible to control chaotic oscillators where we know the position of the UPOs. Our approach is closer to OGY approach in the sense that we also modulate the parameter of the dynamical system. In our method we do not need to know the UPOs and we can also apply our method where only time series is available. In particular, this can have applications in control of chaos especially in controlling experimental time series.

Bibliography

[1] E Ott, C. Grebogi, and J. A. Yorke, Phys. Rev. Lett. 64, 1196 (1990)

[2] W. L. Ditto, S. N. Ranseo and M.L. Spano, Phys. Rev. Lett. 65, 3211 (1990)

[3] E. R. Hunt, Phys. Rev. Lett. 67, 1553 (1991)

[4] E. R. Hunt, Phys. Rev. Lett. 68, 1259 (1992)

[5] K. Pyragas, Phys. Lett. A, 170, 421 (1992)

[6] S. Banerjee and C. Grebogi, Phys. Rev. E 59, 4052(1999)

[7] S. Banerjee, P. Ranjan and C. Grebogi, IEEE Trans. Circuits Systems 47 633 (2000)

[8] C. Grebogi, E. Ott, F. Romeiras and J. A. Yorke, Phys. Rev. A 36, 5365 (1987)

Chapter 8

Conclusion

The main goal of this thesis is to study effects of memory modulation on nonlinear as well as chaotic systems. Control of chaos is one of the most relevant fields for research in nonlinear dynamics. Many methods have been proposed for controlling chaos in last two decades. More recently understanding of usefulness of chaos in physical system has drawn attention of nonlinear dynamicists and has become an active field. In this thesis we have developed memory dependent control algorithms and analysed the resultant dynamics. While external feedback methods are quite common in literature for controlling chaotic dynamics, memory dependent feedback is rare. In iterative maps this technique has been applied in the from of one step memory dependence. We justify the idea of a one step memory dependence as follows. Iterative maps are generated from stroboscopic maps of higher dimensional continuous system. Now a single step in the map corresponds to a fixed time span in the continuous system. In stroboscopic maps we get a section of the continuous system at equal intervals of time. Thus a one step memory in the map is a memory of an event occurring a finite time earlier in the continuous system.

We systematically studied the effects of memory modulation. Logistic map has long been taken as a standard system for exploring the dynamics of one dimensional iterative maps. We suggest a prescription for controlling this map with memory dependent modulation. This modulation not only changes the usual chaotic and non-chaotic ranges it is also able to show richer dynamics. In standard

chaotic maps we can see intermittent transition to chaos from periodic dynamics. In logistic map it occurs through type-I kind of intermittency where local map is quadratic. This intermittent transition predicts the relation between the distance from the periodic window with average length of periodicity in the time series. Under memory modulation the relation changes even if local mapping remains the same. The new idea of re-injection mechanism is included to explain this phenomenon. Various kinds of modulation are possible to implement on maps. We investigated a different kind of modulation on the same logistic map. Different modulations serve different purposes. Unlike previous case here we also studied the interplay between highly chaotic dynamics with stable periodic dynamics. We found that this memory modulated map gives rise to a long sequence of period-adding bifurcation. Period adding bifurcations are usually seen in piecewise linear maps where the periods are generally interspersed with chaotic bands. Here we showed different mechanism (memory modulation) can also generate this phenomenon. We presented a scenario where period adding cascade is much cleaner so that we can analytically calculate the ratio 'δ' of the widths of two adjacent periodic windows. This ratio is universal in the sense that whenever the local map is quadratic under the same mechanism the same analysis follows.

The phenomena of period adding is seen to be ubiquitous in the memory dependent maps. We studied two dimensional discrete Lotka-Volterra system as a natural extension of the one dimensional iterative maps. Discrete Lotka-Volterra shows periodic as well as chaotic dynamics. It also shows invariant cycles as it goes through Neimark-Sacker bifurcation. We studied this system under memory modulation. The existence of both chaotic and periodic dynamics leads to period adding bifurcation. We showed numerically that period adding only occurs in presence of both periodic and chaotic dynamics. Though here we did not see any universal ratio for period adding bifurcation. We need to study this dynamics more in depth in future to explore the underlying dynamics and explain this type of period adding in greater detail.

Finally we showed modulation of chaotic dynamics to periodic limit cycles can be achieved through similar kind of memory dependent modulation. We improved our prescription of memory modulation through low dimensional discrete dynamical systems and eventually applied it to continuous

chaotic systems. Controlling chaos has earlier been suggested by Ott, Grebogi and Yorke (OGY). Unlike OGY method, the controlling methods explained in this thesis control the dynamical system globally. As a natural consequence interplay between chaotic and periodic dynamics becomes important. As a outcome of this interplay many new and rich dynamics can be seen. Memory dependent control methods make the systems discontinuous in general. This discontinuity is often the cause behind the generation of many rich dynamics that was absent in the original systems.